NEW EFFICIENT AC-DC CONVERTERS AND THEIR APPLICATIONS

by

Khalid Saifullah (132407)

Md. Abdullah-Al-Hysam (132434)

Md. Zihad Ul Haque (132445)

Sakif Asif (132484)

A Thesis Submitted to the Academic Faculty in Partial Fulfillment of the Requirements for the Degree of

BACHELOR OF SCIENCE IN ELECTRICAL AND ELECTRONIC ENGINEERING

Department of Electrical and Electronic Engineering

Islamic University of Technology (IUT)

Gazipur, Bangladesh

NEW EFFICIENT AC-DC CONVERTERS AND THEIR APPLICATIONS

Approved by:

Dr. Golam Sarowar

Supervisor and Assistant Professor,

Department of Electrical and Electronic Engineering
Islamic University of Technology (IUT)
Board Bazar, Gazipur-1704
Bangladesh.

Date: 10-11-2017

Table of Contents

LIST OF FIGURES

LIST OF TABLES

Acknowledgements

We wish to express our deepest gratitude to our academic and research advisor **Dr. Golam Sarowar**, Assistant professor, Department of EEE, IUT for his continuous guidance, supervision and invaluable suggestions during the entire project work. We also wish to acknowledge and express our appreciation to friends and others who directly or indirectly helped with, worth suggestions and information in completing this project. Finally, we thank the Electrical and Electronic Engineering Department Laboratory personnel for their patient assistance during the period of the project work.

Chapter 1

Abstract

AC-DC converters are mostly used as power supplies for microelectronic systems, battery chargers, wind energy applications, electric appliances in household and dc motor drives. Switched-capacitor (SC) network based converters can be good solution to the challenges of 21st century having high voltage conversion ratio and low EMI emissions. The application of this type of converters is in microprocessor based systems where the line voltage requires a steep step down to 3V or even less in order to drive integrated circuits (ICs). In this paper, a new high step down bridgeless single switch AC-DC converter with switched capacitor is proposed. The absence of transformer as well as bridge rectifier reduce the components count, size and cost of the converter. Unlike the existing converters, this proposed buck boost converter is able to achieve simple control structure with single switch, high efficiency, low total harmonic distortion (THD) and high input power factor.

Power supplies for microelectronic systems, battery chargers, wind energy applications, electric appliances in the household and dc motor drives require AC-DC converters. The proposed bridgeless Cuk PFC converter in this paper is featured with common ground, transformerless structure, and clear energy delivery process. The absence of bridge rectifiers, transformer and the presence of only two semiconductor switches in the current flowing path during each switching cycle result in less conduction losses and improved thermal management, reducing components count, size and cost of the converter compared to the conventional SEPIC and Cuk PFC converters. Moreover, the presence of two power switches for different half cycles leads to less stress on the power switch. Unlike the existing converters, this proposed bridgeless Cuk PFC converter is able to achieve simple control structure with high efficiency, low total harmonic distortion (THD) and high input power factor.

This letter describes a new application of single-ended primary converter (SEPIC) and Cuk converter for dc bipolar net-work. A dc–dc converter configuration based on a combination of both converters is proposed. In the resulting topology, the switching node is shared by the SEPIC and Cuk converter since they have the same instantaneous duty cycle. The main advantage of this topology is that synchronization of various switches is not required, and control terminal is connected to ground which simplifies the design of the gate drive. On the other hand, this configuration allows the connection of renewable energy sources to microgrids (MG)-type bipolar dc link and to cover the current needs of new distributed generation units with efficient, economical, and easy way. To verify its performance, a prototype was designed. Experimental results show as this combination of two converter topologies with appropriated modulation schemes are adequate to use in dc MG.

Chapter 2

Introduction

2.1 Fundamentals of Power Electronics

This chapter gives a description and overview of power electronic technologies including a description of the fundamental systems that are the building blocks of power electronic systems. Technologies that are described include: power semiconductor switching devices, converter circuits that process energy from one DC level to another DC level, converters that produce variable frequency from DC sources, principles of rectifying AC input voltage in uncontrolled DC output voltage and their extension to controlled rectifiers, converters that convert to AC from DC (inverters) or from AC with fixed or variable output frequency (AC controllers, DC–DC–AC converters, matrix converters, or cyclo- converters). The chapter also covers control of power converters with focus on pulse width modulation (PWM) control techniques.

2.1.1 Definition, History, Applications and Trends of Power Electronics

Power electronics (PE) experienced tremendous growth after the introduction of the first solid-state power switch, the silicon controlled rectifier (SCR) in 1957. Today, almost all of the technologies that require control of power control utilize PE technology. This chapter will give the reader an overview on the field of PE including:

- A description of the fundamentals of the power semiconductor switching devices.
- Converter circuits that process energy from one DC level to another DC level.
- Converters that produce variable frequency from DC sources.
- Principles of rectifying AC input voltage in uncontrolled DC output voltage and their extension to controlled rectifiers.
- Converters that convert to AC from DC (inverters) or from AC with fixed or variable output frequency.
- AC controllers.
- DC–DC–AC converters.
- Matrix converters or cyclo-converters.
- Detailed description of pulse width modulations control techniques.

Power electronic circuits are used to control the power conversion from one or more AC or DC sources to one or more AC or DC loads, and sometimes with bidirectional capabilities. In most power electronics systems, this conversion is accomplished with two functional modules called the control stage and the power stage. Figure 2.1 shows the topology for a single source and single load converter application that includes a power processor (the power stage) and a controller (the control stage). The converter, handles the power transfer from the input to output, or vice versa, and is constituted of power semiconductor devices acting as switches, plus passive devices (inductor and capacitor). The controller is responsible for operating the switches according to specific algorithms monitoring physical quantities (usually voltages and currents) measured at the system input and or output.

The modern PE era began in 1957. It was during that year the first commercial thyristor, or Silicon Controlled Rectifier (SCR), was introduced by General Electric Company. The SCR, started replacing the mercury arc rectifiers, invented in 1902, and the later developed thyratron (invented in 1923) and ignitron (invented in 1931), allowed the commercialization of several industrial circuits conceived during the 1920s and 1940s (like the cyclo-converter, the chopper, and the parallel inverter) as well as the Graetz bridge conceived in 1897.

The SCR was the only available power device for more than 25 years after its invention (and still is very useful for extremely high power applications). Since it is very difficult to impose turn-off conditions for SCR's, faster devices, with higher voltage and current capabilities, with better controllability were developed,

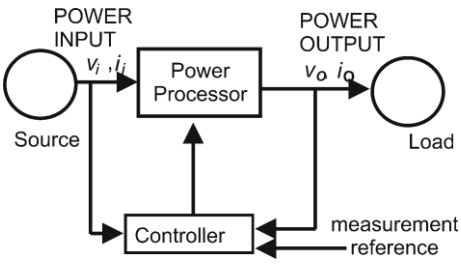

Fig. 2.1 A general power electronic system

including the bipolar junction transistor (BJT) invented in 1970. The BJT was used in applications from low to medium power and frequency and now is considered obsolete. The metal oxide semiconductor field effect transistor (MOSFET) was invented in 1978 and is used for power electronic switching applications of low power and high frequencies. The gate turn-off thyristor (GTO), is used in applications from medium to high power and from low to medium frequencies. The insulated gate bipolar transistor (IGBT) developed in 1983 is used in applications from low to medium power and frequency. The integrated gate commutated thyristor (IGCT) invented in 1997 is used in applications from medium to high power and from low to medium frequencies.

Through the use of this switching technology power electronics systems can operate in the range from few watts up to GW, with frequency range from some 100 Hz up to some 100 kHz, depending on the power handled [1]. The advent of microelectronics and computer control made it possible to apply modern control theory to PE and at same the time made possible very complex circuit functions. Therefore, the area of PE, became interdisciplinary, as indicated in Fig. 2.2. At the high power level, PE deals with static and rotating equipment for generation, transmission, and distribution handling large amount of power. For consumer electronic applications power converters and circuits are important for information processing, employing analog and digital circuits, or microprocessors including microcontrollers, digital signal processors (DSP), and field programmable gate arrays (FPGA). In the area of control, PE deals with stability and response characteristics in systems with feedback loops, based on classical or modern control. With the development of very large system integration (VLSI), ultra large system integration (ULSI), and other sophisticated computer-assisted designs; advanced control systems could be used to develop new power electronic topologies.

The development of devices and equipment able to individually or in combination convert efficiently electric energy from AC to DC, DC to DC, DC to AC, and AC to AC together with the changes that occurred in electrical power engineering has resulted in wide spread of PE in a large spectrum of applications.

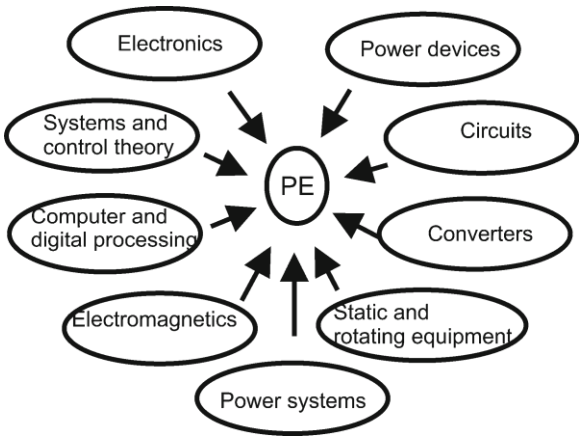

Fig. 2.2 Power electronics and related topics

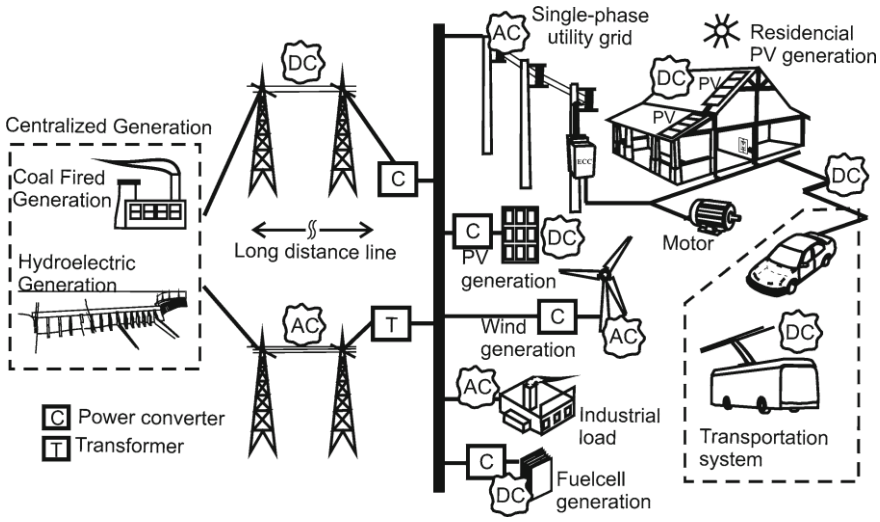

Fig. 2.3 Power electronics and electrical energy generation transmission, storage, and distribution

Figure 2.3 shows how electrical energy generation is distributed for the end-user, showing transmission, distribution, storage, renewable energy sources and users. In fact, nowadays PE is a key technology for all those sub-systems, and has spread in many applications, examples including:

- Residential: heaters, home appliances, electronic lighting, equipment sources;
- Commercial: heaters, fans, elevators Uninterruptible Power Supply (UPS), AC and DC breakers, battery chargers;
- Industrial: pumps, blowers, robots, inductive heaters, welding, machine drive, portable sources;
- Transportation: electrical and hybrid vehicles, battery chargers, railroad electric system;
- Utility systems: high voltage direct current, generators, reactive compensators, interface for photovoltaic, wind, fuel cells systems, Flexible AC Transmission System (FACTS) equipment;
- Aerospace: sources for spacecrafts, satellites, planes;
- Communication: sources, RF amplifiers, audio-amplifiers.

Power electronics will continue to be an enabling technology to address our future electricity needs. It is expected that new power devices for higher power, higher frequency, and lower losses will continue to be invented. Global energy concerns will provoke a large interest in the increase of the conversion efficiency and more application of PE in power quality, distributed generation, energy conservation, and smart grids. The integration of power and control circuitry into functional modules will result in systems solutions that are highly integrated into packaged products that will be both more reliable and affordable.

2.1.2 Power Semiconductor Devices

Electronic switches capable of handling high voltage and current operations at high frequency (HF) are the most important devices needed in the design of energy conversion systems that use PE. For the purposes of this discussion we will define the concept of an ideal switch. An ideal power electronic switch can be represented as a three terminals device as shown in Fig. 2.4. The input, the output, and a control terminal that imposes ON/OFF conditions on the switch. A switch is considered ‘‘ideal’’ when it is open, it has zero-current through it and can handle infinite voltage. When the switch is closed it has zero-voltage across it and can carry infinite current. Also, an ideal switch changes condition instantly, which means that it takes zero-time to switch from ON-to-OFF or OFF-to-ON. Additional characteristics of an ideal switch include that it exhibits zero-power dissipation, carries bidirectional current, and can support bidirectional voltage. If we plot the switch current (*i*) with respect to its voltage (*v*) we define four quadrants that are often referred to as the *v-i* plane and are shown in Fig. 2.5. By definition, an ideal switch can operate in all four quadrants.

Practical or real switches do have their limitations in all of the characteristics explained in an ideal switch. For example, when a switch is on, it has some voltage across it, known as the on-voltage and it carries a finite current. During the off stage, it may carry a small current known as the leakage current while supporting a finite voltage. The switching from ON-to-OFF and vice versa does not happen instantaneously. Of course, all actual switching devices take times to switch and we define these characteristics as the delay, rise, storage, and fall times. As a consequence of the above two non-ideal cases, there is voltage and current across the switch at all times, which will result in two types of losses. The first loss occurs during the on and off-states and is defined as the ‘‘conduction loss’’. The second loss is defined as the ‘‘switching loss’’ which occurs just as the switch changes state as either opening or closing. The switch losses result in raising the overall

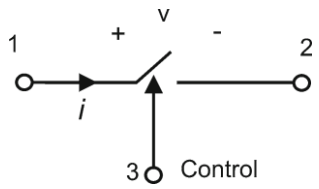

Fig. 2.4 Ideal switch

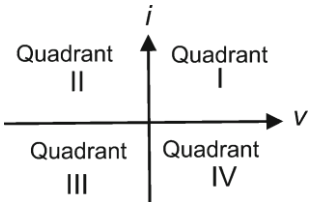

Fig. 2.5 *4-quadrant* switch

v-i characteristics

switch temperature. Further, the ON/OFF-state of the power switch must be controlled though an external signal.

2.1.3 Classifications of Power Switches

The concept of the ideal switch is important when evaluating circuit topologies. Assumptions of zero-voltage drop, zero-leakage current, and instantaneous transitions make it easier to simulate and model the behavior of various electrical designs. Using the characteristics of an ideal switch, there are three classes of power switches:

1. *Uncontrolled switch*: The switch has no control terminal. The state of the switch is determined by the external voltage or current conditions of the circuit in which the switch is connected. A diode is an example of such switch.
2. *Semi-controlled switch*: In this case the circuit designer has limited control over the switch. For example, the switch can be turned-on from the control terminal. However, once ON, it cannot be turned-off from the control signal. The switch can be switched off by the operation of the circuit or by an auxiliary circuit that is added to force the switch to turn-off. A thyristor or a SCR is an example of this switch type.
3. *Fully controlled switch*: The switch can be turned-on and off via the control terminal. Examples of this switch are the BJT, the MOSFET, the IGBT, the GTO thyristor, and the MOS-controlled thyristor (MCT).

2.1.4 Uncontrolled Switches

A diode, also known as rectifier, is an *uncontrolled switch*. It is a two terminal device with a symbol depicted in Fig. 2.6a. The terminals are known as Anode (*A*) and cathode (*K*). In the ideal case, the diode current (i_d) is unidirectional and current can only flow from the anode to the cathode. The diode voltage (v_d) is measured as being positive from the anode to the cathode.

The *v-i* characteristics for a real (non-ideal) diode are shown in Fig. 2.6b. In quadrant I, the diode is in the ON-state, and is known as the forward-biased region. When it is ON the diode carries a positive current while supporting a small voltage. The diode current varies exponentially with the diode voltage. The diode is reversed-biased in quadrant III, which is the OFF-state. When it is OFF, the diode supports a negative voltage and carries a negligible current (leakage current). When the negative voltage exceeds a certain limit, known as the breakdown voltage, the leakage current increases rapidly while the voltage remains at the breaking value, which potentially damages the device. Therefore, operation that exceeds the breakdown voltage must be avoided.

The ideal diode characteristics are shown in Fig. 2.6c. During the ON-state, the diode has zero-voltage across it and carries a positive current. During the OFF- state, the diode carries zero-current and supports a negative voltage.

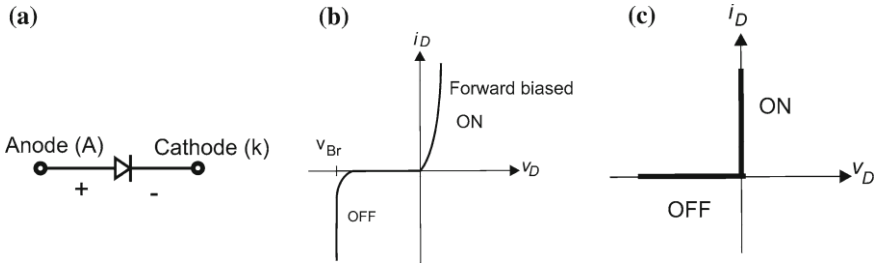

Fig. 2.6 Diode: a symbol, b *i-v* characteristics, and c idealized characteristics

2.1.5 Semi-controlled Switches

The thyristor or SCR is a power semiconductor switch whose turn-on can be activated from the control terminal Gate but once it turns ON, the control terminal becomes ineffective and the thyristor behaves similar to a diode. Therefore, the thyristor is considered a *semi-controlled switch*. The name, controlled rectifier, is an indication that a thyristor is a device that can be considered as a diode whose turn-on can be commanded externally. Figure 2.7a shows the circuit symbol for a thyristor. Although there are similarities between the diode and the thyristor circuit symbols, their operation is very different. The thyristor current, I_A, flows from the anode (A) to the cathode (K) and the voltage V_{Ak}, across the thyristor is positive when the anode is at higher voltage than the cathode. Figure 2.7b shows the *v-i* characteristics of a real or non-ideal thyristor. In quadrant I, in the absence of a gate current, the device is OFF in the forward blocking region and supports a positive voltage. If a gate current is applied, the device switches to the on-state region and the device has a *v-i* characteristic similar to that of a diode. In quadrant III, the device is OFF, and the region is known as the reverse blocking region. Again, the characteristics are similar to those of a diode. Comparing the switching characteristics of a diode and a thyristor, it appears that when the thyristor is OFF, it can block large positive or negative voltage, which is a fundamental feature that is important in circuit applications, such as AC/AC converters. This can be clearly seen in the ideal characteristics of the thyristor as shown in Fig. 2.7c. In the ON- state, the thyristor has zero-voltage across it and carries a positive current. In the OFF-state, the thyristor can support a positive voltage in the forward blocking region or a negative voltage, similar to a diode, in the reverse blocking region. Therefore, the thyristor can be considered to carry a unidirectional current and supports a bidirectional voltage.

The triac, shown in Fig. 2.8a, is also a semi-controlled switch. A triac can be modeled as two thyristors connected back-to-back as shown in Fig. 2.8b. Triacs are considered as bidirectional voltage and bidirectional current devices, as shown by the *v-i* characteristics in Fig. 2.8c. The ideal characteristics are in Fig. 2.8d. As a low-cost bidirectional switch, the triac is the primary switch that is used for low power electronic commercial circuits such as light dimmers and control circuits for single-phase motors used in home appliances.

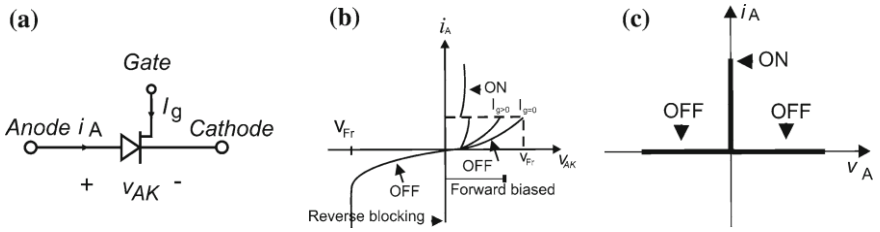

Fig. 2.7 Thyristor: a symbol, b *i-v* characteristics, and c idealized characteristics

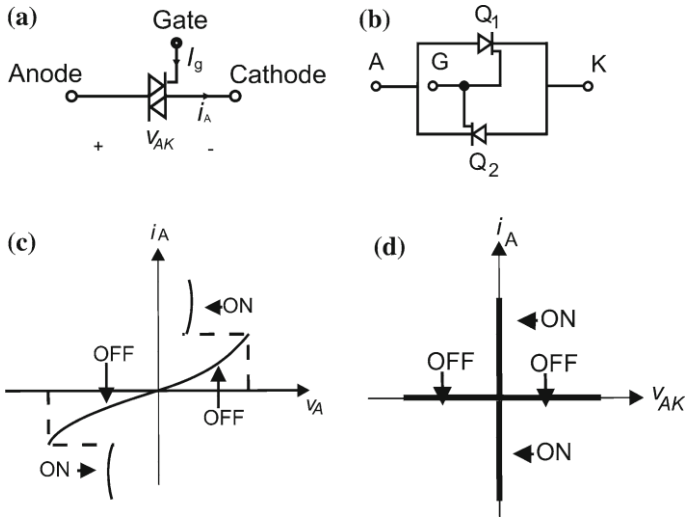

Fig. 2.8 The triac: a symbol, b two-thyristor-representation, c *i-v* characteristics, and d idealized characteristics

2.1.5.1 Fully Controlled Switches

In a fully controlled switch the ON- and OFF-states can be activated externally through a control terminal. A number of power switches fall into the category of controlled switches; some of them are transistor-based devices and others are thyristor-based devices. A brief description of each device is given in the following sections:

2.1.5.1.1 The Bipolar Junction Transistor

Figure 2.9a shows the circuit symbol for an npn-type BJT. The base (*B*) is the control terminal, where the power terminals are the collector (*C*) and the emitter (*E*). The *v-i* characteristics of the device are shown in Fig. 2.9b. The device

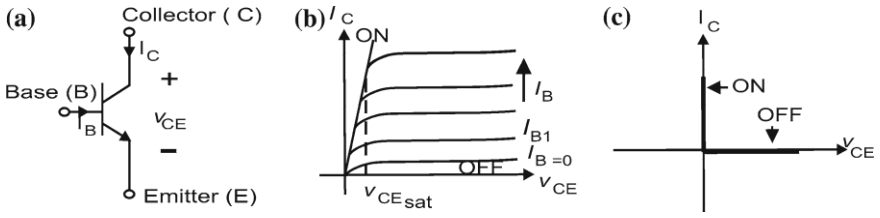

Fig. 2.9 The BJT: a symbol, b *i-v* characteristics, and c idealized characteristics

operates in quadrant I and is characterized by the plot of the collector current versus the collector to emitter voltage. The device has three regions two of them where the device operates as a switch and the third is where the device operates as a linear amplifier. The device is OFF in the region below i_B 0 and is ON in the region where v_{CE} is less than $v_{CE(Sat)}$. Neglecting the middle region, the idealized device characteristics as a switch are shown in Fig. 2.9c. During the ON-

state the device carries a collector current IC > 0 with V_{CE} = 0. In the OFF-state, the device supports positive V_{CE} >0 with IC = 0. Therefore, the BJT is unidirectional current and voltage device. The BJT has historical importance, but today most of its function are covered by devices like the IGBT.

2.1.5.1.2 The Metal Oxide Semiconductor Field Effect Transistor

Figure 2.10a shows the circuit symbol for an n-channel, enhancement mode MOSFET. Similar to the BJT, it has a control terminal known as the gate (*G*) and the power terminals are the drain (*D*) and source (*S*). The device is controlled by supplying a voltage (v_{GS}) between the gate and the source. This makes it a voltage- controlled device compared to the BJT, which is a current-controlled device. The real *v-i* characteristics of device are shown in Fig. 2.10b. Similar to the BJT, the MOSFET operates within three operating regions. Two of the regions are used when the device is operated as a switch, and the third is when the device is used as an amplifier. To maintain the MOSFET in the off-state, v_{GS} must be less than a threshold voltage known as v_T, which is the region below the line marked OFF. And when the device is ON it act as resistance determined by the slope of the line marked ON. The idealized characteristics of a MOSFET switch are shown in Fig. 2.10c. When the device is ON, it has zero v_{DS} and carriers a current I_D>0 and when the device is OFF it supports a positive v_{DS} and has zero drain current (I_D = 0).

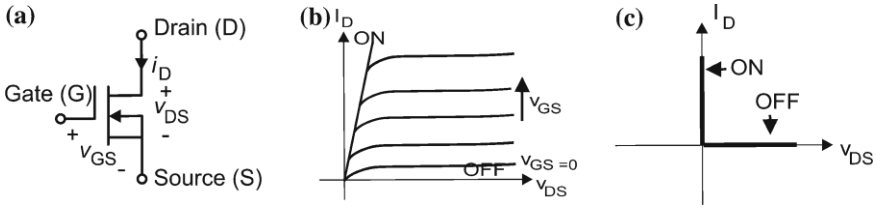

Fig. 2.10 The MOSFET: a symbol, b *i-v* characteristics, and c idealized characteristics

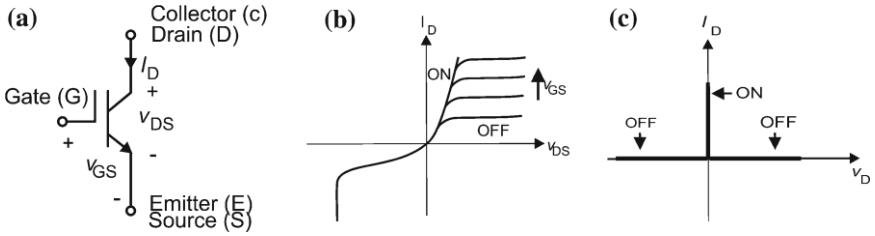

Fig. 2.11 The IGBT: a symbol, b *i-v* characteristics, and c idealized characteristics

Three other MOSFET configurations include: n-channel depletion mode and p-channel enhancement and depletion modes.

2.1.5.1.3 The Insulated Gate Bipolar Transistor (IGBT)

The IGBT is a hybrid or also known as double mechanism device. Its control port resembles a MOSFET and its output or power port resembles a BJT. Therefore, an IGBT combines the fast switching of a MOSFET and the low power conduction loss of a BJT. Figure 2.11a shows a circuit symbol that is used for an IGBT, which is slightly different from the MOSFET with similar terminal labels. The control terminal is labeled as gate (*G*) and the power terminals are labeled as collector (*C*) and emitter (*E*). The *i-v* characteristics of a real IGBT are shown in Fig. 2.11b, which shows that the device operates in quadrants I and III. The ideal characteristics of the device are shown in Fig. 2.11c. The device can block bidirectional voltage and conduct unidirectional current. An IGBT can change to the ON-state very fast but is slower than a MOSFET device. Discharging the gate capacitance completes control of the IGBT to the OFF-state. IGBT's are typically used for high power switching applications such as motor controls and for medium power PV and wind PE.

2.1.5.1.4 The Gate Turn-Off Thyristor

The GTO thyristor is a device that operates similar to a normal thyristor except the device physics, design and manufacturing features allow it to be turned-off by a negative gate current which is accomplished through the use of a bipolar transistor. The circuit symbol for a GTO is shown in Fig. 2.12a. The *v-i* characteristics and the ideal switch characteristics are shown in Fig. 2.12 b, c. Although the device has been in existence since the late 1960s, and it has been successfully used in high power drives, IGBTs have reached price and rating party and are expected to replace GTO's in new power electronic designs.

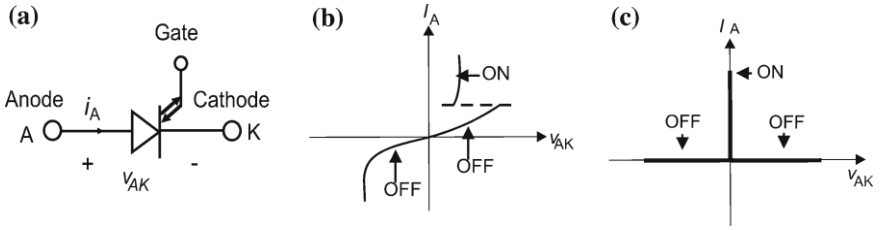

Fig. 2.12 The GTO: a symbol, b *i-v* characteristics, and c idealized characteristics

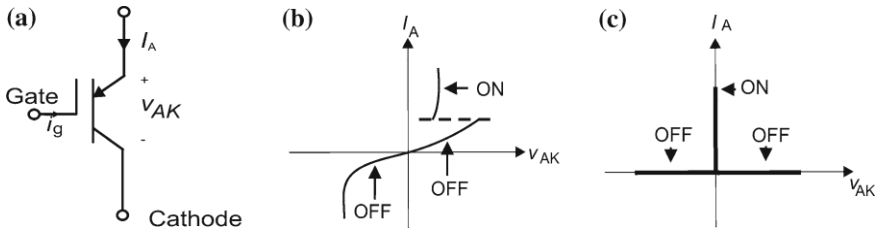

Fig. 2.13 The MCT: a symbol, b *i-v* characteristics, and c idealized characteristics

2.1.5.1.5 The MOS-Controlled Thyristor

Similar to the IGBT, the MCT is a hybrid or double mechanism device that was designed to have a control port of a MOSFET and a power port of a thyristor. The circuit symbol for the device is shown in Fig. 2.13a. The real device characteristics and the idealized characteristics are shown in Fig. 2.13b, c. The characteristics are similar to the GTO, except that the gate drive circuitry for the MCT is less complicated than the design for a GTO as the control circuit of the MCT uses a MOSFET instead of a transistor. As a result, the MCT was supposed to have higher switching frequency. Although the MCT was invented at the same time period of the IGBT it never became fully commercially available and at the time of writing this book it is unknown the future market plans.

2.1.6 Power Electronic Converter Topologies

Power electronic converters are switch-mode circuits that process power between two electrical systems using power semiconductor switches. The electrical systems can be either DC or AC. Therefore, there are four possible types of converters; namely DC/DC, DC/AC, AC/DC, and AC/AC. The four converter types are described below:

1. *DC/DC Converter*: is also known as ‘‘Switching Regulator’’. The circuit will change the level voltage available from a DC source such as a battery, solar cell, or a fuel cell to another DC level, either to supply a DC load or to be used as an intermediate voltage for an adjacent power electronic conversion such as a DC/AC converter. DC/DC converters coupled together with AC/DC converters enable the use of high voltage DC (HVDC) transmission which has been adopted in transmission lines throughout the world.

2. *DC/AC Converter*: Also described as ‘‘Inverter’’ is a circuit that converts a DC source into a sinusoidal AC voltage to supply AC loads, control AC motors, or even connect DC devices that are connected to the grid. Similar to a DC/DC converter, the input to an inverter can be a stiff source such as battery, solar cell, or fuel cell or can be from an intermediate DC link that can be supplied from an AC source.

3. *AC/DC Converter*: This type of converter is also known as ‘‘Rectifier’’. Usually the AC input to the circuit is a sinusoidal voltage source that operates at 120 V, 60 Hz or a 230 V, 50 Hz, which are used for power distribution applications. The AC voltage is rectified into a unidirectional DC voltage, which can be used directly to supply power to a DC resistive load or control a DC motor. In some applications the DC voltage is subjected to further conversion using a DC/DC or DC/AC converter. A rectifier is typically used as a front-end circuit in many power system applications. If not applied correctly, rectifiers can cause harmonics and low power factor when they are connected to the power grid.

4. *AC/AC Converter*: This circuit is more complicated than the previous converters because AC conversion requires change of voltage, frequency, and bipolar voltage blocking capabilities, which usually requires complex device topologies. Converters that have the same fundamental input and output frequencies are called ‘‘AC controllers’’. The conversion is from a fixed voltage fixed frequency (FVFF) to a variable voltage fixed frequency (VVFF). Applications include: light dimmers and control of single-phase AC motors that are typically used in home appliances. When both voltage and frequency are changed, the circuits are called ‘‘Cyclo-converters’’, which convert a FVFF to variable voltage variable frequency (VVVF) and when fully controlled switches are used, this class of circuit is called ‘‘Matrix Converter’’. Another way of achieving AC/AC conversion is by using AC/DC and DC/AC through an intermediate DC link. This type of combined converter approach can be complex as the correct control approach must be implemented including simultaneous regulation of the DC link, injection of power with a prescribed power factor and bidirectional control of energy flow.

2.1.6.1 DC/DC Converters

A generalized circuit for a DC/DC converter is depicted in Fig. 2.14 where all possible switches connecting the input to the output are represented. If one P-switch and one N-switch are used, the resulting circuit is shown in Fig. 2.15a. The switches are controlled ON and OFF within a specified period *T*. The output

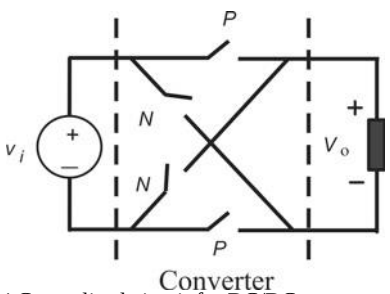

Fig. 2.14 Generalized circuit for DC/DC converter circuits

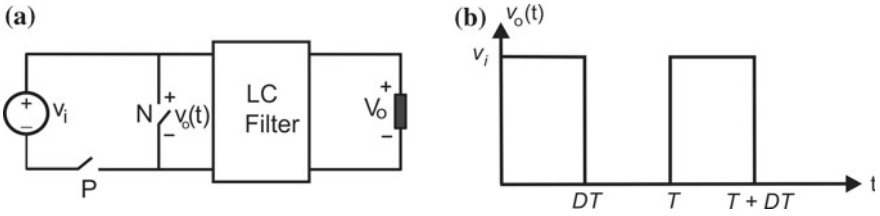

Fig. 2.15 Non-isolated down (buck) DC/DC converter: a circuit and b waveforms

voltage is equal to the input voltage when the P-switch is ON, and is equal to zero when the N-switch is ON. The ratio of the ON-time of switch P switch to the period T is defined as the duty ratio or duty-cycle (D). The waveform of the output voltage $v_o(t)$ is shown in Fig. 2.15b. Since $v_o(t)$ is a pulsating waveform, an LC circuit is used to filter the voltage to a DC. In this case the average V_o or DC component of the output voltage is given by Eq. (2.1),

$$V_{\text{avg}} = \frac{1}{T}\int_0^{DT} V_i = DV_i \qquad (2.1)$$

Since $D<1$, the DC output voltage of this converter is always less than the input voltage.

When all the generalized converter switches are used, the resulting circuit is shown in Fig. 2.16. When the P-switches are ON, the output voltage is equal to the input voltage and when the N-switches are ON, the output voltage is equal to the negative of the input voltage. The resulting waveform is shown in Fig. 2.16b. The DC component or the average of the output voltage is given by:

$$V_{\text{avg}} = \frac{1}{T}\left[\int_0^{DT} V_i \mathrm{d}t + \int_{DT}^{T} -V_i \mathrm{d}t\right] = (2D-1)V_i \qquad (2.2)$$

Equation (2.2) indicates that the output voltage is less than the input voltage with a changed polarity. For duty-cycle $D>0.5$ the output has a positive value and for

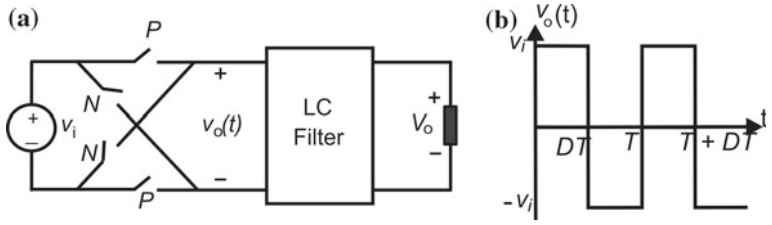

Fig. 2.16 Full-bridge non-isolated down (buck) DC/DC converter: a circuit, and b waveforms

duty-cycle $D<0.5$ the output has a negative value. The LC circuit in the design is used to filter the harmonic components of the output voltage so that the load receives a DC voltage with negligible ripple. Both voltages given by Eqn. (2.1) and (2.2) indicate that output has a lower DC value than the input voltage. Therefore, the converters are referred to as step down or buck converters.

Two other basic DC/DC converters include the boost and buck/boost converters. A boost converter can be defined as when the DC output voltage is higher than the input voltage. This design is also referred to as a step-up converter and a typical design is shown in Fig. 2.17. In this circuit, the switches are inserted between the inductor and the capacitor. If the converter is lossless, the ratio of the output DC voltage to the input DC voltage is given by Eq. (2.3). Since D is less than one, the output voltage is always higher than the input voltage.

$$V_{avg} = \frac{V_i}{D} \qquad (2.3)$$

A buck/boost or step-up/down converter is shown in Fig. 2.18. This converter is capable of providing a DC output voltage that can be lower or higher than the input DC voltage. The input/output conversion ratio is given by Eq. (2.4).

$$\frac{V_o}{V_i} = \frac{D}{1-D} \qquad (2.4)$$

When the *D*, is less than 0.5 the converter operates as a buck or step-down converter and when *D*>0.5 the converter operates as step-up or boost converter. For all basic DC/DC converters discussed so far. The switch is implemented by a controlled switch (transistor) and an uncontrolled switch (diode). When the transistor and the diode are alternately switched, the mode of operation is referred to as

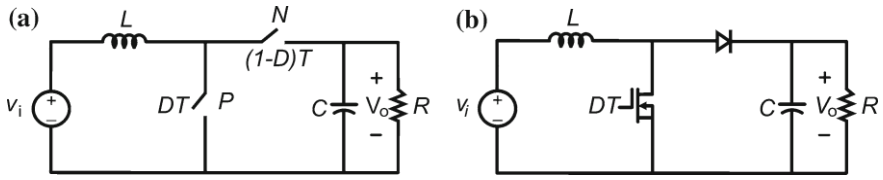

Fig. 2.17 Non-isolated boost (*up*) DC/DC converter: a circuit, and b switch implementation

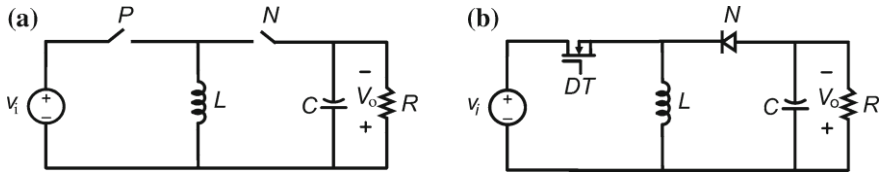

Fig. 2.18 The buck-boost (*up/down*) non-isolated DC/DC converter: a circuit, and b switch implementation

continuous conduction mode (CCM). In this mode, the inductor current never reaches zero and the output voltage-to-input voltage conversion ratio becomes only a function of the duty ratio. If the inductor current is zero for a portion of the cycle, the mode of operation is known as the discontinuous conduction mode (DCM). The converter will operate at DCM when circuit parameters such as inductance is decreased or when the switching frequency is decreased or when the load resistance is increased. Therefore, the output-input conversion ratio is a function of the duty ratio and several of those parameters.

The three basic DC/DC converters discussed so far are referred to as non- isolated converter topologies. Another class of converter is called isolated converters whose utilize a transformer that is placed directly between the input and output and usually have more switches and more filter components than non- isolated converters. Isolated DC/DC converters can be designed to provide multiple output DC voltages. There are some non-isolated converters that use higher order filter such as the Cuk converter, the SEPIC converter and the ZETA converter. For complete types and analysis of non-isolated and isolated converters, please refer to Chaps. 6 and 7 in [1], Chaps. 7 and 10 in [2], Chaps. 4 and 5 in [3] and Chaps. 6 and 7 in [4].

2.1.6.2 DC/AC Converters (Inverters)

Inverters are power electronic circuits that transform DC voltage from sources such as batteries, solar cells or fuel cells (or the output of a rectifier) into AC, for powering motor drives, providing stand-alone AC output, or interconnecting to the AC grid. Inverters can be usually classified according to their AC output as single- phase or three-phase and also as half- and full-bridge converters.

2.1.6.2.1 Single-Phase Inverters

Figure 2.19a represents a generalized DC/AC single-phase inverter. Figure 2.19b shows the resulting AC waveform when the P- and N-switches operate at a $D = 0.5$. The graph shows that the AC waveform is a square wave $D = 0.5$. Further, the voltage has no DC component which can also be shown by substituting $D = 0.5$ in Eq. (2.2). A half-bridge converter can be obtained using two DC sources of equal voltages, one P-Switch and one N-switch as shown in Fig. 2.20. The output is a square wave with a period T, which corresponds to an AC fundamental frequency as:

$$f = \frac{1}{T} \text{ Hz} \quad \text{or} \quad \omega = 2\pi f = \frac{2\pi}{T} \text{ rad/s} \qquad (2.5)$$

The amplitude of the n[th] sinusoidal voltage can be evaluated by Fourier series of the square wave $v_o(t)$ as

$$v_{on} = \frac{2}{T}\int_0^T v_o(t) \sin n\omega_a t dt = \frac{4V_i}{n\pi} \quad \rightarrow n = 1, 3, 5, \ldots \text{odd} \qquad (2.6)$$

A filter such as a resonant LC-type circuit can be designed to filter most of the harmonics present in the square wave and prevent them from appearing across load. The fundamental voltage available from the square voltage has a fixed amplitude (as obtained by substituting $n = 1$ in Eq. (2.6). Half-bridge converters have

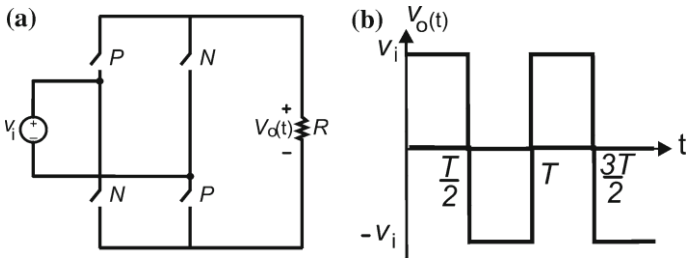

Fig. 2.19 Full bridge (*FB*) DC/AC converter: a circuit, and b waveforms

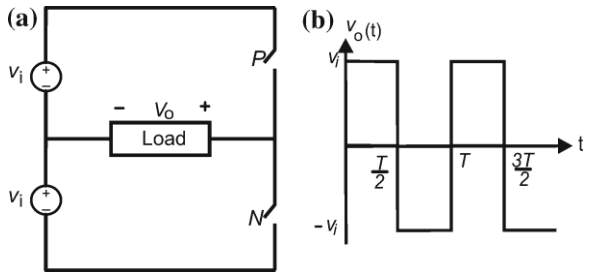

Fig. 2.20 Half-bridge (*HB*) DC/AC converter (inverter): a circuit, and b waveforms

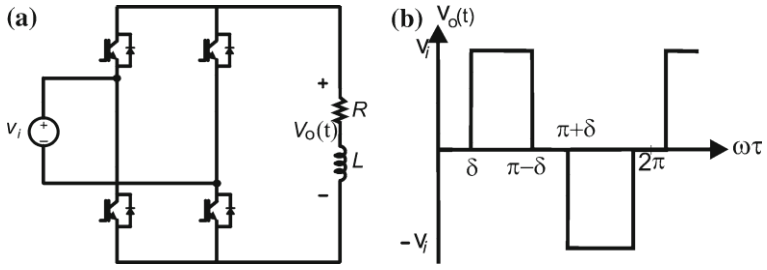

Fig. 2.21 Full-bridge (*FB*) DC/AC converter with variable AC voltage: a circuit, and b waveforms

fixed amplitude, but the full-bridge ones (as shown in Fig. 2.21) do not have this limitation.

Rather than having the voltage v_o to have only two levels V_{dc} or $-V_{dc}$, a third level can be used where the voltage v_o is zero and is called a three-level inverter. The resultant voltage waveform is shown in Fig. 2.21b. The angle d is a phase-shift between the two transistor legs and is used to control the amplitude of the sinusoidal n[th] voltage, as demonstrated by Fourier series of v_o.

$$v_{on} = \frac{4}{T}\int_0^T v_o(t)\sin n\omega_a t \; \mathrm{d}(\omega t) = \frac{4V_i}{n\pi}\cos n\delta \quad \rightarrow n = 1, 3, 5, \ldots \text{odd} \qquad (2.7)$$

It can be seen that by varying δ from zero to π, the output voltage can be varied from a fixed voltage at $\delta = 0$ to zero-voltage at $\delta = \pi$. This δ-control introduces a variable AC voltage and also can eliminate one harmonic voltage as long as Eq. (2.8) is observed.

$$\cos n\delta = 0, \text{ which means } n\delta = \frac{\pi}{2} \qquad (2.8)$$

For example, if the third harmonic voltage is chosen to be eliminated then $d = p/6$. This method of harmonic elimination is known as active filtering contrasted to passive filtering that requires actual filter components. Another method of active filtering is known as harmonic cancellation where harmonics are eliminated by processing waveforms. Figure 2.22shows two converters where both converters are switched at a steady square wave voltage. The output waveforms $v_{o1}(t)$ and $v_{o2}(t)$ of the two converters are shown in Fig. 2.22b. It can be seen that each of the two converters produces a fixed two-level square wave voltage. By shifting the control of one converter by angle d, and adding the two voltage the resulting output voltage $v_o(t)$ is a variable three-level inverter, similar to the one shown in Fig. 2.21. Each of the inverters output contains a third harmonic. However, by adding the two inverters output, the resulting voltage will not have third harmonic voltage if d is chosen to be 30°. Numerous control methods for

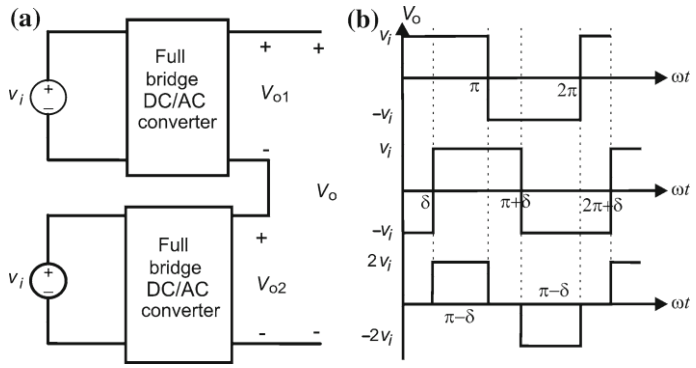

Fig. 2.22 Active filtering using harmonic elimination: a circuit, and b waveforms

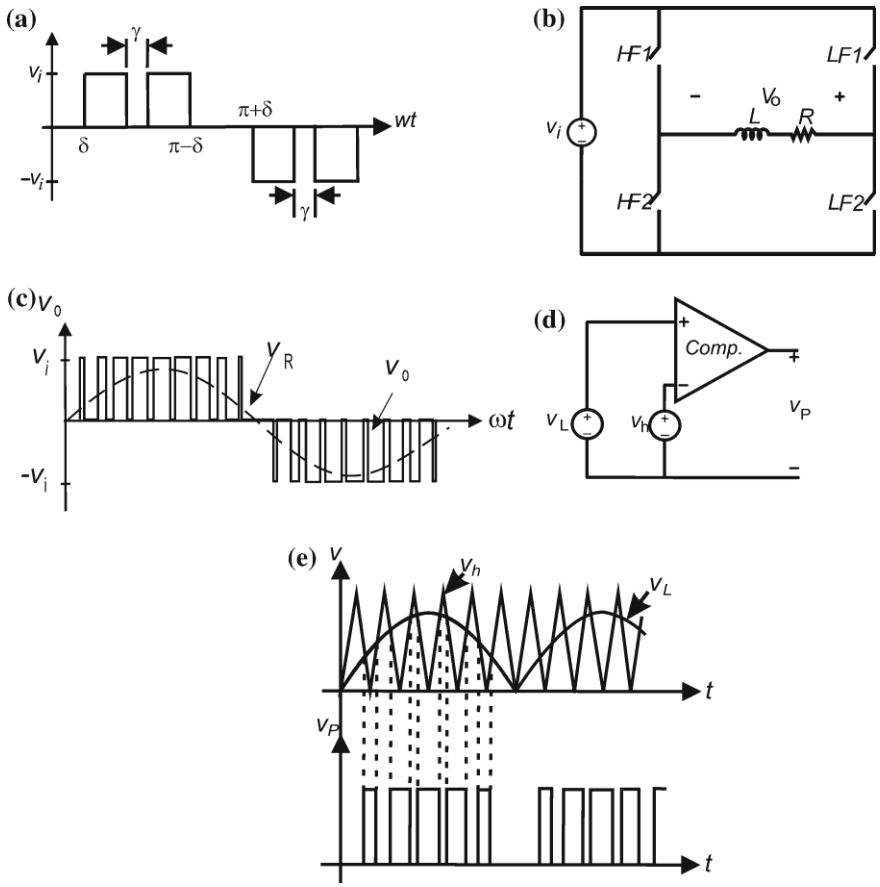

Fig. 2.23 Pulse-width modulation (*PWM*) switching technique: a multiple harmonic elimination, b PWM circuit, c PWM AC output, d PWM generation, and e PWM signal

harmonic elimination and harmonic cancellation have been proposed in the literature. These methods have resulted in two major breakthroughs in active-wave shaping or active filters; namely the method of pulse-width modulation (PWM) and the method of multilevel inverters, which will briefly be discussed later.

The *d*-control method imposes a zero-voltage on the output voltage and if more of the zero-voltage segments are introduced, the harmonic content of the AC voltage can be reduced. For example, if two segments are introduced as shown in Fig. 2.23a, with $d = 30^{\circ}$ and $c = 12°$, then it can be shown that both the third and fifth harmonic voltages can be eliminated [1]. Also, if these zero-voltage regions can be introduced at high frequency (HF) with a variable width that is sinusoidally distributed at the fundamental frequency of the AC voltage, the resulting AC voltage will contain only the fundamental AC component and components at the HF of the *d*-control.

Figure 2.23b shows a converter similar to the full-bridge topology where the switches are controlled at either HF or a low frequency (LF). The HF switches operate at a frequency known as the carrier frequency, which is much higher than the fundamental AC frequency. The LF switches are operated at the fundamental frequency, referred to as the modulating frequency. During the positive half cycle of the LF switches, the HF switches are alternating at the constant carrier frequency with different on-times, i.e., a variable duty ratio. The duty ratio can be obtained by comparing a triangular wave signal at the carrier frequency with a sine wave signal at the modulating frequency, as shown in Fig. 2.23c. The resulting output waveform has a constant frequency with a modulated pulse width, so this technique is called PWM. Although no specific harmonic elimination (or cancellation) is introduced, the unwanted frequencies are pushed to higher frequency decades above the fundamental AC frequency and, as a result, the amount of passive filtering that is required can be minimized.

2.1.6.3 Three-Phase Inverters

Three-phase DC/AC converters can be constructed using single-phase DC/AC converters (one leg branch). Three single-phase inverters can be connected to a common DC source, as shown in Fig. 2.24a. Their switch controls are shifted by 120°, with resulting output voltages shown in Fig. 2.24b. The three outputs can be connected in *Y* or D as shown in Fig. 2.24c. It can be shown that the number of switches for the three independent single-phase bridge converters can be reduced to six switches rather than twelve and this design is shown in Fig. 2.25a and b. This converter design is the standard circuit topology that is used for conversion of DC to three-phase AC. The AC output depends on the control of the six switches. For example, if the switches are controlled with a phase-shift command of 60°, the resulting waveforms are shown in Fig. 2.25c.

When a DC voltage is the input to a converter, the design is defined as voltage- fed inverter (VFI) or voltage source inverter (VSI). When a DC current is the input to a converter it is defined as either a current-fed inverter (CFI) or current source inverter (CSI) as depicted in Fig. 2.26. The CSI operation constraints are: (1) there must always exist a current path for the current source; (2) the output phases cannot be short-circuited. The DC current is unidirectional, and only two switches conduct at same time providing the path for current circulation. The switch types for this design must be fully controlled in current and bidirectional in voltage. Switches that meet this requirement include: SCR, GTO, and the recently introduced IGBT.

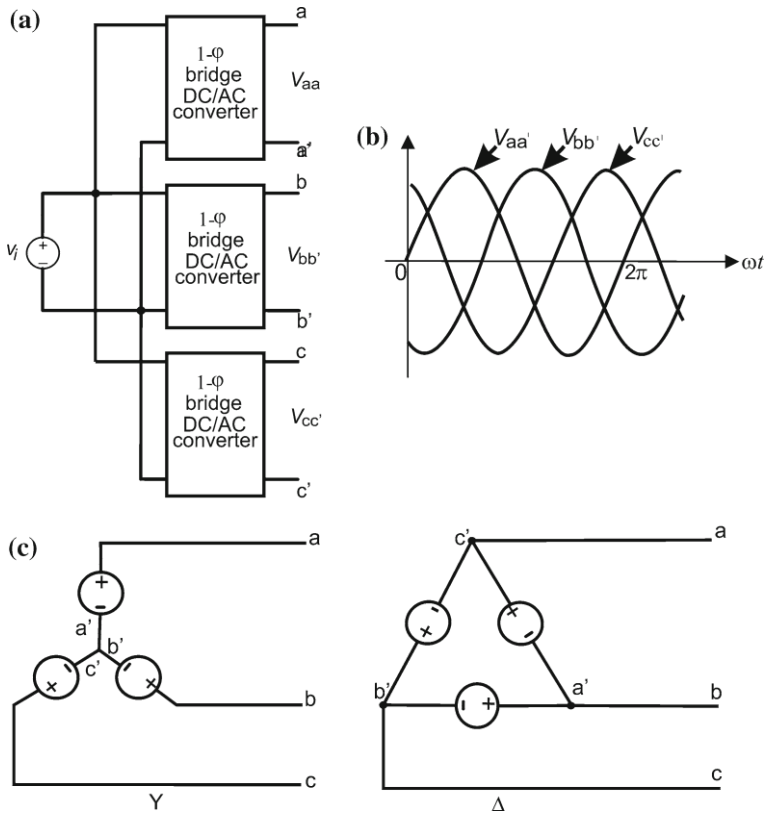

Fig. 2.24 Three-phase AC/DC converter: a circuit, b waveforms, and c connections

2.1.6.3.1 AC/DC Converters (Rectifiers)

AC/DC converters are called rectifiers circuits, which can be broadly classified based on the type of AC source and the type of semiconductor switch is used as shown in Fig. 2.27. Rectifiers are usually used in either single-phase orthree-phase applications, but multi-phase topologies are possible for high power applications. Switches that are used in rectifier's designs can be either uncontrolled (diode) or controlled devices (thyristor). Single-phase rectifiers can be classified as

either half-wave or full-wave circuits. Three-phase rectifiers are classified based on the number of pulses of the rectified output voltage, i.e., 3-pulse rectifiers, 6-pulse, 12- pulse, or more generally 3 9 2^n-pulse (where $n = 0, 1, 2, 3\ldots$). The number of pulses is the ratio of the fundamental frequency of the rectifier output to the frequency of the AC input.

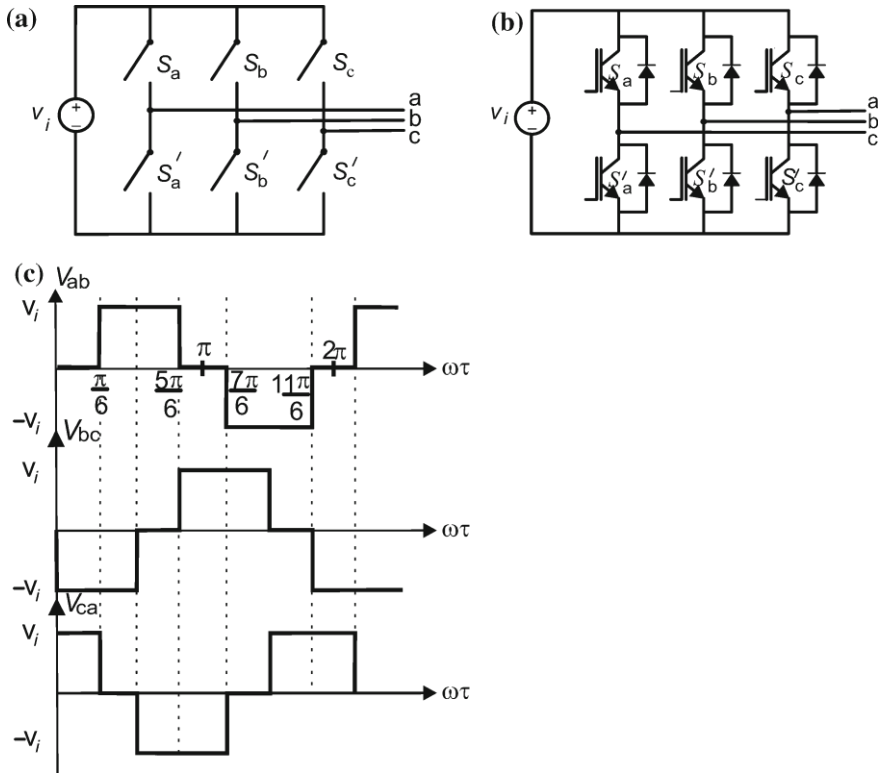

Fig. 2.25 Six-step inverter and waveforms: a circuit, b switch implementation, and c waveforms

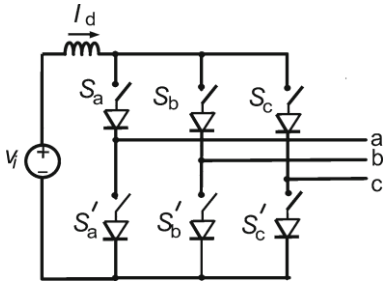

Fig. 2.26 Current source inverter (*CSI*)

2.1.6.3.1 Single-Phase Rectifiers

A general circuit for a single-phase rectifier is illustrated in Fig. 2.28. Note that this design is the same as the generalized DC/DC converter shown in Fig. 2.14 except that a sinusoidal voltage replaces the input DC source. The basic single- phase rectifier circuits are completed by setting the P- and N-switches to be either permanently closed or open. For example, if all the N-switches are permanently open and the bottom P-switch is permanently closed, the resulting circuit is a half-wave rectifier circuit. If the remaining P-switch is a thyristor, then the resulting circuit is a controlled half-wave rectifier. A depiction of this topology is shown in Fig. 2.28b and resulting waveforms are shown in Fig. 2.28c. In such case, the angle *a* is the thyristor turn-on delay angle, which is measured starting at the zero- crossings of the input voltage source.

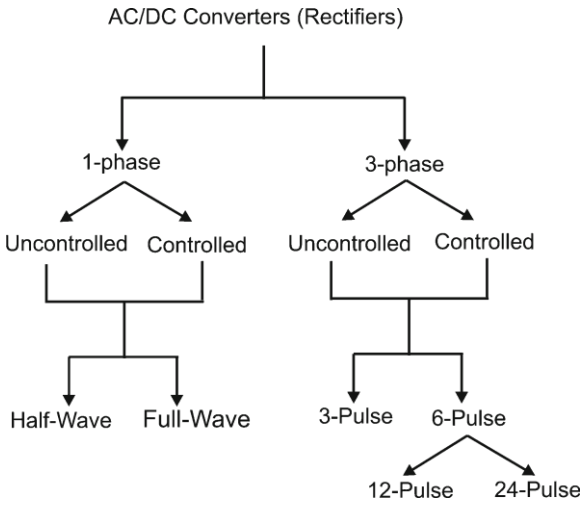

Fig. 2.27 Classifications of rectifier circuits

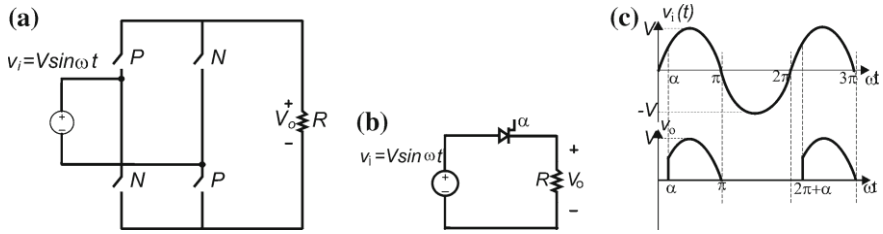

Fig. 2.28 a General 1-phase rectifier circuit, b 1-phase controlled rectifier, and c Input and output voltage waveforms

The output waveform has an average value (the required DC component), which can be calculated using Eq. (2.9) as,

$$V_{\text{avg}} = \frac{1}{T}\int_0^T v(t)\,\mathrm{d}t = \frac{1}{2\pi}\int_\alpha^\pi V\sin\omega t\,\mathrm{d}(\omega t) = \frac{V}{2\pi}(1+\cos\alpha) \qquad (2.9)$$

Equation (2.9) shows that the value of the DC voltage can be varied as *a* is changed. A half-wave uncontrolled rectifier is possible when the remaining P- switch is implemented through the use of a diode; this circuit is the same as in

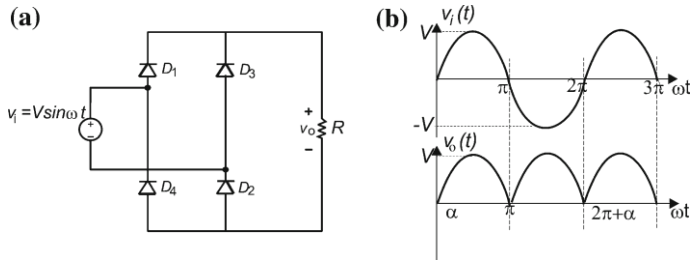

Fig. 2.29 Examples of uncontrolled rectifiers: a full-bridge (*FB*), and b waveforms

Fig. 2.28b except the thyristor is replaced by a diode. Since the diode is an uncontrolled switch, *a* is set to zero and the diode will turn-on at the zero-crossings of the supply voltage. When $a = 0$ is substituted into Eq. (2.9) then average voltage is given as:

Equation (2.10) shows that the DC voltage is fixed and cannot be changed and as a result this type of rectifier is defined as uncontrolled.

If all the switches of Fig. 2.28a are used, then the resulting circuit is a full-wave rectifier as shown in Fig. 2.29a. When all the switches are diodes, the resulting waveform is illustrated in Fig. 2.29b. The DC voltage in a full-wave rectifier design will be double the one from the half-wave rectifier.

There are circuit topologies, such as one-quadrant, two-quadrant, and four- quadrant, for half- or full-wave types. Some of them are uncontrolled, and others are fully controlled depending on the combination of diodes and thyristors, which are usually classified as semi-controlled or hybrid rectifiers. Some rectifiers use transformers for isolation for further rectification capability [1, 2].

$$V_{avg} = \frac{1}{2\pi}\int_0^{\pi} V \sin \omega t \, \mathrm{d}(\omega t) = \frac{V}{\pi} \qquad (2.10)$$

2.1.6.3.4 Three-Phase (3-U) Rectifiers

As mentioned in the classification of three-phase rectifiers, the output is defined in terms of the number of pulses per one cycle of the input voltage. The 3-pulse rectifier is a basic three-phase rectifier circuit (connected to a three-phase system), and can be used as building block for most of other three-phase rectifiers. Each of the three-phase input voltages can be determined using Eq. (2.11). The operation of a three-phase 3-pulse rectifier is shown in Fig. 2.30a, b.

$$\begin{aligned} v_a &= V \sin \omega t \ \text{V} \\ v_b &= V \sin(\omega t - 120°) \ \text{V} \\ v_b &= V \sin(\omega t + 120°) \ \text{V} \end{aligned} \qquad (2.11)$$

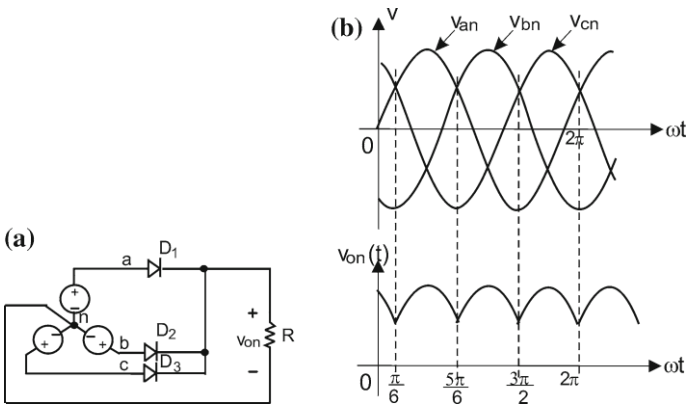

Fig. 2.30 three-phase, 3-pulse rectifier circuit: a circuit and b waveforms

In this case the switches are implemented with diodes (uncontrolled rectifier). A diode will turn-on when its voltage is higher than the other two diodes, i.e., the diode connected to the highest of the three voltages will conduct. The resulting output is shown in Fig. 2.30b; notice that the diode conduction starts and ends when two of the three voltages are equal. Also, each diode conducts for an angle of 120°, and the output voltage has 3 pulses, during one cycle of the input. Therefore, the fundamental frequency of the output voltage is three times the frequency of the input voltage. The DC component of the output of each of them can be calculated by the average over its period as:

$$V_{avg} = \frac{1}{(2\pi/3)} \int_{\frac{\pi}{6}}^{\frac{5\pi}{6}} V \sin \omega t \, d(\omega t) = \frac{3\sqrt{3}V}{2\pi} \qquad (2.12)$$

The DC voltage, given by Eq. (2.12), is higher than the output voltage of a single-phase full-wave rectifier. Of course, the drawback is the need of a three- phase source, which is most common for industrial applications.

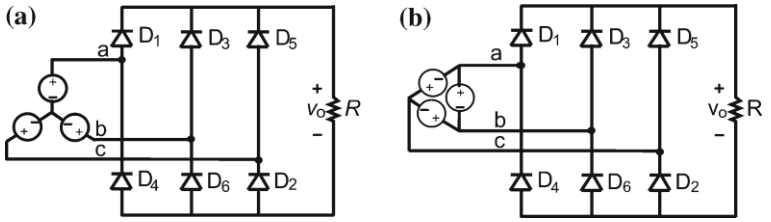

Fig. 2.31 6-pulse rectifier circuits: a *Y*-connected source, and b D-connected source

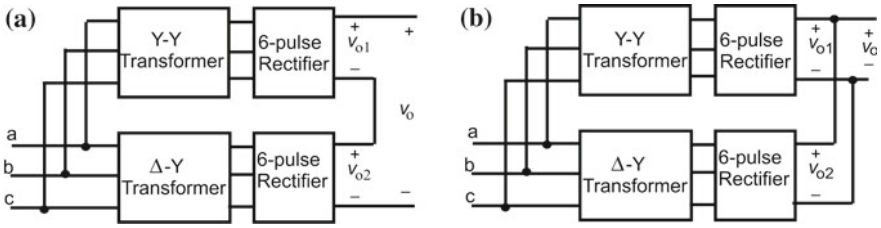

Fig. 2.32 12-pulse rectifier circuits: a high voltage 12-pulse rectifier, and b high current 12- pulse rectifier

If two 3-pulse rectifiers are connected the resulting topology is shown in Fig. 2.31. This circuit is known as a 6-pulse rectifier, and it is the building block for all high power multiple-pulse rectifier circuits.

Two 6-pulse rectifier circuits can be connected through the use of Y-Y and D-Y transformers for building 12-pulse rectifiers. If the two rectifiers are connected in series, the resulting circuit is shown in Fig. 2.32a and is suitable for high voltage, whereas the converter is connected in parallel as shown in Fig. 2.32b, the circuit is suitable for high current.

2.1.6.3.5 Controlled Rectifiers

When diodes are replaced by thyristors, the three-phase rectifier circuit becomes a controlled one, and the delay angle *a* (measured relative to the time where the diodes start to conduct) will control the output voltage. Similar to single-phase rectifiers, there are combinations of switches and transformers that result in higher pulse three-phase rectifiers. For complete understanding on the types and analyses of single-phase and three-phase rectifiers, the reader is referred to Chaps. 4 and 5 of reference [1], Chap. 7 of reference [2], Chaps. 5 and 6 of reference [3], and Chaps. 4 and 5 of reference [4].

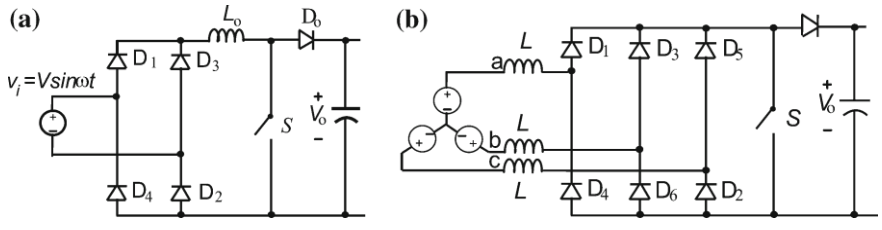

Fig. 2.33 PWM rectifier: a single-phase, and b three-phase

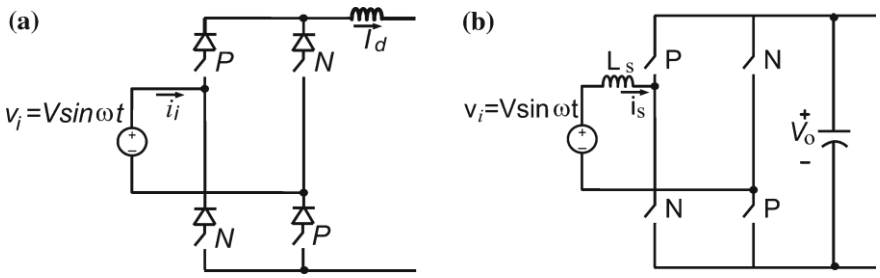

Fig. 2.34 Single-phase PWM rectifiers

2.1.6.3.6 PWM Rectifiers

PWM rectifiers can be implemented as unidirectional or bidirectional as regarding their power flow capabilities. A basic unidirectional boost version consists of an uncontrolled diode bridge followed by a boost converter as shown in Fig. 2.33a. When the switch is ON the inductor current increases proportionally to the input voltage (which is sinusoidal). When the switch is OFF, the inductor current decreases, and its energy is transferred to the capacitor, repeating such cycle with variable input voltage. The boost converter regulates the capacitor voltage, and also impresses a sinusoidal input current profile, which improves the input power factor. Since this converter can operate in either Continuous Conduction Mode (CCM) or in Discontinuous Conduction Mode (DCM), its control should be designed to be stable and work in both conditions. A three-phase version of the unidirectional boost rectifier is shown in Fig. 2.33b, but the inductors are connected at the AC side.

In order to implement a bidirectional converter fully controlled switches replace the diodes, as shown in Fig. 2.34a. This topology is called a current source rectifier (CSR). In this design, the output voltage, V_0, is smaller than the amplitude of the input voltage, V, as indicated in Eq. (2.13). Therefore, the CSR is also defined as a Buck Rectifier, where the objective is to provide a constant current I_d at the output.

$$V_0 < \frac{\sqrt{3}}{2} V \qquad (2.13)$$

The boost function is possible by connecting the boost converter inductor on the AC side, as shown in Fig. 2.34b. When the AC voltage is positive and the switch T_2 is ON, the inductor current increases proportionally to the AC voltage and when T_2 turns-off the inductor energy is pumped to the capacitor via diodes $D1$ and $D4$. Similarly, when the AC voltage is negative $T4$ is turned-on. When it turns-off the energy flows via diodes $D2$ and $D3$. This topology is known as the voltage source rectifier (VSR). In VSR the output voltage, V_0 is greater than the amplitude of the input voltage, V, as indicated in Eq. (2.14).

$$V_0 > V \qquad (2.14)$$

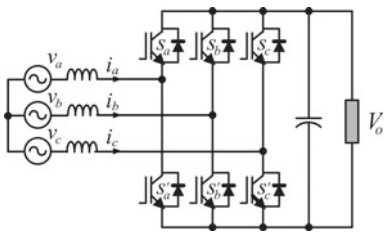

Fig. 2.35 Implementation of the three-phase VSR

The VSR is also known as Boost Rectifier with objective to provide a constant voltage V_0 at the output. The CSR and the VSR are dual from each other. Figure 2.35 shows the implementation of a three-phase version of the PWM VSR (with IGBTs). The VSR requires a large capacitor across the output, it is inherently bidirectional and can be applied in several applications where the line side converter must be able to deliver energy back to the source, such as in locomotives, cranes, and renewable energy sources connected to the DC link side.

2.1.6.4 AC/AC Converters

AC/AC converters are used to interconnect AC sources, for example from single- phase or a three-phase source to single-phase or a three-phase source. In applications that require variable AC such as light dimmers and AC motor drives, energy is converted from a FVFF to a single-phase or three-phase VVFF or VVVF. A very simple AC/AC converter circuit, to regulate the AC power for a resistive load is shown in Fig. 2.36a and the waveform shown in Fig. 2.36b. This circuit is known as AC controller, which converts from single-phase AC FVFF to VVFF single-phase AC. The fundamental frequency of the input and output is the same. By varying the switch turn-on delay angle, *a*, the amplitude of the fundamental voltage is varied. Typical applications of this circuit are light dimmers and single-phase motor drives used in home appliances. The switch implementation is usually a

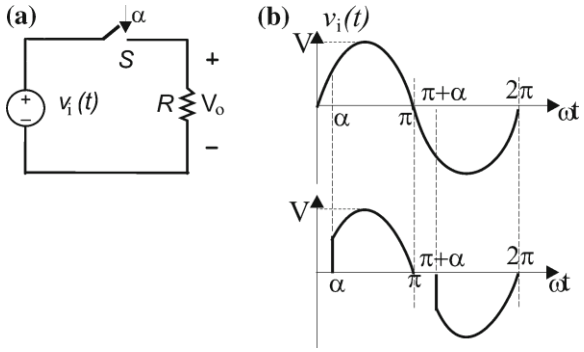

Fig. 2.36 Variable voltage fixed frequency (*VVFF*) AC/ AC converter

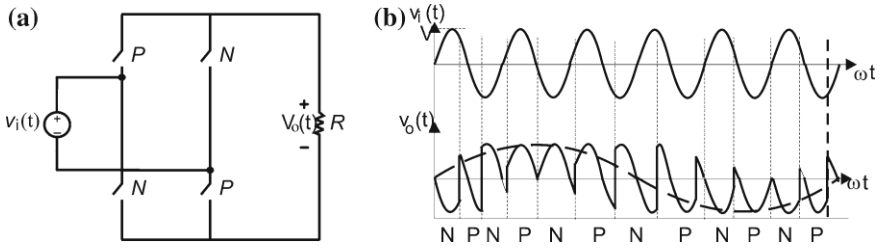

Fig. 2.37 Cyclo-converter as VVVF AC/AC converters

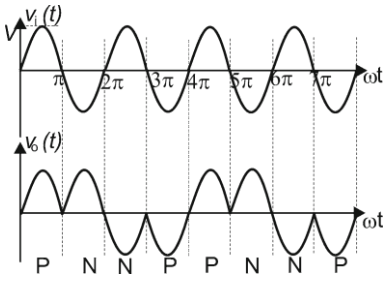

Fig. 2.38 Integral-cycle control for (VVVF) AC/AC converter

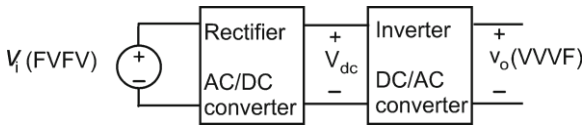

Fig. 2.39 FVFF to VVVF AC/AC converter through a DC link

triac (combination of two SCR's in anti-parallel) controlling the positive half cycle of the AC source with one thyristor and the negative half cycle with the other one. The circuit shown in Fig. 2.37a is a general AC/AC converter, referred to as a cyclo-converter. The switches can be controlled to produce an output voltage with variable amplitude and variable frequency. This is referred to as VVVF output as shown in Fig. 2.37b [1]. The P- and the N-switch are controlled to achieve an output voltage at a frequency lower than the input frequency. Another possible approach for controlling AC/AC converter is known as integral-cycle control, as shown by the waveforms in Fig. 2.38, exemplifying a case where the fundamental frequency of the output is twice the input [2].

AC/AC conversion can also be obtained by cascading an AC/DC converter with a DC/AC converter, as shown in Fig. 2.39; the approach is known as ''DC link conversion'' approach. The implementation of this converter with IGBTs is shown in Fig. 2.40. This design allows two-way energy flow and four-quadrant operation and is usually applied to motor drives, electric power generation using asynchronous machines, energy storage systems (such as batteries, UPS, and flywheel energy systems), and the connection of two independent grids. Because a CSR can

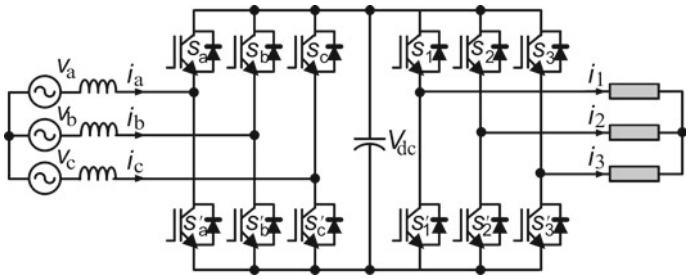

Fig. 2.40 Implementation of a FVFF to VVVF AC/AC converter through a DC link

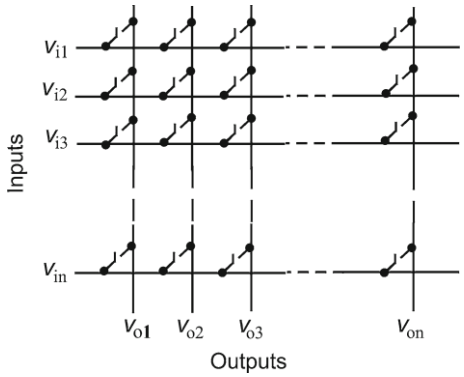

Fig. 2.41 Generalized matrix converters

be modeled as a controllable DC current source, the natural load is a CSI that supports a FVFF to VVVF AC/AC converter through an inductive DC link.

2.1.7 Advanced Converter Topologies

Several advanced circuits have been developed and the field of PE is still an emerging and rapidly growing field with new converters. Some of those topologies are application-specific and will be discussed in the next sections.

2.1.7.1 The Matrix Converter

A matrix converter consists of a multi-input multi-output switching matrix that can represent all the switching converters. It can be considered as a fully controlled four-quadrant bidirectional switch, which allows HF operation. Figure 2.41 has an example of a matrix converter with n-inputs and m-outputs. Figure 2.42a shows a specific case where $n = m = 3$, i.e., a three-phase to three-phase AC/AC

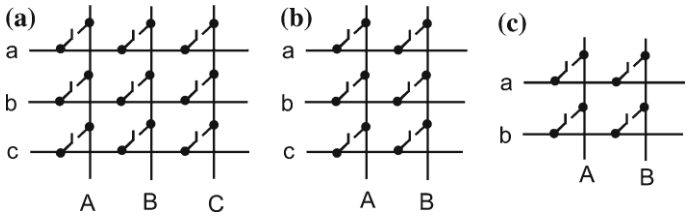

Fig. 2.42 Examples of converters derived from the matrix converter: a AC/AC, b AC/DC, and c AC/DC and DC/DC

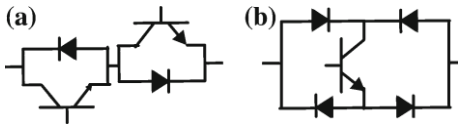

Fig. 2.43 Implementation of a fully bidirectional switch

converter, while Fig. 2.42b shows the case for $n = 3$ and $m = 1$, which can be either a three-phase AC/DC converter or a DC to three-phase AC converter. Figure 2.42c shows the converter for $n = m = 1$ (i.e., any DC/DC converter, single-phase AC/DC converter, or DC to single-phase AC converter).

The bidirectional voltage and current switch can be made of diodes and con- trolled switches as indicated in Figs. 2.43a, b. A three-phase AC to AC converter is shown in Fig. 2.44. Although the matrix converter topology has been around for quite some time, it has gained attention in many applications because of the recent availability of switching power electronic devices and controllers.

2.1.7.2 Multilevel Inverters

Multilevel inverters are AC/DC converters where a series connection of power electronic devices and split capacitors allow high voltage applications. These inverters are modulated in a way such that the output voltage resembles a staircase

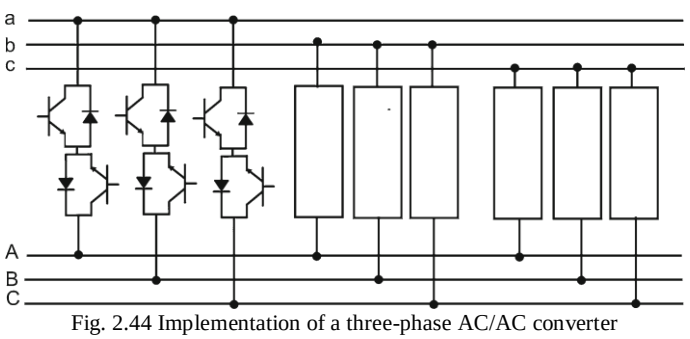

Fig. 2.44 Implementation of a three-phase AC/AC converter

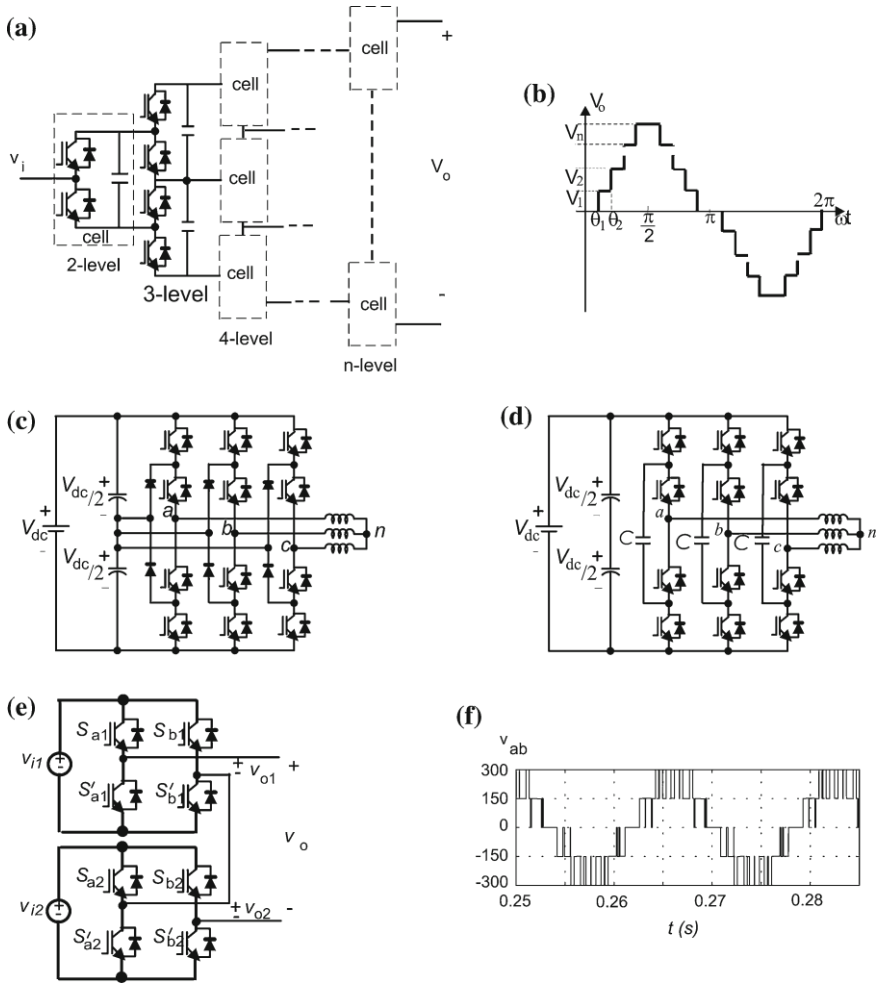

Fig. 2.45 Multilevel inverter: a generalized multi-level converter, b generalized waveforms, c NPC inverter, d flying capacitor inverter, e H-bridge cascaded inverter, and f NPC line voltage waveform

as shown by the generalized multilevel inverter in Fig. 2.45a. A three-level converter consists of series capacitor with a center tap as the neutral where each phase leg of the converter has two pairs of switching devices in series. As the number of levels increase, the synthesized output waveform adds more steps, producing a more refined staircase wave with minimum harmonic distortion, as shown in Fig. 2.45b. Of course, a zero-harmonic distortion of the output wave can be obtained by an infinite number of levels. More levels also mean that series device can provide higher output voltages without any device voltage-sharing problems. Such multiple switches and circuits usually make multilevel inverters more expensive than two-level inverters and are cost-effective only for very specific utility and transmission or distribution power system applications. Different multilevel inverter topologies can be developed from the basic circuit of Fig. 2.45, for example the Diode Clamped (or Neutral-Point Clamped, NPC), and of the Capacitor Clamped or flying capacitor (FC) inverters, as shown in Fig. 2.45c, d, respectively, for three-level inverters. Another popular configuration is the Cascaded H-Bridge, with separate DC sources that is evolved from the two-level inverter, shown in Fig. 2.45e for five-level inverter. All these inverters can also be controlled by PWM techniques [5, 6], of which one example is shown in Fig. 2.45f for the three-level NPC inverter.

2.1.8 Control of Power Converters

There are several objectives in the applications of the power converters, such as control of grid voltage, control of current, control of DC link voltage or current, as load or DC connection, control of AC load voltage or current, control of harmonics, control of speed, and so on. The control strategy applied to these cases often deal with the regulation of two variables with different dynamics, one is probably slow and another fast. Examples are: (1) for a rectifier: capacitor voltage (slow) and grid current (fast), (2) for a motor drive: motor speed (slow) and motor current (fast), (3) grid connected inverter: output current (slow) and input voltage (fast).

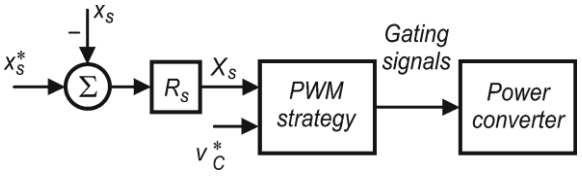

Fig. 2.46 Slow variable controller

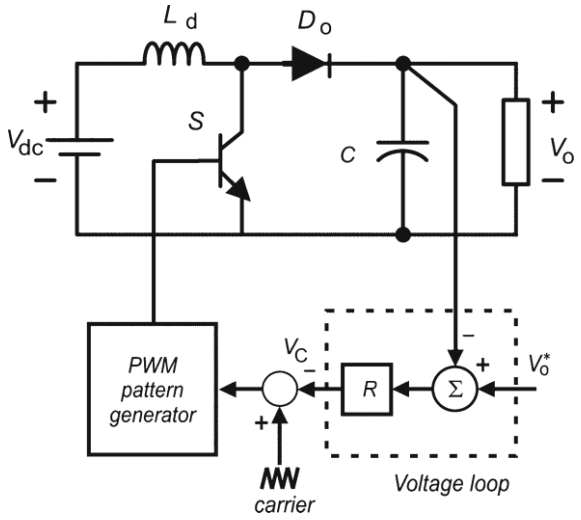

Fig. 2.47 Voltage control of a boost converter

This section will only consider the control of voltages and currents. Figure 2.46 shows a typical PWM control for a slow variable, defined as X_s is compared with its reference X_s^m. The resulting error is regulated by the slow variable regulator, R_s: This regulator has a dynamic performance such as D is directly adjusted so that the slow variable remains regulated. This scheme can be directly applied to DC/DC converters. An example is for a boost DC/DC converter shown in Fig. 2.47, where the objective is to regulate the output voltage, V_O: For this, the error between the reference and the actual output voltage typically feeds a proportional-integrative (PI) regulator, R. The output of the regulator, the voltage control X_s v_c is compared to the carrier signal to produce a direct duty ratio PWM control. This type of control can also be employed when only one variable is controlled, such as the voltage in the PWM VSI, and the current in the PWM CSI.

The control scheme can be generalized by using a cascaded strategy, in which any external (slow variable) control defines the reference for an internal (fast variable) control. This kind of control is most often stable since both loops have different dynamics. In order to ensure a desired fast variable profile, the output of regulator R_s is synchronized with a template signal to define the internal control reference, x_f^m: As an example, for obtaining near unity power factor operation, the PWM input line current pattern is synchronized with the grid voltage. This can be achieved in two ways: (1) the grid voltage, after filtering, can be used directly as a template for current, or (2) the zero crossing of the grid or the capacitor voltage can be used as a synchronization signal.

Two schemes for internal control will be now considered: the first one is shown in Fig. 2.48, where x_f is compared with the internal loop reference, x_f^m; in order to generate the gating pulses. Considering only CCM operation, this comparator can:

(1) employ hysteresis (bang–bang) techniques, in which the regulated variable is maintained inside a tolerance band; (2) compare directly x_f^m and x_f, and (3) compare the integral of x_s with x_f^m: These three principles are indicated in Fig. 2.49 when the controlled variable is the current and the template is a sinusoidal waveform. In the hysteresis technique shown in Fig. 2.49a the measured current is compared with a tolerance band around the reference. The corresponding switch is turned-on when the current reaches the lower limit of the band, Imm in; and is turned-off when the actual current reaches the upper

limit of the band, Imm ax. The switching frequency varies along the current waveform. Different from the previous technique, case (2),

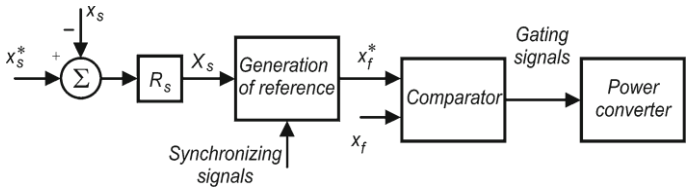

Fig. 2.48 Block scheme for both slow and fast variable control

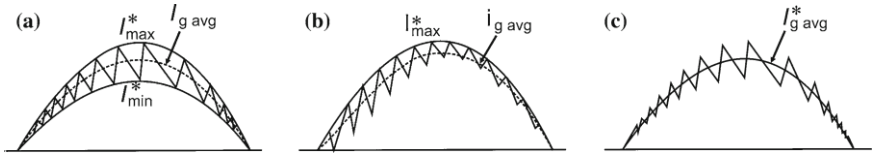

Fig. 2.49 CCM: a hysteresis control, b current peak control, and c average current control

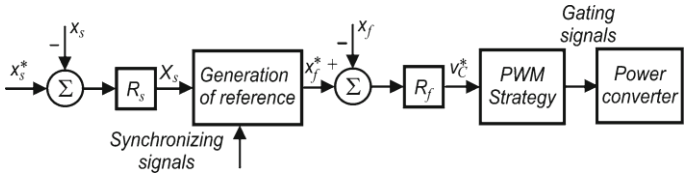

Fig. 2.50 Generalized control strategy applied to power converters

Fig. 2.49b, operates with constant switching frequency: the corresponding switch is turned-on by a clock at the beginning of each switching interval and is turned-off when the actual current tries to go beyond the reference. This technique is known as current peak control. In Fig. 2.49c the measured current is integrated so that its average value can be compared with the current reference. For this reason, this approach is known as average current control. For more information on these and other current control schemes the reader is referred to [7– 9].

A possible scheme is given in Fig. 2.50 where the control error is regulated by the regulator R_f, whose output furnishes the modulating signal to be applied to the chosen PWM strategy.

Consider, as an example, the control of the PWM VSR circuit, as shown in Fig. 2.51. In this case, the output voltage and the grid current are the main objectives of the converter control. In the scheme of Fig. 2.51, x_s is the capacitor

voltage and x_f is the grid current.

The scheme in Fig. 2.51 includes a fast current controller, a slow DC voltage controller, such as PI, P, Fuzzy or other, and a PWM generator. Since, for power factor control, the input current reference, i^{m}; must be sinusoidal, and the voltage controller output is multiplied by a sinusoidal signal (template signal) with the same frequency and the same phase-shift angle of the mains supply. This template is used to produce the PWM pattern that forces the input currents to follow the desired current template I^{m}: This voltage source current controlled PWM rectifier is simpler and more stable than the voltage source voltage controlled PWM rectifier method. Its stability can be ensured by adequate choice of the controller gains [9].

Other control strategies such as the space vector scheme are also used (Fig. 2.52). In this case the voltage controller provides the value of the reference of the *d* component current, X_d^{m}; while the reference of the *q* component current, X_q^{m}; is fixed to zero in order to obtain unitary power factor. These references are compared with the input currents that are represented in *d-q* coordinates.

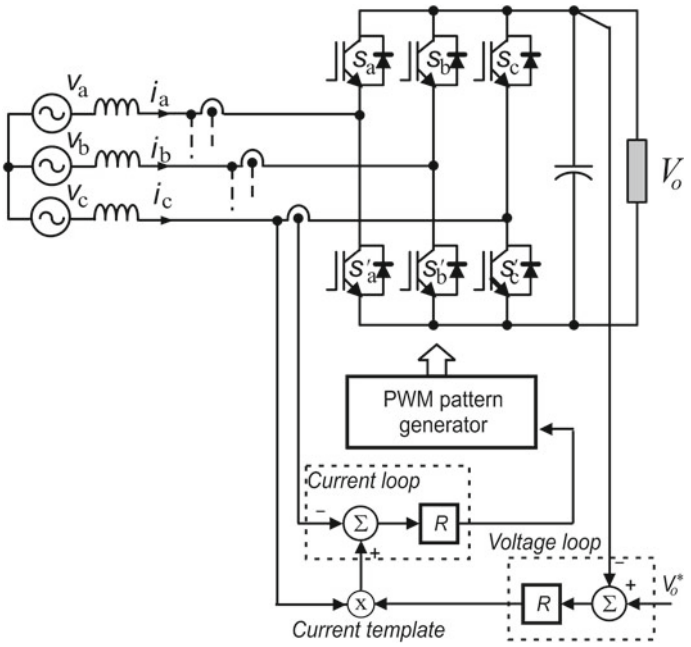

Fig. 2.51 Voltage current controlled PWM rectifier

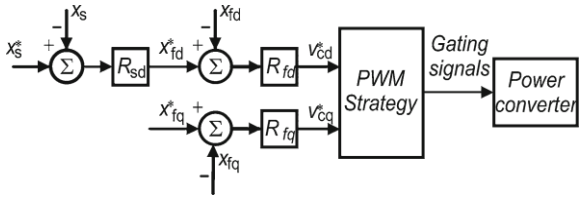

Fig. 2.52 Space-vector control scheme

Two controllers, typically PI, give the control values v_{cd}^m and v_{cq}^m that generate the PWM pattern which controls the VSR. The inverse transformation *dq/abc* allows for obtaining the gate drive pulses for the switches.

An important point is that the current controller can be modified by other signals like the signal of balancing capacitor voltages in NPC multilevel converter.

2.1.9 Pulse Width Modulation

A PWM pattern is essential in the schemes shown in Figs. 2.46, 2.48, and 2.52. The following sections will present more advanced PWM strategies that are used in control of DC/DC and DC/AC converts. The PWM strategies will be applied to a three-phase PWM VSI and then used for a PWM CSR. It will also be indicated how these strategies can also be applied to three-phase PWM CSIs and PWM VSRs.

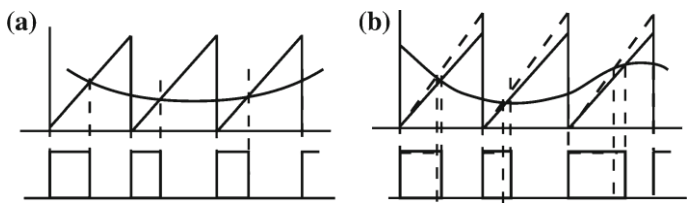

Fig. 2.53 Two principles of PWM modulators: a variation of the control voltage and saw-tooth carrier with constant slope, and b variation of the carrier amplitude

2.1.10 PWM Techniques for DC/DC Converters

The most popular DC PWM is the voltage-mode control. It is obtained by com- paring a saw-tooth (carrier) with a control voltage (modulating signal). The adjustment of the control voltage allows adjustment of the output pulse width and is shown in Fig. 2.53a. As the control voltage is increased or decreased, the *D* is increased or decreased, causing an increase or decrease in the converter output voltage. For this reason, the voltage-mode control is also called duty-cycle control, which is largely employed to control DC/DC power converters. The pulse-width control can also be obtained by varying the carrier amplitude as shown in Fig. 2.53b. For digital implementation, a digital comparator and the modulating signal are replaced by a sampled signal [8].

2.1.11 PWM Techniques for Two-Level Voltage Source *Converters*

PWM has been the subject of intensive research and is widely employed to control the output voltage of static power converters. A large variety of feed forward and feedback control schemes has been described in the literature [5, 10], such as the Selective Harmonic Elimination PWM, but the most widely used methods of PWM are the sinusoidal pulse-width modulation (SPWM), the non-sinusoidal carrier PWM techniques, the space vector modulation (SVPWM), and the hybrid PWM (HPWM) [11].

Although most of comments in the following will be addressed to the VSIs, PWM rectifiers are very important because of several advantages such as: regulation of input power factor to unity, minimum harmonic distortion of input line currents, near sinusoidal current waveforms, precise regulation of output DC voltage, and bi-directional power flow.

The PWM techniques discussed for the VSI can be directly applied to the VSR or Boost Rectifier. Although the basic operation principle of VSR consists in keeping the load DC link voltage at a desired reference value, the PWM scheme for the VSR must provide an adjustable modulation index for the DC voltage

control in addition to the reduction in the total harmonic distortion at the input current, mainly by controlling the input power factor.

2.1.11.1 Selective Harmonic Elimination PWM

Selective harmonic elimination (SHE) PWM can be explained from the output voltage waveform in Fig. 2.54, obtained by operating the circuit in Figs. 2.3 and 2.19, with 2Vi Vdc and four extra commutations per cycle in relation to the square wave. The choice of the values of the angles a1 and a2 allows to eliminate or reduce two selected harmonics in the square-wave form. The Fourier analysis of the waveform given in Fig. 2.19 allows for determining the amplitude of the fundamental and harmonic voltage content of the pole voltage waveform, that is,

$$V_{ao(n,m)} = \frac{4}{\pi}\frac{V_{dc}}{2}\left(\frac{1 - 2\cos n\alpha_1 + 2\cos n\alpha_2}{n}\right) \qquad (2.15)$$

Specific harmonics will be eliminated when the numerator of Eq. (2.15) is set equal to zero for a given value of *n*. For example, the third and fifth harmonics are the largest present in the square-wave voltage, and because they are relatively close to the fundamental frequency they are also the most difficult to filter. Their elimination is obtained by solving two trigonometric equations issued from (2.15), assuming that $0^\circ<a_1<90^\circ$; $0^\circ<a_2<90^\circ$ and $a_1<a_2$; which results in

$$\alpha_1 = 23.62^\circ \qquad (2.16)$$

$$\alpha_2 = 33.30^\circ \qquad (2.17)$$

However, in most multiple phase circuits the third harmonics and multiples are eliminated by connections that include the addition of the two ‘‘notches’’ in the voltage waveform can eliminate the fifth and seventh harmonics, allowing for no harmonics below the eleventh on the inverter output voltage waveform. The angles a_1 and a_2 for this case are

$$\alpha_1 = 16.25^\circ \tag{2.18}$$

$$\alpha_2 = 22.07^\circ \tag{2.19}$$

More harmonics can be eliminated by the introduction of additional notches.

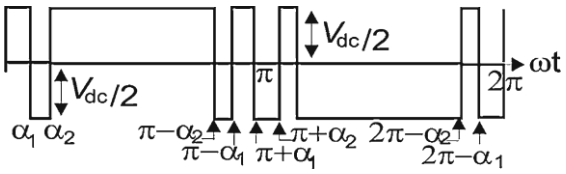

Fig. 2.54 Selective harmonic elimination PWM

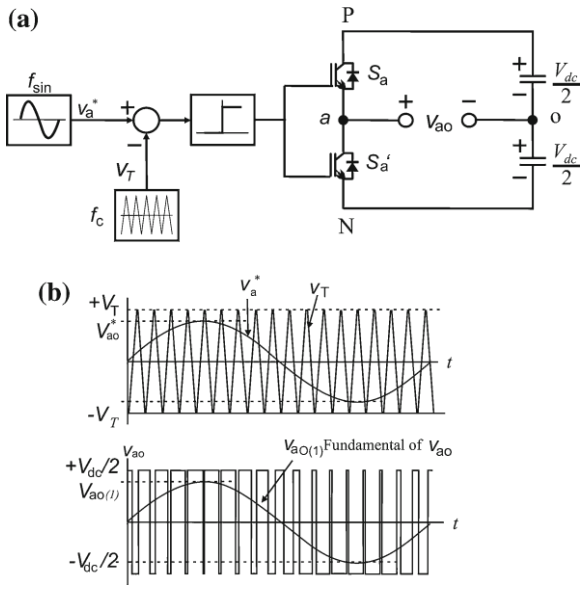

Fig. 2.55 Sinusoidal PWM a bipolar voltage switching for half-bridge inverter, b control signals (*upper*) and pole voltage (*lower*)

2.1.11.2 Carrier Modulation

In Sect. 2.3, a modulated pulse width is obtained by comparing a triangular wave at the carrier frequency with a sine wave signal at the modulating frequency. This technique is known as Sinusoidal PWM [1, 3, 5, 12). Its principle is shown in Fig. 2.55a, b, for a half-bridge inverter. When the modulating signal, v^*_a; is higher

than the carrier signal, v_T; the upper switch is turned on and the inverter leg assumes a switching state ‘‘P’’. The pole voltage is then equal to V_{dc}=2: When the modulating signal is lower than the carrier signal, the lower switch is turned-on, and the inverter leg assumes a switching state ‘‘N’’. The pole voltage is then equal to V_{dc}/2:

The ratio between the amplitudes of the sine wave and the carrier signals is defined as amplitude modulation ratio m_a; and that between the carrier frequency and the modulating frequency is defined as the frequency modulation ratio, m_f: In order to avoid the effects of sub-harmonics m_f should be an odd integer.

When m_f is high enough, the amplitude of the fundamental frequency component of the pole voltage, V_{ao}; in Fig. 2.55a is linear with the variation of m_a; that is,

$$V_{Ao1m} = m_a \frac{V_{dc}}{2} \qquad (2.20)$$

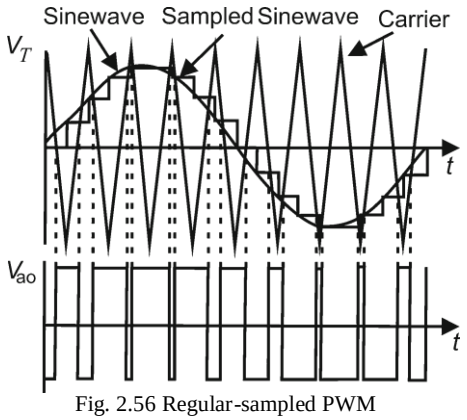

Fig. 2.56 Regular-sampled PWM

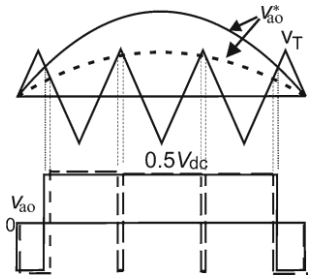

Fig. 2.57 Operation in over modulation region

Also, the harmonics of the output voltage waveform appear centered around harmonics m_f; $2m_f$ and so on, as sidebands.

The pulses are almost centered inside the switching interval; the use of high switching frequencies to improve this location can be avoided by sampling the signals as done for the regular sampled modulation (RSPWM) [13] shown in Fig. 2.56. Nevertheless, sinusoids will continue to be used in the examples that follow.

A value of m_a>1 causes over modulation with a reduction in the number of pulses in the pole voltage v_{ao1} waveform, as shown in Fig. 2.57, and loss of linearity. However, the addition of an adequate zero-sequence component, either continuous or discontinuous, to each of the pole voltage reference waveforms makes possible to increase in 15.5 % the fundamental of the output voltages [14]. Figure 2.58 shows an example of the third harmonic injection PWM (THIPWM), which is somewhat flattened on the top [15]. Injection of other zero-sequence components makes possible to generate different PWM strategies such as Symmetrical PWM and Discontinuous PWM [5, 14–20].

The above concept can be expressed in terms of the sinusoidal reference plus a zero-sequence signal v_h; that is,

$$v_a^{*'} = v_a^* + v_h \qquad (2.21)$$

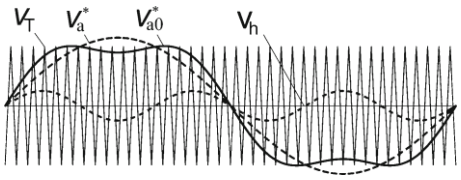

Fig. 2.58 Operation in over modulation region—non-sinusoidal PWM: sinusoidal reference, v_a^*, modulating signal generated, v_{ao}^*; and zero-sequence signal v_h (*middle*) for the THIPWM strategy

From (2.21), the SPWM corresponds to $v_h = 0$. For the three-phase inverter shown in Fig. 2.59a there are three modulating signals, one for each of the phases, and one carrier signal, as shown in Fig. 2.59b. This figure shows the pole voltage and the line–line voltage of the inverter.

In the following section, it will be shown how to build different PWM techniques for the three-phase VSI, using the concepts mentioned above. The extension of Eq. (2.21) to the three-phase case results in

$$v_j^{*'} = v_j^* + v_h \quad (j = a, b, c) \tag{2.22}$$

An important feature is that the injected zero-sequence signal v_h will not increase the LF harmonic distortion in the inverter output voltage.

The most used v_h signal can be easily determined for any of the Sectors from I to VI, which divide the fundamental period, as shown in Fig. 2.60, from [21].

$$v_h = \frac{v_M + v_m}{2} \tag{2.23}$$

That is, from the average value of vM+vm; where v_M and v_m are the maximum and the minimum values among the three sinusoidal reference voltages, v_a; v_b and v_c; respectively. In the switching interval considered, v_a and v_c have the maximum and minimum values, respectively, while v_b is at an intermediate value. Therefore, in the case, v_h corresponds to the intermediate values, v_{mid}; along the three references along the fundamental period (see the dashed line in Fig. 2.60), since v_a; v_b and v_c change position in the different sectors. The continuous line in Fig. 2.61 represents the new modulating signal for one phase.

As mentioned, many other continuous and discontinuous zero-sequence components can be employed in Eq. (2.22), resulting in different non-sinusoidal carrier-based PWM techniques, but their discussion is out of the scope of this chapter. The combination of the conduction of the switches ''P'' (upper switches) and the switches ''N'' (lower switches) in legs *a*, *b*, and *c* of the inverter in Fig. 2.59a, allows for eight possible switch combinations, denoted by SC_i (i = 0, 1…7). Six of these switch combinations, SC_1 = PNN, SC_2 = PPN, SC_3 = NPN, SC_4 = NPP, SC_5 = NNP, and SC_6 = PNP, apply voltage to the output (active switch combinations) while switch combinations SC_0 = NNN and SC_7 = PPP correspond to the short circuiting of the lower switches and of the upper switches, respectively.

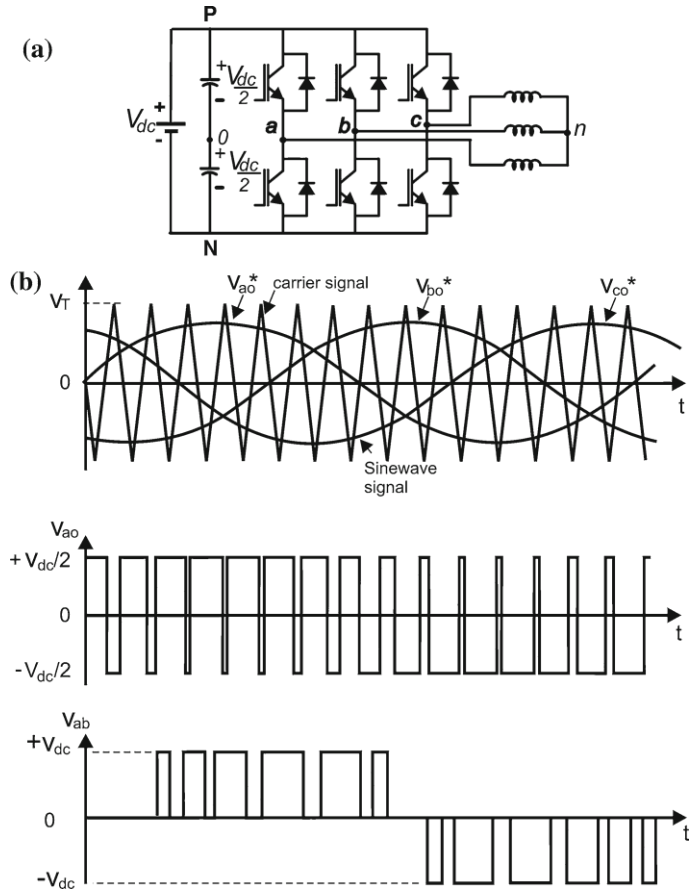

Fig. 2.59 Three-phase sinusoidal PWM: a inverter circuit, b principle, pole voltage, and inverter output voltage

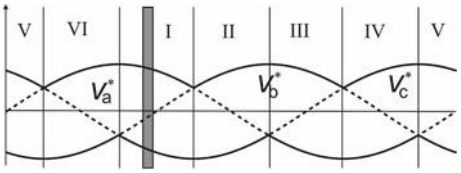

Fig. 2.60 Sectors inside one period

Figure 2.62 shows the representation of the modulated pulse waveforms inside a switching interval of Sector I. The intersection of modulating voltages (references) v_M v_a^* v_m v_b^*, and v_{mid} v_c^* with the triangle defines: (1) the pulse widths for each of the phase voltages, s_1; s_2; and s_3; (2) the distances between the switching instants for phases *a*, *b*, *c*, the delay of the first switching procedure t_{01}; the distances of the switching instants, t_1 and t_2; and the remaining time of the

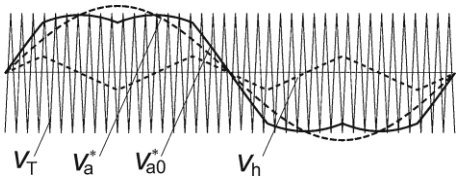

Fig. 2.61 Operation in over modulation region—non- sinusoidal PWM: v_a^*; modulating signal generated, v_{ao}^*; and zero-voltage signal v_h (*middle*) generated for Symmetric PWM

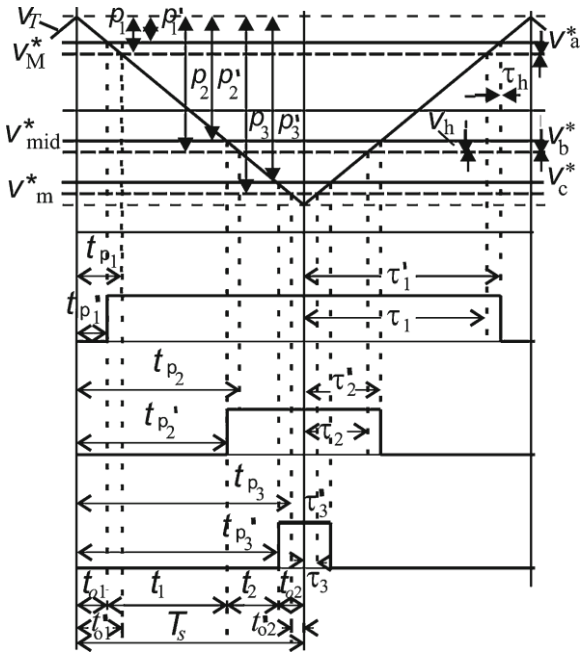

Fig. 2.62 Pole voltage pulse width inside a switching interval

sampling period t_{02}; and (3) the time intervals t_{p1}; t_{p2}; and t_{p3} (switching delays) before each leg changes in a given switching interval. When the zero-sequence component is added to the sinusoidal reference, the intervals t_1 and t_2 between the phase pulses remain the same. Instead, the pulse widths for each of the phase voltages, s_1; s_2; and s_3; do change, and become s_1'; s_2'; and s_3': Note that, inside the switching interval, the intervals t_{01}; t_1; t_2, and t_{02} indicate the duration of the

switch combinations NNN, ONN, PPN, and PPP, which occur in all switching periods inside Sector I. Note, also, that

$$t_z = t_{01} + t_{02} = T_s - (t_1 + t_2) \qquad (2.24)$$

In Eq. (2.24), $t_z = t_{01} + t_{02}$ constitutes the total freewheeling interval. Note, finally, that t_{01} and t_{02} are equally distributed at the beginning and at the end of the switching interval. In reality, these zero interval constituents can assume different values provided that the condition in (2.24) is observed.

2.1.11.3 Space Vector Modulation

The space vector pulse-width modulation (SVPWM) technique [4, 5] does not consider each of the three-phases as a separate entity. The three-phase voltages are simultaneously performed within a two-dimensional reference frame (plane), the complex reference voltage vector being processed as a whole. Because of its flexibility of manipulation, the SVPWM technique became popular [5, 10, 26, 27].

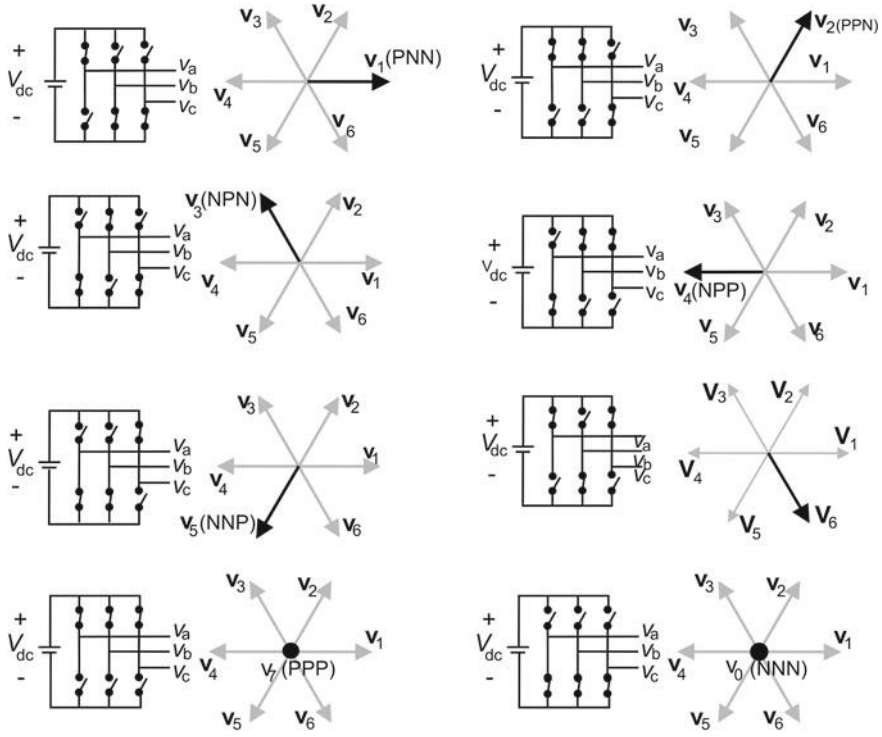

Fig. 2.63 Relation of the inverter switching configurations and the state vectors

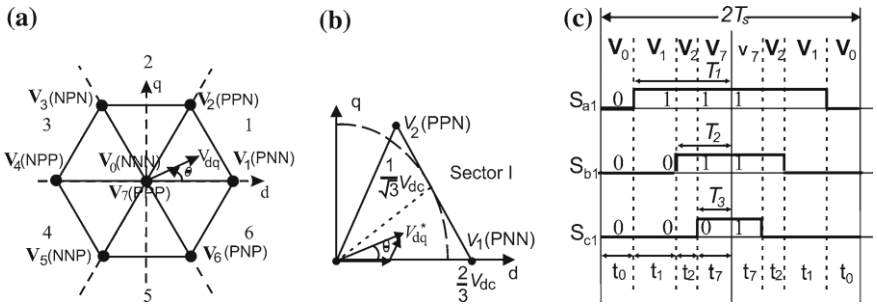

Fig. 2.64 a Space vector diagram and sector definition, b synthesis of the reference state vector in *Sector I* using switching vectors $\mathbb{V}_0$; $\mathbb{V}_1$; $\mathbb{V}_2$; and $\mathbb{V}_7$, and c switching pattern

2.1.12 PWM Techniques for Other Two-Level Converters

In the following section on the PWM techniques for the CSI and the CSR and AC/ AC converters will be introduced.

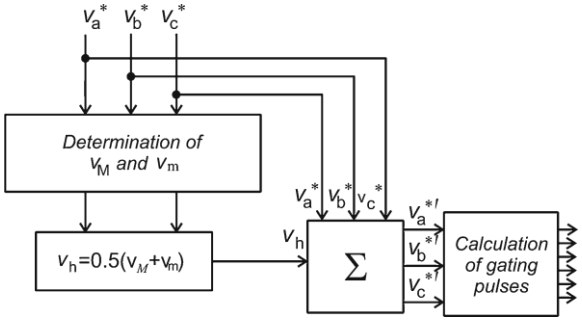

Fig. 2.65 Block diagram for calculation of the pulse width

A. Current Source Converters

The three-phase CSI is the dual of the voltage source three-phase inverter [29, 30]. Because of this the line-to-line output voltage waveform of a VSI is the line output current waveform of a CSI. Using this knowledge, the CSI can be controlled by the same PWM techniques used to control the VSI. However, there are two differences [29]:

1. In CSI the current signals are used as references, instead of voltages as in VSI.
2. For VSI, the PWM pattern can be used to directly control the switching devices and in the CSI the phase switching states cannot be used directly to control the switching devices, since these are controlled by line switching states [5]. References [29–31] have established an PWM equivalence between these circuits so that any PWM techniques developed for VSI can also be applied to current-type inverters, such as SHE PWM [32], SVPWM, HPWM, and other techniques, including those of third harmonic injection and discontinuous PWM to reduce losses [11].

High power and its high quality as current source PWM has applications in AC drives, VAR generator, active filters, and superconductive magnetic energy storage (SMES) [33]. But it is much less used than the VSR. The PWM techniques used for the CSI can be directly applied to the CSR. However, the PWM scheme for the CSR must provide an adjustable modulation index for the DC current control in addition to the reduction in the total harmonic distortion. CSR or Buck Rectifier

B. AC/AC Converters

PWM techniques for indirect and direct (matrix) AC/AC converters will be examined next. Due to the fact that the VSR can be modeled as a controllable DC voltage source, its natural load is a VSI. The connection of these two voltage source converters sharing a common capacitor DC link (as in Fig. 2.40) allows two-way energy flow and four-quadrant operation. This four-quadrant converter is presently applied to asynchronous drives, electric power generation using asynchronous, energy storage systems, like UPS and flywheel energy storage systems, and transmission and distribution systems multilevel converter-based (Universal Power Flow Controller, UPFC, High Voltage DC-Light, HVDC-Light, Dynamic Voltage Regulation, DVR) [34, 35].

The major objective in matrix converters is to simultaneously control their input currents, managing inclusively the reactive power flowing between the grid and the load. This is also the major difficulty found in PWM schemes to control these converters. Many schemes have been proposed to solve this problem [36]. This problem does not exist in indirect converters because of the independent control of the input currents (at the rectifier stage) an output voltage is independent from the control (in the inverter stage) due to the capacitor in DC link. The two-stage direct power converter (DPC) topology has a structure similar to the AC/DC/AC converter, but without the DC link capacitor [37, 38]. Based on this, *dissociation* between input currents and output voltages controls in the matrix converter was proposed in [37]. The space vector modulator implemented includes the adaptation of the DPC duty-cycles to the matrix converter topology.

The technique was also implemented using a generalized PWM strategy similar to those studied for two-level converter to control both input currents and output voltages. This technique is well detailed in [39].

2.1.13 PWM Techniques for Multilevel Converters

Multilevel inverters have emerged as the solution for working with higher voltage levels. They have been considered for an increasing number of applications due to not only their high power capability, but also lower output harmonics and lower commutation losses.

The three-level NPC inverter topology shown in Fig. 2.66a will be used as an example. This topology has 12 active switches (note that the number of switches increases with the number of level *K*). In each leg of the inverter, the switches can be positive (S_1 and S_2) or negative (S_3 and S_4), which in turn can be external (S_1 and S_4) or internal (S_2 and S_3), in phase *a* of inverter. Also, each inverter leg can assume three switching states, ‘‘P’’, ‘‘O’’, and ‘‘N’’, as shown from the equivalent circuit in Fig. 2.66b. Taking into account the three-phases, the inverter has a total of 27 possible combinations of switching states as indicated in the three-level space vector diagram in Fig. 2.67, obtained through the same procedure used for the two-level inverter. Such representation allows not only to establish the correlation between the state vectors and the switching configurations but, also, to visualize the division of the voltage vectors into four groups as a function of the vector amplitude: Large Vectors, when the three pole voltages assume only the states *P* and *N*; Medium Vectors, when the three pole voltages assume the states *P*, *O*, and *N*; Small Vectors, when the three pole voltages assume only the states *P* and *O* or *O* and *N*; Null Vectors: NNN, PPP, OOO. In SVPWM, in order to optimize the modulation, each sector is typically divided into four triangles (regions 1 to 4). The knowledge of the position of the reference vector inside a region of a certain sector allows for

calculating the pulse widths of the gating pulses. One possibility is to consider the space vector diagram as formed of six small two-level hexagons, each of them centered in one vector of the small vectors

$\vec{V}_1$; $\vec{V}_2$;$\vec{V}_6$; as shown in Fig. 2.67. Using the adjacent state vectors of the small hexagon reproduces a partial reference vector. The reference voltage vector V^m is then obtained by subtracting the center vector of the corresponding small hexagon from the original reference vector (see vectors in triangle *D* of Sector I). This means that in that region the pole voltage modulates, for instance, between *P* and *O* levels. For a *K*-level inverter, its state phase-diagram is simplified to that of a $K-1$ level inverter and so on, till that of the two-level inverter.

Alternatives are the use of SHE modulation or the use a carrier-based PWM, such as the in-phase disposition (IPD) modulation [6] illustrated in Fig. 2.68a for the three-level inverter ($K = 3$). The number of carrier signals is $K-1 = 2$. For this reason, the modulating signal intersects two triangular waves, generating the pulse widths of each pole voltage.

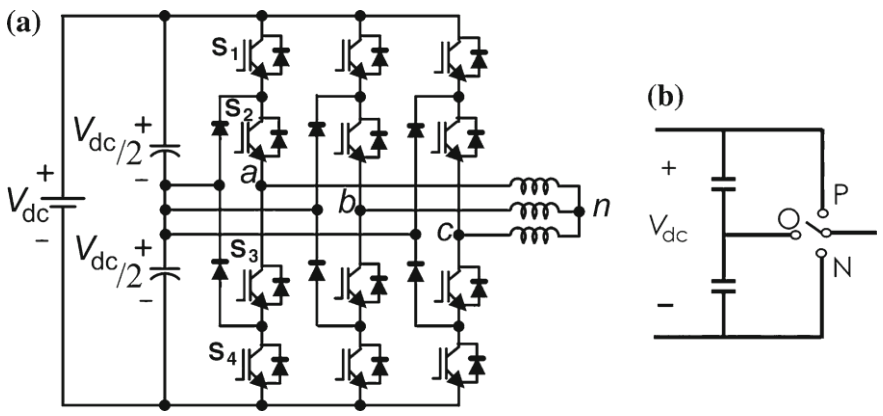

Fig. 2.66 a Three-level NPC inverter topology and b equivalent circuit

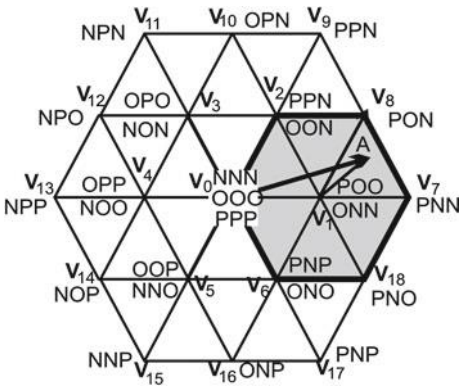

Fig. 2.67 Space vector diagram of a three-level converter

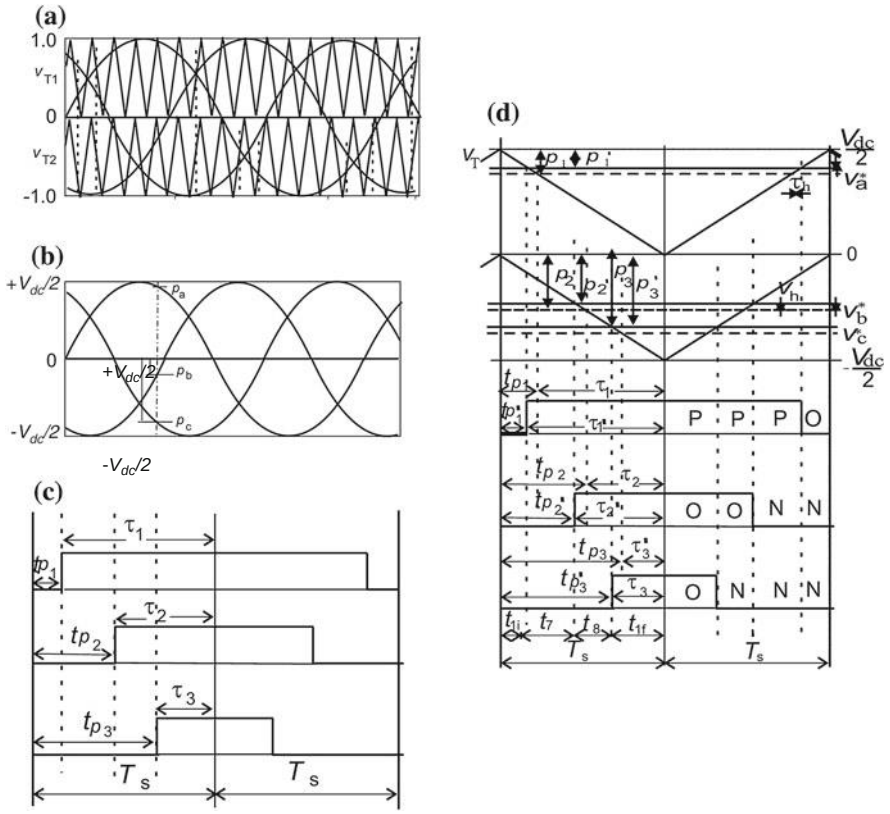

Fig. 2.68 Three-level inverter: a modulation principle (IPD), b definition of pi (i = 1, 2, 3), c the relation of pi with the pulse delays in the switching interval tpi, and d the switching interval considering the addition of the zero-sequence signal, vh

2.2 Types of AC-DC Converters

2.2.1 Buck Converter

The step-down dc–dc converter, commonly known as a buck converter, is shown in Fig. 2.69a. It consists of dc input voltage source VS, controlled switch S, diode D, filter inductor L, filter capacitor C, and load resistance R. Typical waveforms in the converter are shown in Fig. 2.69b under assumption that the inductor current is always positive. The state of the converter in which the inductor current is never zero for any period of time is called the continuous conduction mode (CCM). It can be seen from the circuit that when the switch S is commanded to the on state, the diode D is reverse biased. When the switch S is off, the diode conducts to support an uninterrupted current in the inductor. The relationship among the input voltage, output voltage, and the switch duty ratio D can be derived, for instance, from the inductor voltage vL waveform (see Fig. 2.69b).

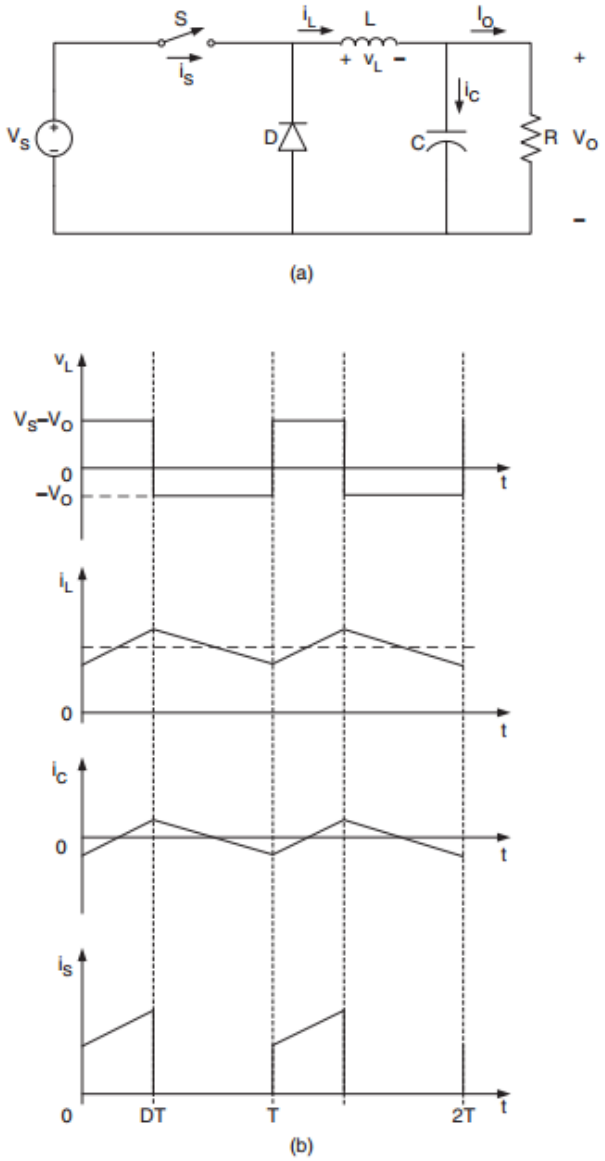

Fig. 2.69: Buck converter: (a) circuit diagram and (b) waveforms

According to Faraday's law, the inductor volt–second product over a period of steady-state operation is zero. For the buck converter

$$(Vs - Vo)DT = -Vo(1 - D)T \qquad (2.25)$$

Hence, the dc voltage transfer function, defined as the ratio of the output voltage to the input voltage, is

$$MV \equiv Vo/Vs = D \qquad (2.26)$$

It can be seen from Eq. (2.26) that the output voltage is always smaller than the input voltage. The dc–dc converters can operate in two distinct modes with respect to the inductor current iL. Figure 2.69b depicts the CCM in which the inductor current is always greater than zero. When the average value of the input current is low (high R) and/or the switching frequency f is low, the converter may enter the discontinuous conduction mode (DCM). In the DCM, the inductor current is zero during a portion of the switching

period. The CCM is preferred for high efficiency and good utilization of semiconductor switches and passive components. The DCM may be used in applications with special control requirements, since the dynamic order of the converter is reduced (the energy stored in the inductor is zero at the beginning and at the end of each switching period). It is uncommon to mix these two operating modes because of different control algorithms. For the buck converter, the value of the filter inductance that determines the boundary between CCM and DCM is given by

$$Lb = \frac{(1-D)R}{2f} \qquad (2.27)$$

For typical values of D = 0.5, R = 10, and f = 100 kHz, the boundary is Lb = 25 μH. For L > Lb, the converter operates in the CCM. The filter inductor current iL in the CCM consists of a dc component IO with a superimposed triangular ac component.

Almost all of this ac component flows through the filter capacitor as a current *ic*. Current *ic* causes a small voltage ripple across the dc output voltage *VO*. To limit the peak-to-peak value of the ripple voltage below certain value *Vr*, the filter capacitance *C* must be greater than

$$Cmin = \frac{(1-D)\,VO}{8VrLf^{\,2}} \qquad (2.28)$$

At *D* = 0.5, *Vr*/*VO* = 1%, *L* = 25 μH, and *f* = 100 kHz, the minimum capacitance is *Cmin* = 25 μF. Equations (2.27) and (2.28) are the key design equations for the buck converter. The input and output dc voltages (hence, the duty ratio *D*), and the range of load resistance *R* are usually determined by preliminary specifications. The designer needs to determine values of passive components *L* and *C*, and of the switching frequency *f*. The value of the filter inductor *L* is calculated from the CCM/DCM condition using Eq. (2.27). The value of the filter capacitor *C* is obtained from the voltage ripple condition Eq. (2.28). For the compactness and low conduction losses of a converter, it is desirable to use small passive components. Equations (2.27) and (2.28) show that it can be accomplished by using a high switching frequency *f*. The switching frequency is limited, however, by the type of semiconductor switches used and by switching losses. It should be also noted that values of *L* and *C* may be altered by effects of parasitic components in the converter, especially by the equivalent series resistance of the capacitor.

2.2.2 Boost Converter

Figure 2.70a depicts a step-up or a PWM boost converter. It is comprised of dc input voltage source Vs, boost inductor L, controlled switch S, diode D, filter capacitor C, and load resistance R. The converter waveforms in the CCM are presented in Fig. 2.70b. When the switch S is in the on state, the current in the boost inductor increases linearly. The diode D is off at the time. When the switch S is turned off, the energy stored in the inductor is released through the diode to the input RC circuit. Using the Faraday's law for the boost inductor

$$VsDT = (Vo - Vs)(1 - D)T \qquad (2.29)$$

from which the dc voltage transfer function turns out to be

$$MV \equiv Vo/Vs = 1/1 - D \qquad (2.30)$$

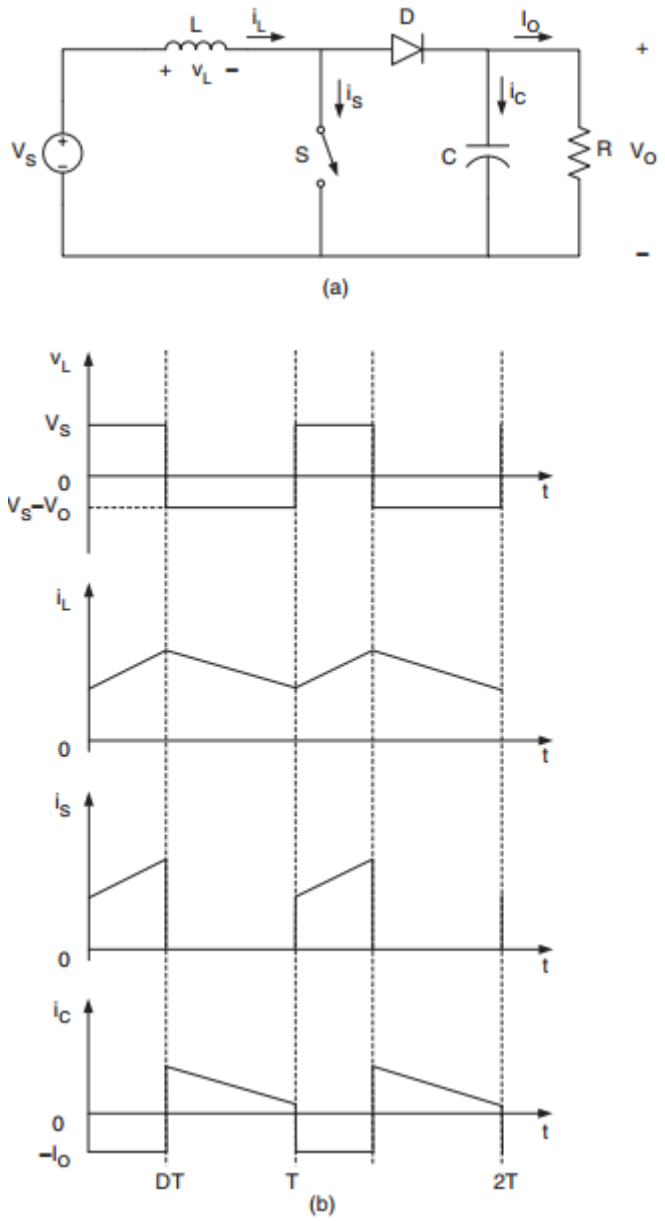

Fig. 2.70: Boost converter: (a) circuit diagram and (b) waveforms

As the name of the converter suggests, the output voltage is always greater than the input voltage. The boost converter operates in the CCM for L > Lb where

$$Lb = (1 - D)^2 DR/2f \qquad (2.31)$$

For D = 0.5, R = 10, and f = 100 kHz, the boundary value of the inductance is Lb = 6.25 μH. As shown in Fig. 2.70b, the current supplied to the output RC circuit is discontinuous. Thus, a larger filter capacitor is required in comparison to that in the buck-derived converters to limit the output voltage ripple. The filter capacitor must provide the output dc current to the load when the diode D is off. The minimum value of the filter capacitance that results in the voltage ripple Vr is given by

$$Cmin = DVo/(Vr\ Rf) \qquad (2.32)$$

At D = 0.5, Vr/Vo = 1%, R = 10 , and f = 100 kHz, the minimum capacitance for the boost converter is Cmin = 50 μF. The boost converter does not have a popular transformer (isolated) version.

2.2.3 Buck-Boost Converter

A non-isolated (transformerless) topology of the buck–boost converter is shown in Fig. 2.71a. The converter consists of dc input voltage source VS, controlled switch S, inductor L, diode D, filter capacitor C, and load

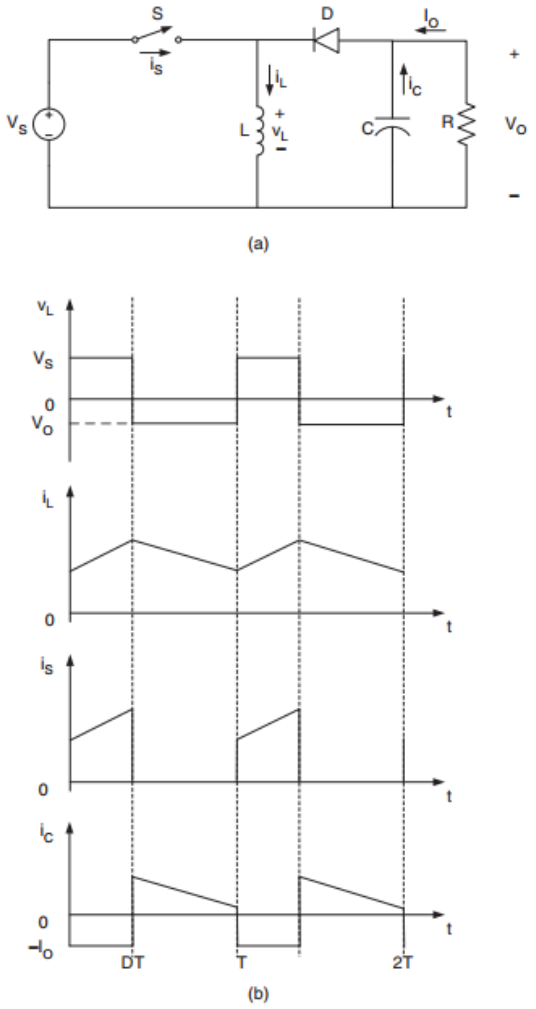

Fig. 2.71 Buck–boost converter: (a) circuit diagram and (b) waveforms

resistance R. With the switch on, the inductor current increases while the diode is maintained off. When the switch is turned off, the diode provides a path for the inductor current. Note the polarity of the diode which results in its current being drawn from the output. The buck–boost converter waveforms are depicted in Fig. 13.10b. The condition of a zero volt–second product for the inductor in steady state yields

$$VsDT = -Vo/(1 - D)T \quad (2.33)$$

Hence, the dc voltage transfer function of the buck–boost converter is

$$MV \equiv Vo/Vs = -D/(1 - D) \quad (2.34)$$

The output voltage Vo is negative with respect to the ground. Its magnitude can be either greater or smaller (equal at D = 0.5) than the input voltage as the converter's name implies. The value of the inductor that determines the boundary between the CCM and DCM is

$$L_b = (1 - D)^2 R/2f \qquad (2.35)$$

The structure of the output part of the converter is similar to that of the boost converter (reversed polarities being the only difference). Thus, the value of the filter capacitor can be obtained from Eq. (2.32).

2.2.4 Cuk Converter

The circuit of the Cuk converter is shown in Fig. 2.72a. It consists of dc input voltage source V_s, input inductor L1, controllable switch S, energy transfer capacitor C1, diode D, filter inductor L2, filter capacitor C, and load resistance R.

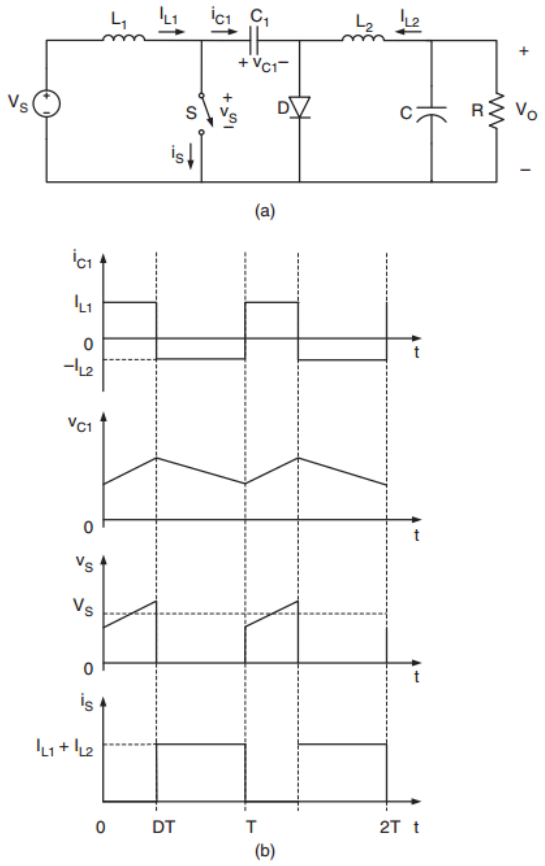

Fig. 2.72: Cuk converter: (a) circuit diagram and (b) waveforms.

An important advantage of this topology is a continuous current at both the input and the output of the converter. Disadvantages of the Cuk converter include a high number of ` reactive components and high current stresses on the switch, the diode, and the capacitor C1. Main waveforms in the converter are presented in Fig. 2.72b. When the switch is on, the diode is off and the capacitor C1 is discharged by the inductor L2 current. With the switch in the off state, the diode conducts currents of the inductors L1 and L2 whereas capacitor C1 is charged by the inductor L1 current. To obtain the dc voltage transfer function of the converter, we shall use the principle that the average current through a capacitor is zero for steady-state operation. Let us assume that inductors L1 and L2 are large enough that their ripple current can be neglected. Capacitor C1 is in steady state if

$$I_{L2}DT = I_{L1}(1 - D)T \qquad (2.36)$$

For a lossless converter,

$P_S = V_S I_{L1} = -V_O I_{L2} = P_O$ (2.37)

Combining these two equations, the dc voltage transfer function of the Cuk converter is

$M_V \equiv V_O/V_S = -D/((1 - D)$ (2.38)

This voltage transfer function is the same as that for the buck–boost converter. The boundaries between the CCM and DCM are determined by

$L_{b1} = (1 - D)R/2Df$ (2.39)

for L_1 and for L_2,

$L_{b2} = (1 - D)R/2f$ (2.40)

The output part of the Cuk converter is similar to that

$C_{min} = (1 - D)V_O/8V_r L_2 f^2$ (2.41)

The peak-to-peak ripple voltage in the capacitor C_1 can be estimated as

$V_{r1} = \frac{DVo}{C1Rf}$ (2.42)

A transformer (isolated) version of the Cuk converter can be obtained by splitting capacitor C_1 and inserting a high frequency transformer between the split capacitors.

Chapter 3

Related Field Study

3.1 Buck-Boost Converter

Conventional AC-DC converters for buck, boost, buck-boost, Cuk, SEPIC and Zeta are not equipped to provide the required voltages from the line voltages for many modern applications. In future, instead of using 5V power supply, microprocessors will be using any range of power from 1V to 3V. This is to reduce the CPU power loss [40]. In modern times, for obvious reasons, we need the voltage conversion ratio of the converters be extremely high and extremely low for various applications. In case of automobile head lamps, the high intensity discharge lamps (HID) at start-up require at least 100V at 35W to light up from 12V car battery [41]. For power supply applications, 1V is required from 12V supply and sometimes from 48V which is possible only if the conversion ratio of the converters can somehow be increased without incurring any major drawbacks in its output quality [40]. The 48V supply from dc battery has to be boosted up to 380V supply in intermediate dc bus in case of providing internet by telecom standard equipment [42]. In order to make these possible, the converters are needed to be operated higher than 0.9 duty cycle for step up conversion and lower than 0.1 duty cycle for step down conversion. However, these extreme duty cycles reduce the efficiency and deteriorates the transient response of the system [43]. Moreover, such an extreme duty cycle requires very expensive and super-fast comparators within the control circuit. The short conduction due to high switching frequency also can lead to malfunction in the diode for step up converters and in the active transistor for step down converters.

The easiest and simplest solution would be to use transformer for having the required conversion ratio, for instance, forward or flyback converter. But introducing transformer in industrial applications where dc isolation is not absolutely necessary will only increase the expense, loss and volume of the system. On top of that, voltage stress on primary elements will be much higher when a large transformer is used with a very high turns ratio, resulting in low efficiency.

Recently, voltage regulators for 1V supply needed in microprocessors are being researched and developed [44]. They can handle the high load current and fast dynamics that are required of them, but still need a lot to improve. Although the switched-capacitor converters which were proposed in the 1990s presented with steep conversion ratio, they also brought many disadvantages along, such as poor efficiency [45]. As for the cascade converters, they are ruled out from the race as the overall efficiency is the product of individual efficiencies of the circuits in series. The use of single driven transistor in Quadratic converters can solve the efficiency problem of Cascade converters [46] [47] but they suffer from voltage and current over stress.

For the very first time, a new structure of converter was proposed with topological converters [48] that is based on the duality between switching capacitor cell and switching inductor cell and also the duality between a voltage driven converter and a current driven converter. Regardless, the limitation of this converter type is the use of maximum two switches and not so high conversion ratios.

A novel approach of simple switching dual structures is proposed in this paper formed by either two capacitors and 2– 3 diodes, or two inductors and 2– 3 diodes are defined. These circuit blocks can provide either a step down of the input voltage or a step up of it [49]. They can be inserted in classical buck–boost converter to give a steep voltage conversion ratio retaining all the positives of the topological converter without the expense of major disadvantages.

When the active switch of the converter is on, the capacitors in the C-switching blocks are discharged in parallel. When the active switch of the converter is off, the capacitors in the C-switching blocks are charged in series.

The proposed converter can step down the line voltage more than the classical buck-boost topology can do as reflected by its voltage gain formula,

$$\frac{\mathrm{Vo}}{\mathrm{Vin}\,|\sin wt|} = -\frac{\mathrm{D}}{(1-\mathrm{D})(2-\mathrm{D})}$$

What this proposed converter contains is comparable with the quadratic buck boost converters in terms of its number of circuit elements. And the performance of this converter design is superior to the available quadratic converters as it improves the dc gain, voltage and current stresses on the active switch and diodes.

The conventional buck-boost converter has a number of disadvantages which need to be tackled. An input filter is needed to lower the effects of ripple current in buck-boost converters and fulfil the electromagnetic interference (EMI) requirements as the input current is pulsating because of the switching of the power switch. Large output capacitor has to be introduced to reduce the ripple current and make up for the discontinuous conduction current. These issues are solved by introducing switched capacitors before the switch [50]. The circuit diagram for this configuration is shown in Fig. 1. But still there is an input bridge rectifier which arises many problems. Most importantly, it causes much conduction loss due to hysteresis and magnetization of components. Consequently, efficiency is hampered. The rectification stage of traditional bridge configuration suffers several problems such as, distorted input current, high conduction loss, low power factor, and low conversion efficiency due to extremely low duty cycles [51]- [54]. Total harmonic distortion (THD) is caused by distorted input current. THD can be minimized by introducing a L-C filter in the input side. However, it doesn't improve power factor. To improve power factor, the most used methodology is to use cascade buck-boost PFC (CBB-PFC) converter. But the major drawback of CBB-PFC converter is high conduction loss which is not desirable [55]. So, to solve these two problems (low power factor and conduction loss) simultaneously, a new bridgeless buck-boost topology is proposed. This proposed circuit design reduces the number of conduction semiconductors. And hence reduces conduction loss, improves converter efficiency.

3.2 Cuk Converter

In recent years, SMPS technologies have been developed significantly. Most SMPS supplies are used to convert AC to DC sources in different applications. DC-output voltage can be achieved easily using a transformer, a bridge rectifier, and capacitors, but the input current may be distorted severely. Therefore, PFC converters are necessarily required for AC-DC conversion [56-57]. Numerous circuit topologies have been introduced for PFC applications.

In future, instead of using 5V power supply, microprocessors will be using any range of power from 1V to 3V. This is to reduce the CPU power loss [58]. In modern times, for obvious reasons, we need the voltage conversion ratio of the converters be extremely high and extremely low for various applications. For power supply applications, 1V is required from 12V supply and sometimes from 48V which is possible only if the conversion ratio of the converters can somehow be increased without incurring any major drawbacks in its output quality [58].

In order to make these possible, the converters are needed to be operated higher than 0.9 duty cycle for step up conversion and lower than 0.1 duty cycle for step down conversion. However, these extreme duty cycles reduce the efficiency and deteriorates the transient response of the system [59]. Moreover, such an extreme duty cycle requires very expensive and super-fast comparators within the control circuit. The short conduction due to high switching frequency also can lead to malfunction in the diode for step up converters and in the active transistor for step down converters.

The simplest and easiest way would be introducing transformer in industrial applications where dc isolation is not absolutely necessary will only increase the expense, loss and volume of the system. Most importantly, voltage stress on primary elements will be much higher when a large transformer is used with a very high turns ratio, resulting in low efficiency.

All the conventional boost, buck-boost, SEPIC, and Cuk PFC converters can be used in DCM or CCM. These converters have intrinsic PFC characteristics at fixed duty ratio while it is in DCM operation to shape the input current sinusoidally and so there is no need of any control circuit. However, high-current stress on semiconductor devices and discontinuous input current occur in buck-boost converter operating in DCM, which ultimately increases the THD. On the other hand, the SEPIC and Cuk converters have continuous input currents when it is in DCM operation with output voltage lower than its input voltage.

In PFC applications, the Cuk converter has many advantages, such as easy implementation of transformer isolation, natural protection against inrush current at start-up or overload current, lower input ripple current, and reduced electromagnetic interference (EMI) associated with the DCM topologies. Unlike SEPIC converter, Cuk converter has both continuous input and output currents with a low current ripple, making it a better choice than other basic converter topologies.

Considerable research works have been directed toward the development of efficient bridgeless PFC circuit topologies [60]–[63] to maximize the power supply efficiency. Compared to the conventional PFC circuit, a bridgeless PFC circuit allows the current to flow through a minimum number of switching devices. Therefore, the converter conduction losses can significantly be reduced, cost can be reduced, and high efficiency can be obtained.

A novel structure of converter was proposed with topological converters [64] that is based on the duality between switching capacitor cell and switching inductor cell and also the duality between a voltage driven converter and a current driven converter. However, this converter type is limited by the use of maximum two switches and not so high conversion ratios.

A new approach of simple switching dual structures is proposed formed by two capacitors and 2– 3 diodes are defined. These circuit blocks can provide a step down of the input voltage [65]. They can be inserted in classical Cuk converter to give a steep voltage conversion ratio retaining all the positives of the topological converter without at the cost of no significant disadvantages. The capacitors in the C-switching blocks are discharged in parallel when the active switch of the converter is on. When the active switch of the converter is off, the capacitors in the C-switching blocks are charged in series. In this paper, both bridge and bridgeless topologies are proposed, shown in figure 1(a) and 1(b) respectively. The voltage gain of these two topologies are given by,

$$\frac{\mathrm{Vo}}{\mathrm{Vin}\,|\sin wt|} = -\frac{\mathrm{D}}{2(1-\mathrm{D})}$$

3.3 SEPIC-Cuk Combination Converter

AC networks have been the standard choice for the distribution and transmission of electricity in the last century. This type of network has the advantage that transforms voltages at different levels easily, therefore, facilitates power transmission over long distances and it is possible to easily generate the energy with rotating machines. On the other hand, keep in mind that during this century most of the loads are AC type. So, from the point of view of the generation, transmission and use of energy is justified the choice of such networks. In the last two decades, distributed generation systems, energy storage, communications technology and the advancement of power electronics have led to a redesign of traditional power systems. The distribution system should be more flexible and configurable, allowing efficient energy management in the presence of new distributed generation units. So, MG have proved to be very attractive structures that meet these premises [66]. They allow the integration of Distributed Generation (DG) based on Renewable Energy Units (RES) [67-70] and facilitate the implementation of: Energy Storage Systems (ESS), Smart Grids (SG), Power Quality (PQ), Static Var Compensator (SVC), Transmission and distribution (T&D), including Medium Voltage and High Voltage Direct Current (HVDC), Flexible AC Transmission Systems (FACTS), Shunt and Series Compensation, and Universal Power Flow Control (UPFC). A MG allows operation in two basic modes: isolated and connected to the utility grid [71]. In the first, the network is managed in isolation; managing devices connected to the microgrid and controlling the balance generation-consumption. In the second mode, bidirectional energy flow between the MG and the utility grid is allowed. A MG can be operated based on two principles: as an AC power system or as a DC power system. The use of DC technology was almost discarded in the power transmission systems. DC power systems have been used in applications like avionic, automotive, marine, rural areas, telecommunication infrastructures and point-to-point transmissions over long distances or via sea cables and for interconnecting AC grids with different frequencies. Today's consumer equipment such as computers, fluorescent lights or LED lighting, households, businesses, industrial appliances and equipment need the DC power for their operation. However, all these DC loads require conversion of the available AC power into DC for use and the majority of these conversion stages typically use inefficient rectifiers. On the other hand, most of renewable energy units generate in DC form or they have outputs voltage/frequency variable, which requires power electronic devices to adapt its output to network conditions. These DC–AC–DC power conversion stages result in substantial energy losses. Therefore, in many cases it is justified to use DC microgrids. Such systems have mainly the following advantages over AC microgrids [72]:

- More efficiency and more power transmission.
- Require few wires.
- More stable.
- No reactance in the line.
- Frequency is zero, so no need of frequency monitoring.
- No transient stability problems.

- No electromagnetic interference.
- Have lower line resistance.

In a DC microgrid, energy can be transmitted with single cable, two cables, or even three cables, what leads to consider three DC link types: Monopolar, Bipolar and Homopolar. Monopolar DC link uses a single voltage wire (Fig. 1a). The return conductor may be land or metallic, the first has advantages from an economic point of view to use a single cable, however, some countries prohibits their use by corrosion problems in pipelines and other buried metal objects. The metallic return avoids these drawbacks. Bipolar DC link has two wires (Fig. 1b): one with positive polarity and one with negative polarity. In normal operation, the current through ground is zero. It has two voltage levels, allowing fault conditions a monopolar operation. It is also possible a metallic return with appropriate control strategies. Homopolar DC link (Fig. 1c) has two or more wires with the same polarity, usually negative. The return may be by land or metallic. Its main advantage is the reduction of the costs of insulation, however, the return current is double and in the case two conductors this drawback overcomes the advantage of the insulation

Of all these topologies, bipolar DC link is one of the most used. This topology has a higher technical complexity and cost than the monopolar DC link, but has going for it the following advantages:

- In normal operation, the current through the return wire is smaller, so the power losses are reduced.
- When a failure occurs in one of the lines, the other continues to operate normally.
- For the same transmission power, in a bipolar DC link, the current is half.

This topology allows to have two different voltage levels. This is useful when some loads consume high power, because the current drawn is reduced. The DC-DC converters that are employed to balance the DC supply voltages and/or balance its transmitted powers are key elements in Bipolar DC link. Configurations widely used in Bipolar DC link [73], use two or four controlled switches: Half Bridge type, and Full-Bridge type, which difficult the implementation of strategies to voltage balancing in DC microgrid.

Chapter 4

Proposed Circuits

4.1 Principle of Operation

4.1.1 Bridgeless Hybrid Buck-Boost Converter Topology

In this topology, two switched capacitor networks are introduced, one for each half cycle as illustrated in Fig. 4.2. Bridge rectifier has been discarded since two different paths have been introduced for two half cycles. Switching loss remains same despite using more components in the proposed topology as compared to single stage switched capacitor network [50]. Hence, the basic operation of both the above mentioned circuits are identical. However, this proposed topology is expected to have higher efficiency since effort reduces hysteresis and excess energy loss may occur due to magnetization of the components in case of single stage switched capacitor network.

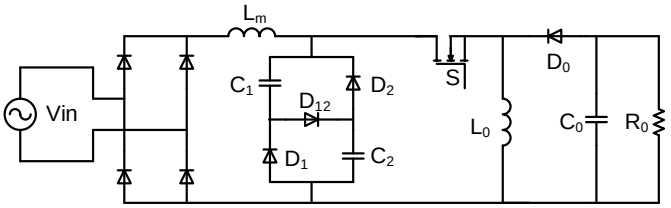

Fig. 4.1: Single Stage Switched Capacitor Network

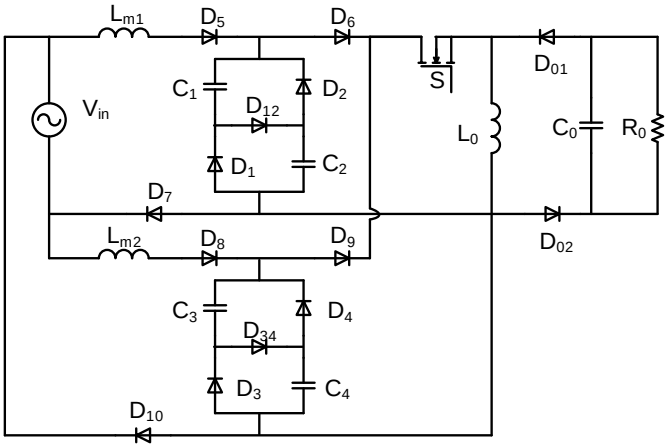

Fig. 4.2: Double Stage Switched Capacitor Network

During T_{on}, (for positive half cycle as illustrated in Fig. 4.3(a), for negative half cycle as illustrated in Fig. 4.3(b)) the buck-boost inductor L_0 and output capacitor C_0 are charged by the switched capacitors (C_1, C_2 for positive half cycle and C_3, C_4 for negative half cycle) with half of the DC link voltage since these switched capacitors become parallel due to the reverse bias of D_{12} and forward bias of D_1 and D_2 during positive cycle and diodes D_3, D_4 and D_{34} provide separate path for negative half cycle. However, during T_{off}, (for positive half cycle as illustrated in Fig. 4.3(a), for negative half cycle as illustrated in Fig. 4.3(b)) C_1, C_2 for positive half cycle and C_3, C_4 for negative half cycle are charged in series with the DC link voltage since D_{12} for positive half cycle and D_{34} for negative half cycle become forward biased. Furthermore, current in the buck-boost inductor L_0 continuing through the freewheeling diode D_0 charges the output capacitor C_0.

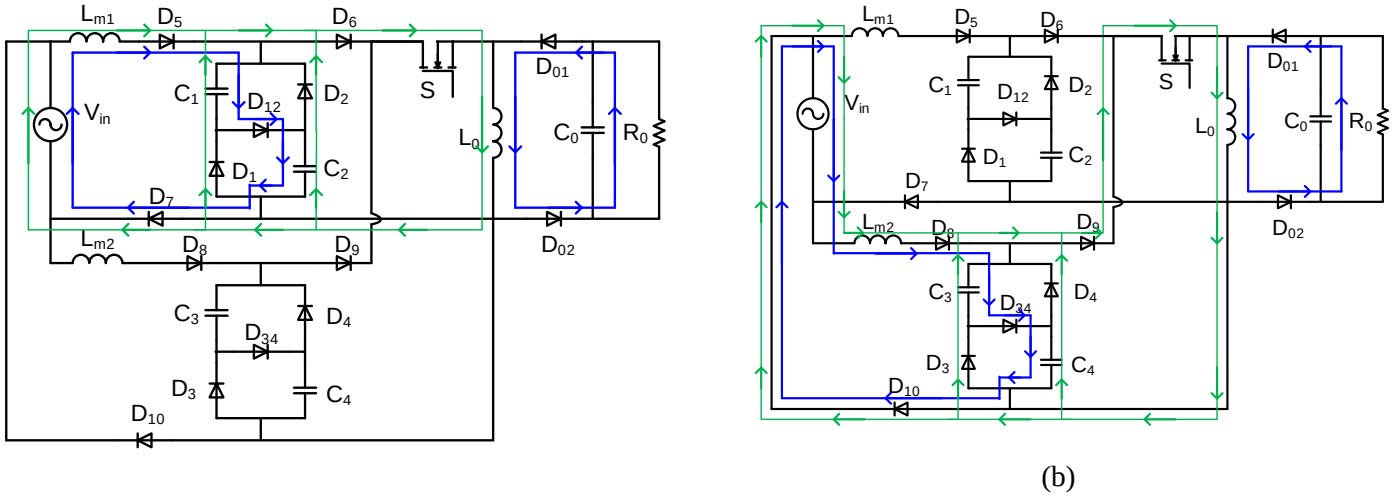

Fig. 4.3: Operation Principles of Double Stage Switched Capacitor Network (a)Positive half cycle (b)Negative half cycle (T_{on} = Green, T_{off} = Blue)

4.1.2 Hybrid Cuk Converter Topologies

Proposed Topology with Single Switched Capacitor Network: The first topology comprises of a basic single-phase rectifier followed by a switched capacitor network and a high frequency DC to DC converter as illustrated in Fig. 4.4(a). Here, a single switched capacitor network is adopted for both positive and negative cycle of operation.

Proposed Topology with Two Switched Capacitor Network: Unlike the first topology, here, two switched capacitor networks are introduced, one for each half cycle as illustrated in Fig. 4.4(b). Bridge rectifier has been discarded since two different paths have been introduced for two half cycles. Switching loss remains same despite using more components in the proposed topology as compared to single stage switched capacitor network. Hence, the basic operation of both the above-mentioned circuits are identical. However, this proposed topology is expected to have higher efficiency since effort reduces hysteresis and excess energy loss may occur due to magnetization of the components in case of single stage switched capacitor network.

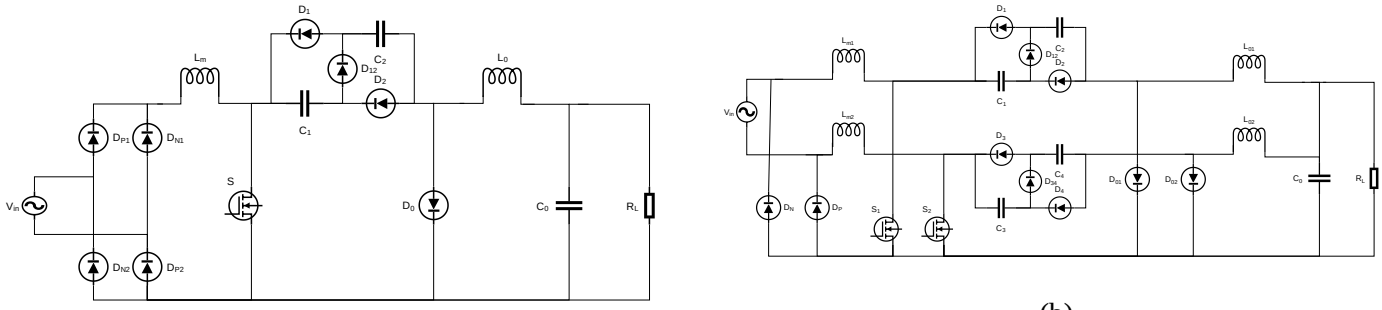

Fig. 4.4: Proposed Topology with (a)Single Switched Capacitor Network (b)Two Switched Capacitor Network

For the first topology, during T_{on}, (for positive half cycle as illustrated in Fig. 4.5(a), for negative half cycle as illustrated in Fig. 4.5(b)) the Cuk inductor L_0 and output capacitor C_0 are charged by the switched capacitors (C_1 and C_2) with half of the DC link voltage since these switched capacitors become parallel due to the reverse bias of D_{12} and forward bias of D_1 and D_2. However, during T_{off}, (for positive half cycle as illustrated in Fig. 4.5(a), for negative half cycle as illustrated in Fig. 4.5(b)) C_1 and C_2 are charged in series with the DC link voltage since D_{12} becomes forward bias. Furthermore, current in the Cuk inductor L_0 continuing through the freewheeling diode D_0 charges the output capacitor C_0. In case of second topology, the circuit operation is identical as the first topology during positive half cycle. However, for negative half cycle, a separate path is introduced to avoid magnetization loss as illustrated in Fig. 4.6(b).

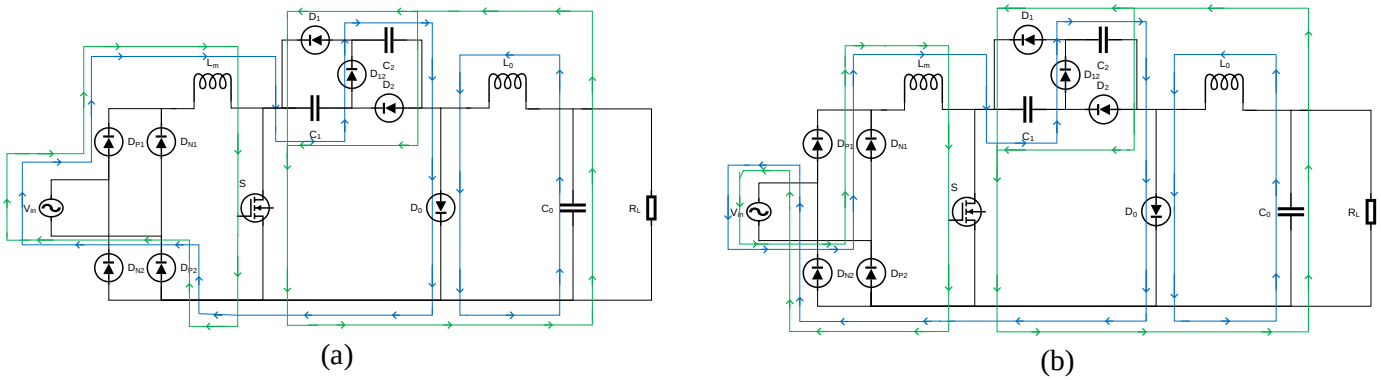

Fig. 4.5: Operation Principles of Single Switched Capacitor Network (a)Positive half cycle (b)Negative half cycle (Ton = Green, Toff = Blue)

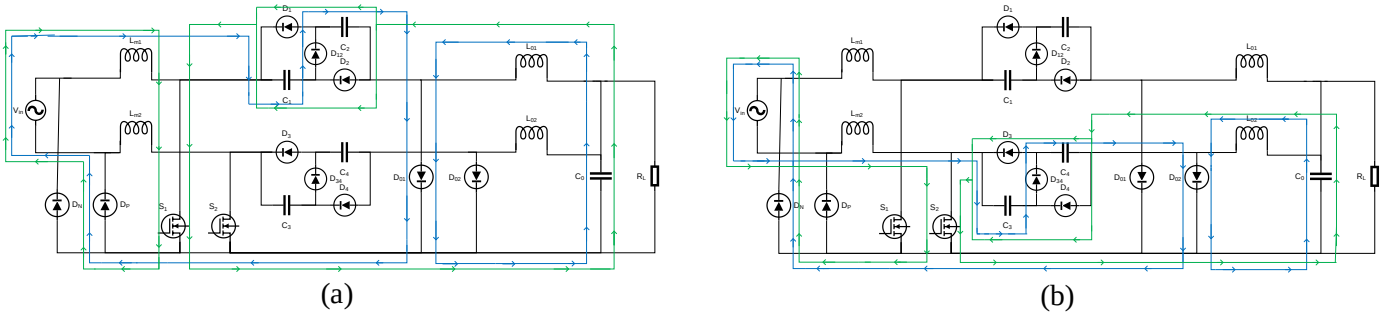

Fig. 4.6: Operation Principles of Two Switched Capacitor Network (a)Positive half cycle (b)Negative half cycle (Ton = Green, Toff = Blue)

4.2 Voltage Gain Analysis:

4.2.1 Hybrid Buck-Boost Converter

In this proposed circuit, there are two different current paths for positive and negative half cycles. Both the paths are identical in terms of voltage gain and efficiency analysis. So, only the positive half cycle will be analyzed.

The voltage gain of the proposed converter can be obtained from the volt-sec balance across inductors over the switching frequency. The step by step analysis of voltage gain is as follows.

Using volt-sec balance for inductors L_{m1} and L_0,

$$(\mathrm{Vin}|\sin wt| - \mathrm{Vc})\mathrm{DT} + (\mathrm{Vin}|\sin wt| - \mathrm{Vc})(1 - \mathrm{D})\mathrm{T} = 0 \quad (4.1)$$

$$\mathrm{Vc\ DT} + \mathrm{Vo}(1 - \mathrm{D})\mathrm{T} = 0 \quad (4.2)$$

From equation (1) and (2) we get the voltage gain as follows,

$$\frac{\mathrm{Vo}}{\mathrm{Vin}\,|\sin wt|} = -\frac{\mathrm{D}}{(1-\mathrm{D})(2-\mathrm{D})} \quad (4.3)$$

Here D is the duty-cycle of the proposed buck-boost converter. For conventional buck-boost converter, the voltage gain is expressed as follows,

$$\frac{\mathrm{Vo}}{\mathrm{Vin}\,|\sin wt|} = -\frac{\mathrm{Dc}}{(1-\mathrm{Dc})} \quad (4.4)$$

Here Dc is the duty-cycle of conventional buck-boost converter.

Comparing (4.3) and (4.4), we can see that (4.3) has an extra term (2-D) in denominator. As duty-cycle ranges from $0 < D < 1$, the term (2-D) is always higher than 1. That means, the proposed converter has higher step down capability than the conventional one.

4.2.2 Hybrid Cuk Converter

Although two proposed topologies are different in terms of architectural point of view, their operating principle is similar. The voltage gain of our converters can be obtained from the volt-sec balance across inductors over the switching frequency. The step by step analysis of voltage gain is as follows.

Using volt-sec balance for inductors L_m and L_0,

$$\mathrm{Vin}|\sin wt|\mathrm{DT} + (\mathrm{Vin}|\sin wt| - 2\mathrm{Vc})(1 - \mathrm{D})\mathrm{T} = 0 \quad (4.5)$$

$$(\mathrm{Vo} + \mathrm{Vc})\ \mathrm{DT} + \mathrm{Vo}(1 - \mathrm{D})\mathrm{T} = 0 \quad (4.6)$$

From equation (1) and (2) we get the voltage gain as follows,

$$\frac{\mathrm{Vo}}{\mathrm{Vin}\,|\sin wt|} = -\frac{\mathrm{D}}{2(1-\mathrm{D})} \quad (4.7)$$

For conventional Cuk converter, the voltage gain is expressed as follows,

$$\frac{\mathrm{Vo}}{\mathrm{Vin}\,|\sin wt|} = -\frac{\mathrm{D}}{(1-\mathrm{D})} \tag{4.8}$$

Comparing (4.7) and (4.8), we can see that this proposed converters step down two times steeper than that of conventional Cuk converter.

4.3 Efficiency Analysis

4.3.1 Hybrid Buck-Boost Converter

The efficiency of our proposed converters is expressed as follows,

$$\eta = \frac{\mathrm{Po}}{\mathrm{Pin}} = \frac{\mathrm{Vo}}{|\mathrm{Vin}|}\frac{(1-\mathrm{Dc})(2-\mathrm{Dc})}{\mathrm{Dc}} \tag{4.9}$$

And the efficiency of the conventional buck-boost converter is

$$\eta_c = \frac{\mathrm{Po}}{\mathrm{Pin}} = \frac{Vo}{|Vin|}\frac{(1-Dc)}{Dc} \tag{4.10}$$

Comparing (4.9) and (4.10), we got

$$\eta = \eta c\,(2-\mathrm{Dc}) \tag{4.11}$$

Since, the term (2-D) is always greater than 1, the efficiency of our proposed converters is greater than the conventional one for any duty cycle.

4.3.2 Hybrid Cuk Converter

The efficiency of our proposed converters is expressed as follows,

$$\eta = \frac{\mathrm{Po}}{\mathrm{Pin}} = \frac{\mathrm{Vo}}{|\mathrm{Vin}|}\frac{2(1-\mathrm{D})}{\mathrm{D}} \tag{4.12}$$

And the efficiency of the conventional Cuk converter is

$$\eta_c = \frac{\mathrm{Po}}{\mathrm{Pin}} = \frac{Vo}{|Vin|}\frac{(1-D)}{D} \tag{4.13}$$

Comparing (4.12) and (4.13), we got

$$\eta = 2\times\eta c \tag{4.14}$$

So, it's clear that these proposed converters have twice the efficiency than that of conventional one for any duty cycle.

4.4 Approach to Model a New Converter

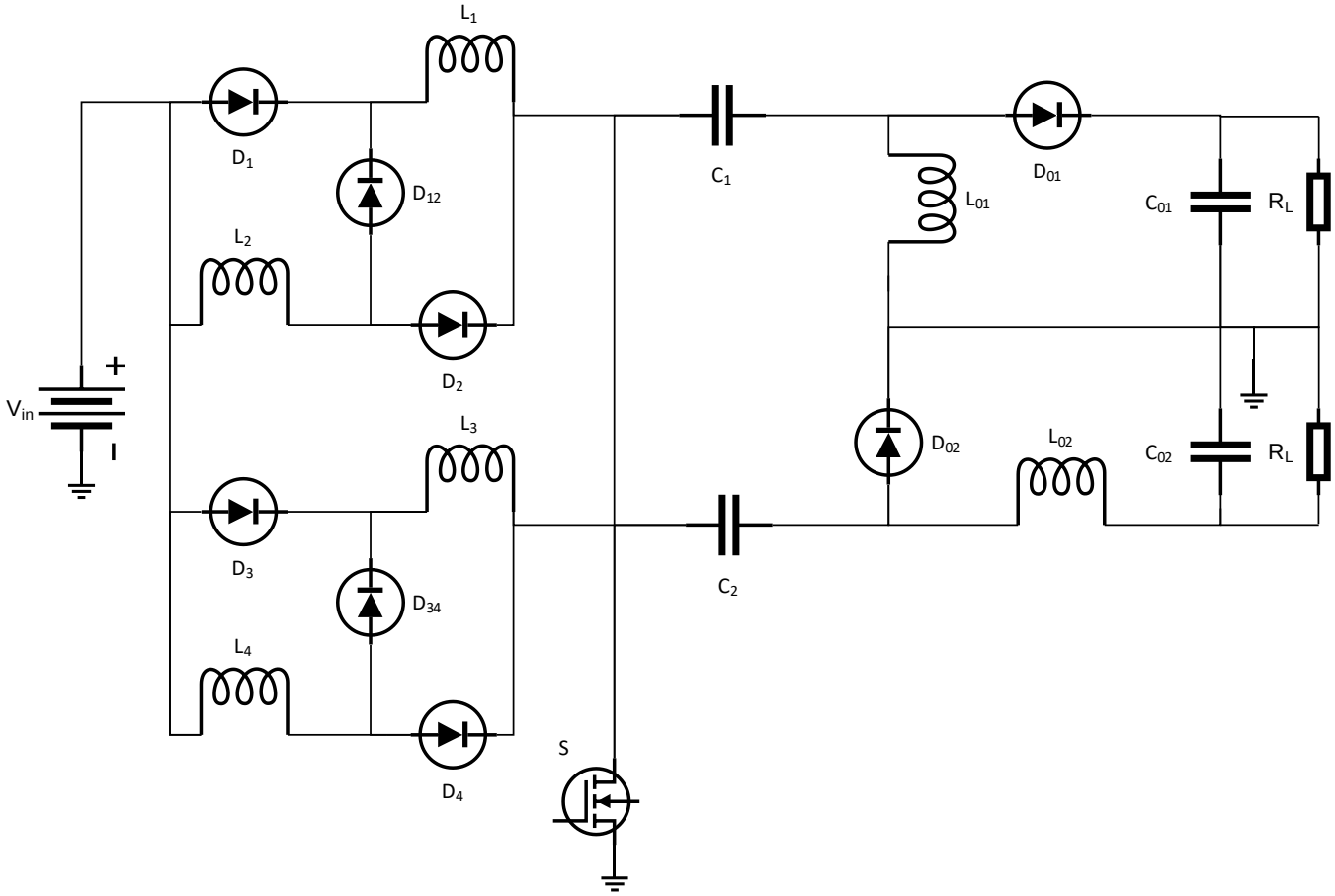

Fig. 4.7: Bipolar DC Link Based on SEPIC-Cuk Combination

Voltage conversion ratio of SEPIC side is $\frac{Vo}{Vin} = \frac{D(1+D)}{1-D}$ (4.15)

Voltage conversion ratio of Cuk side is $\frac{Vo}{Vin} = -\frac{D(1+D)}{1-D}$ (4.16)

Voltage across two ends is $\frac{Vo}{Vin} = \frac{D(1+D)}{1-D} - \left(-\frac{D(1+D)}{1-D}\right) = \frac{2D(1+D)}{1-D}$ (4.17)

Chapter 5

Simulation and Results

5.1 Assumptions

Following assumptions were made to simplify the theoretical analysis.

- All the components are assumed to be ideal.
- For the simplification of analysis, |Vin| was considered as a purely rectified sinusoidal source.
- Larger value of output capacitor C_0 was considered to refer V_0 as a pure dc voltage.
- Both the converters have been simulated using PSPICE for the following data specifications:

  $L_m = L_{m1} = L_{m2} = 10mH$

  $C_1 = C_2 = C_3 = C_4 = 1\mu F$

  $L_0 = 5mH$

  $C_0 = 330\mu F$

  $R_0 = 100\Omega$

5.2 Comparative Analysis

5.2.1 Hybrid Buck-Boost Converter

5.2.1.1 Input Power Factor Comparison

Our proposed topology has higher power factor compared to both the conventional buck-boost converter and the single stage switched capacitor network as illustrated in Fig. 5.1. The input inductor L_m followed by the switched capacitor network form an input L-C type filter for each half cycle of operation. This L-C input filter reduces the input current ripple and harmonics. Thus, it improves the input power factor in our proposed topology.

Duty Cycle	Conventional	Single Stage	Double Stage
5%	0.20330521	0.30781072	0.35726913
10%	0.2770445	0.40827239	0.5082502
15%	0.3336645	0.53588037	0.63587218
20%	0.38109973	0.64497323	0.74975702
25%	0.42256877	0.70916865	0.80295909

30%	0.45988344	0.73252044	0.83463638
35%	0.49402272	0.75755227	0.86170401
40%	0.5257054	0.7705437	0.87245564
45%	0.55500941	0.79844083	0.8908741
50%	0.58198889	0.81634614	0.91353324

Table 5.1: Input PF Comparison of Different Buck-Boost Converters

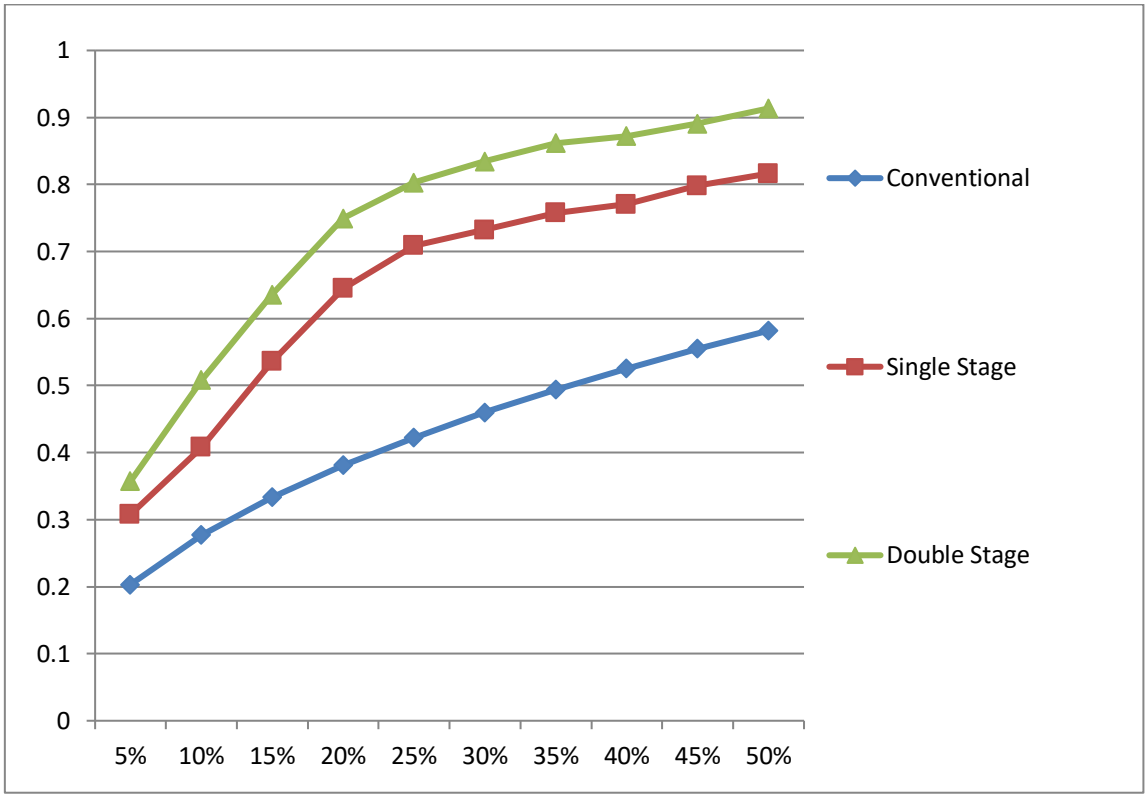

Fig. 5.1: Input PF Comparison of Different Buck-Boost Converters

5.2.1.2 Efficiency Comparison

Our proposed topology has greater efficiency compared to both the conventional buck-boost converter and the single stage switched capacitor network as illustrated in Fig. 5.2. The most efficient configuration is the double stage bridgeless switched capacitor network based buck-boost converter which has been proposed in this paper since there are separate paths introduced for each half cycle of operation. As two separate paths are used for two half cycles of operation, there are less reduction of hysteresis and loss of energy due to magnetization. Mathematically it is proved that our topology has greater efficiency compared to both the conventional as well as the single stage switched capacitor network based buck-boost converter.

Duty Cycle	Conventional	Single Stage	Double Stage
5%	0.755664537	0.780377564	0.820771773
10%	0.816365014	0.862233878	0.96174351
15%	0.844871616	0.896810261	0.979619007
20%	0.875023318	0.91574194	0.983565431
25%	0.897262748	0.939519235	0.987588079
30%	0.915415425	0.959175116	0.986668072
35%	0.931154884	0.968125983	0.989079807
40%	0.950369048	0.971716348	0.990046182
45%	0.95855238	0.976951005	0.991046219
50%	0.961007767	0.978104775	0.994066345

Table 5.2: Efficiency Comparison of Different Buck-Boost Converters

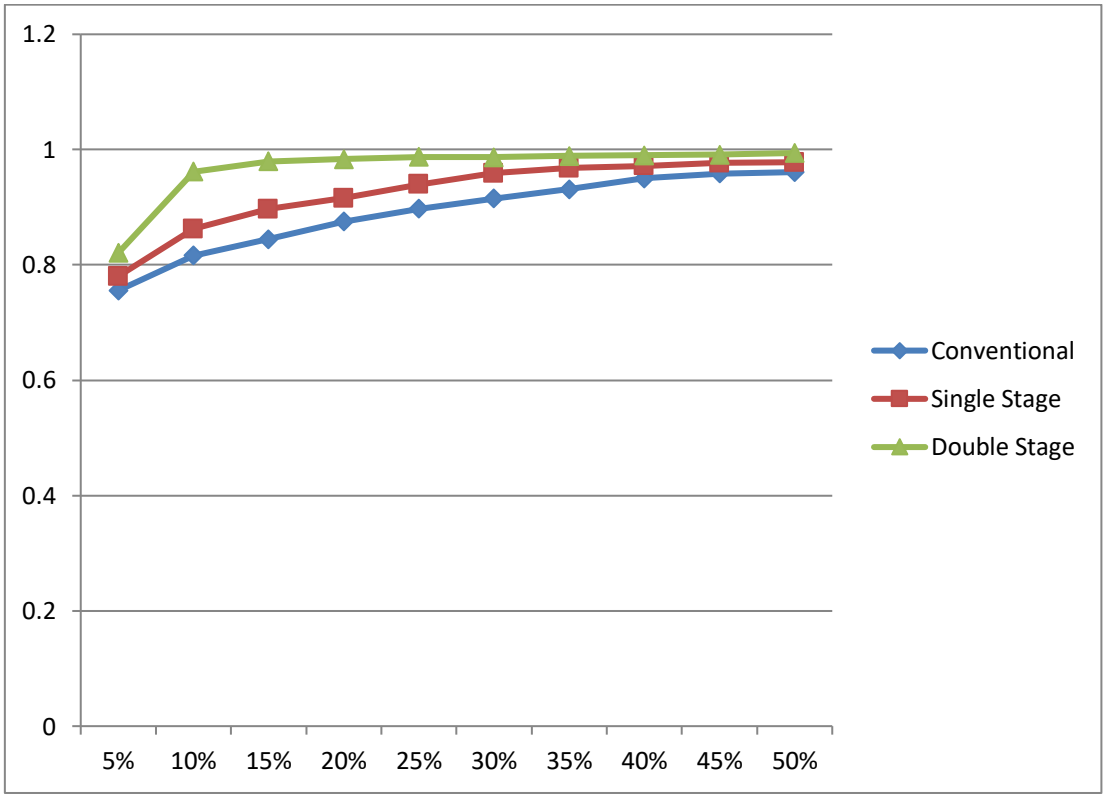

Fig. 5.2: Efficiency Comparison of Different Buck-Boost Converters

5.2.1.3 THD of Input Current Comparison

Our proposed topology has less total harmonic distortion (THD) of input current compared to both the conventional buck-boost converter and the single stage switched capacitor network as illustrated in Fig. 5.3. An input inductor followed by a switched capacitor network is introduced which formed an L-C input filter for each half cycle of operation. This L-C input filter reduces the input current ripple resulting in lower total harmonic distortion with respect to both the conventional as well as the single stage switched capacitor network based buck-boost converter.

Duty Cycle	Conventional	Single Stage	Double Stage
5%	4.7997019	3.6023178	2.6068043
10%	3.4461317	2.6559119	1.6556891
15%	2.7966135	2.095927	1.1958669
20%	2.38968	1.57575646	0.87625578
25%	2.0988676	1.12177655	0.72912508
30%	1.8733915	0.9372822	0.61887549
35%	1.6878313	0.78080035	0.56354391
40%	1.5285002	0.75774144	0.55422278
45%	1.3873519	0.72754263	0.53586287
50%	1.258749	0.70393323	0.51503457

Table 5.3: THD of Input Current Comparison of Different Buck-Boost Converters

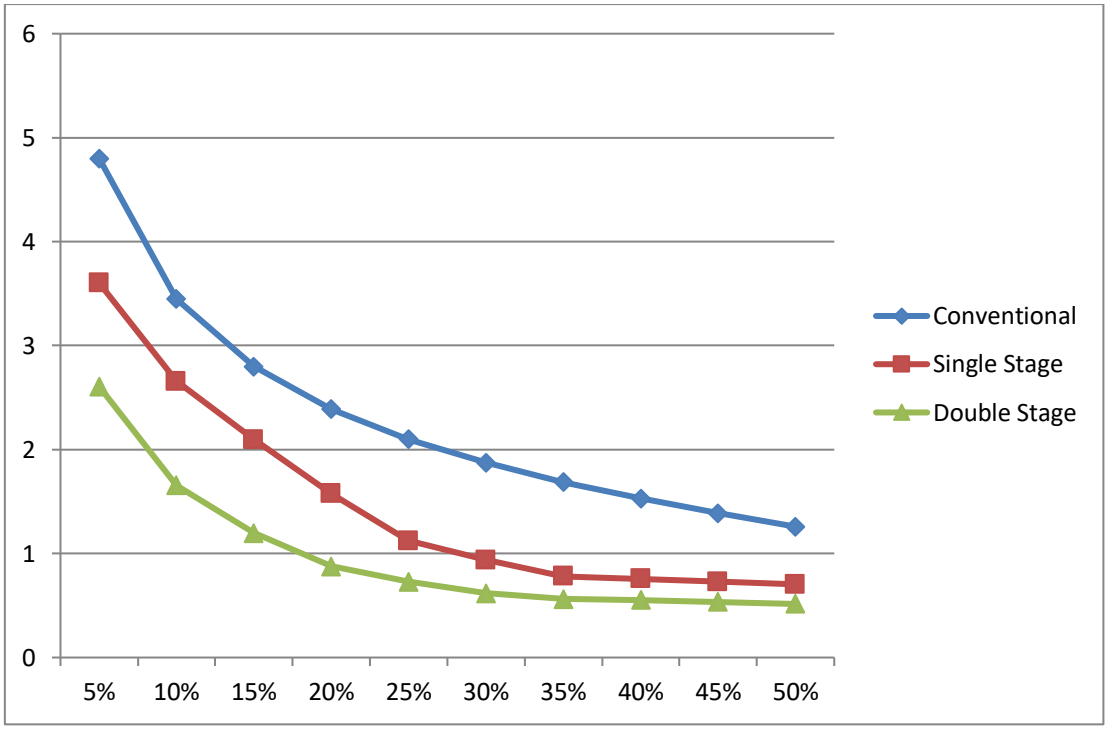

Fig. 5.3: THD of Input Current Comparison of Different Buck-Boost Converters

5.2.2 Hybrid Cuk Converter

5.2.2.1 Input Power Factor Comparison

Both the proposed topologies have higher power factor compared to the conventional Cuk converter as illustrated in Fig. 5.4. The input inductor Lm followed by the switched capacitor network form an input L-C type filter for each half cycle of operation. This L-C input filter reduces the input current ripple and harmonics. Thus, it improves the input power factor in this proposed topology.

Duty Cycle	Conventional	Single Stage	Double Stage
5%	0.40645362	0.44671204	0.50176994
10%	0.4967621	0.59472574	0.63385031
15%	0.6106245	0.70781529	0.73288949
20%	0.70261439	0.77442883	0.80143058
25%	0.77534506	0.80270234	0.83965325
30%	0.80485198	0.83847545	0.86115889
35%	0.8169007	0.85801791	0.87968577
40%	0.8207417	0.86724483	0.89156349

45%	0.8376546	0.89002888	0.91099008
50%	0.85761291	0.90474411	0.93522289

Table 5.4: Input PF Comparison of Different Cuk Converters

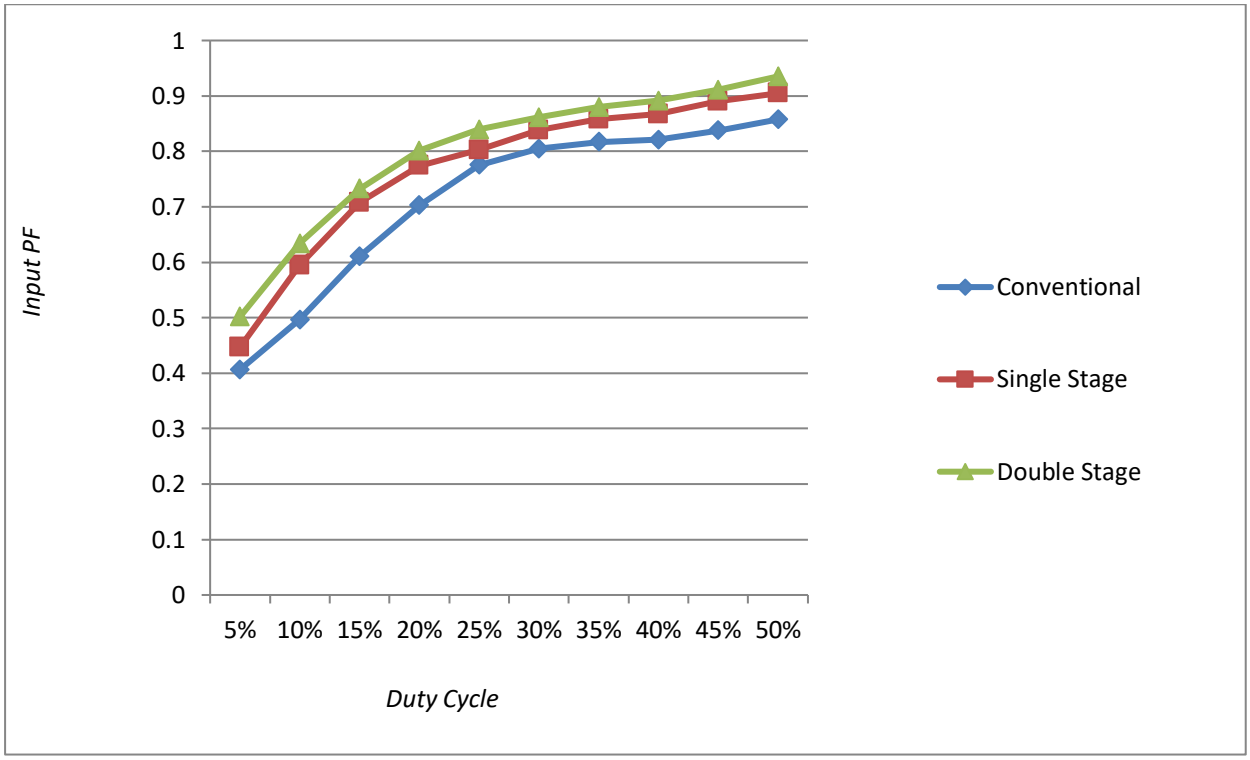

Fig. 5.4: Input PF Comparison of Different Cuk Converters

5.2.2.2 Efficiency Comparison

Both the proposed topologies have greater efficiency compared to the conventional Cuk converter as illustrated in Fig. 5.5. The most efficient configuration is the double stage bridgeless switched capacitor network based Cuk converter since there are separate paths introduced for each half cycle of operation. As two separate paths are used for two half cycles of operation, there are less reduction of hysteresis and loss of energy due to magnetization. Mathematically it is proved that both the topologies have greater efficiency compared to the conventional Cuk converter.

Duty Cycle	Conventional	Single Stage	Double Stage
5%	0.722550111	0.767694934	0.803173359
10%	0.750443156	0.792349328	0.827176156
15%	0.785823848	0.820961602	0.848819516

20%	0.817378931	0.844798081	0.867360639
25%	0.838089049	0.862801215	0.887052097
30%	0.855441903	0.880690356	0.902865673
35%	0.872621709	0.905178347	0.928283982
40%	0.890724011	0.921473827	0.939563495
45%	0.908739852	0.932664831	0.948696934
50%	0.918690151	0.948729757	0.958764401

Table 5.5: Efficiency Comparison of Different Cuk Converters

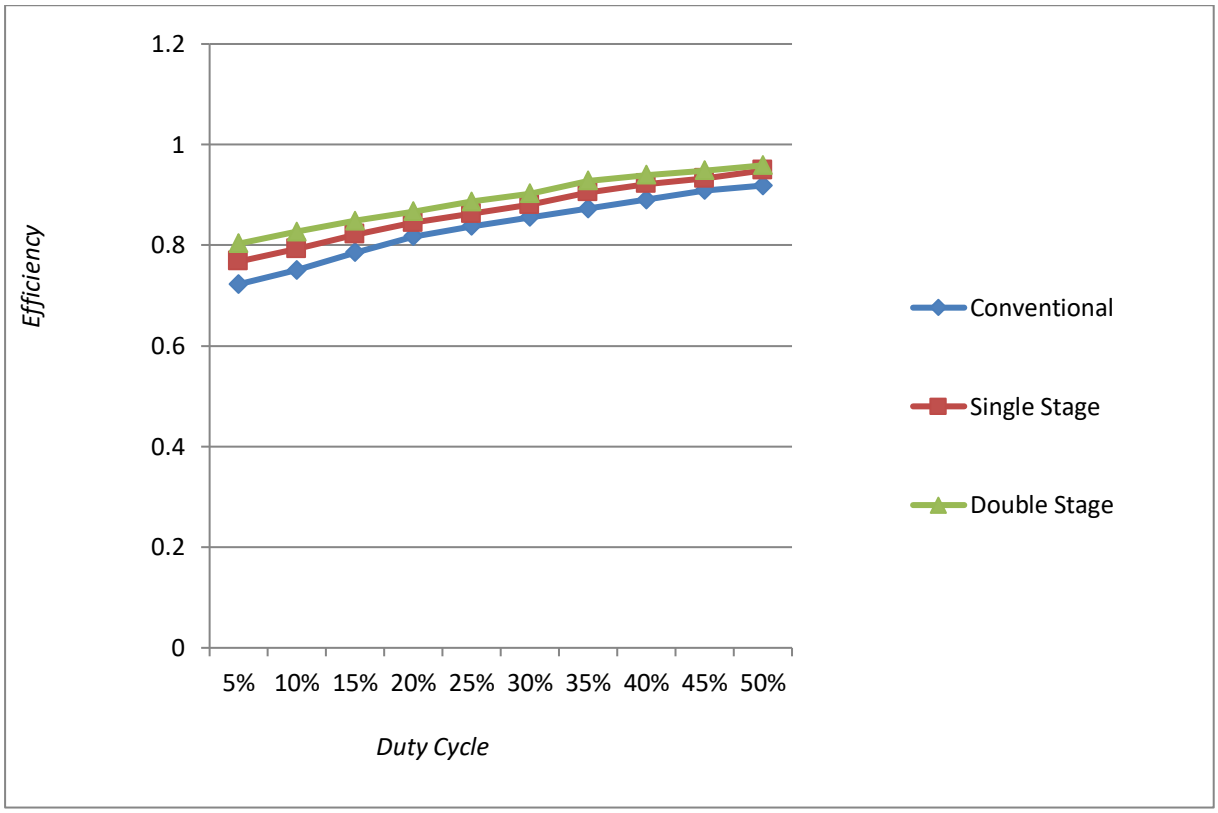

Fig. 5.5: Efficiency Comparison of Different Cuk Converters

5.2.2.3 THD of Input Current Comparison

Both the proposed topologies have less total harmonic distortion (THD) of input current compared to the conventional Cuk converter as illustrated in Fig. 5.6. An input inductor followed by a switched capacitor network is introduced which formed an L-C input filter for each half cycle of operation. This L-C input filter reduces the input current ripple resulting in lower total harmonic distortion with respect to the conventional Cuk converter.

Duty Cycle	Conventional	Single Stage	Double Stage
5%	1.7115743	1.342944	1.215438
10%	1.15647646	0.9980138	0.93173868
15%	0.9862886	0.83262408	0.76752166
20%	0.87063577	0.73496993	0.67959925
25%	0.75882945	0.63557231	0.58935167
30%	0.64286979	0.57152866	0.5047073
35%	0.59808386	0.50927184	0.44501911
40%	0.55121595	0.45005705	0.4067281
45%	0.50559907	0.43126578	0.38354148
50%	0.48653834	0.40701299	0.36227401

Table 5.6: THD of Input Current Comparison of Different Cuk Converters

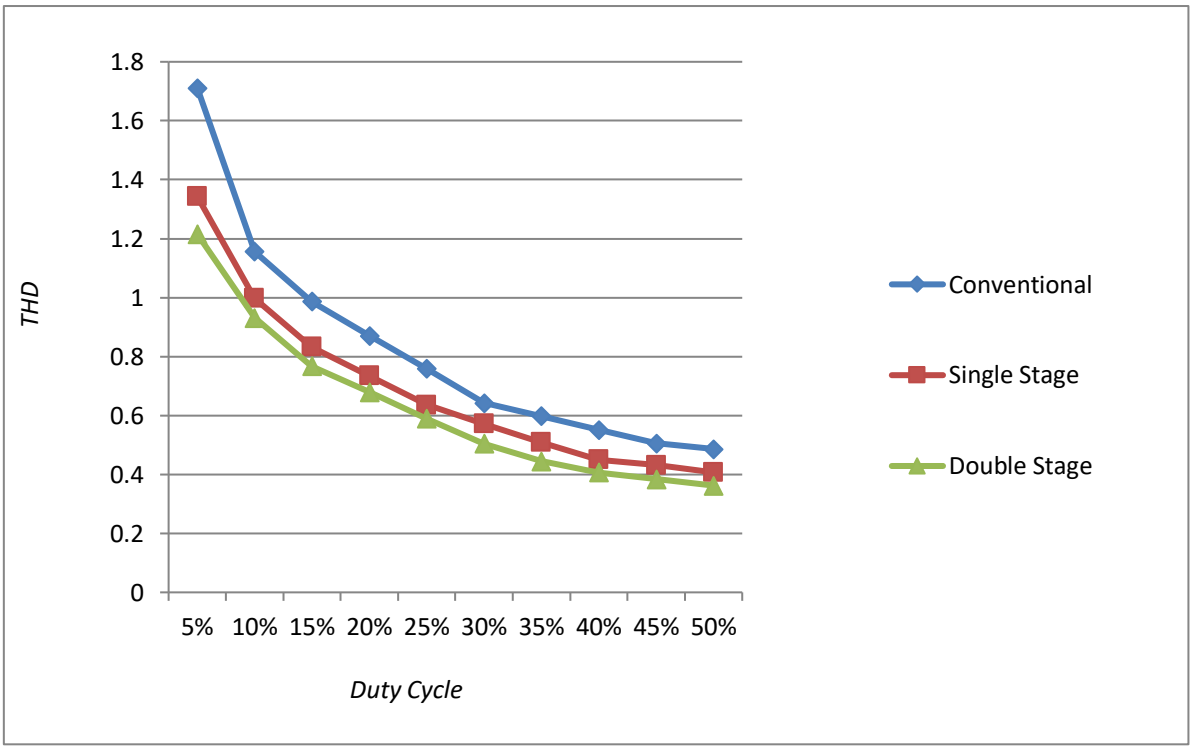

Fig. 5.6: THD of Input Current Comparison of Different Cuk Converters

Chapter 6

Application

6.1 Grid Connected Photovoltaic System

A new application of single-ended primary converter (SEPIC) and Cuk converter for dc bipolar network. A dc–dc converter configuration based on a combination of both converters is proposed. In the resulting topology, the switching node is shared by the SEPIC and Cuk converter since they have the same instantaneous duty cycle. The main advantage of this topology is that synchronization of various switches is not required and control terminal is connected to ground which simplifies the design of the gate drive. On the other hand, this configuration allows the connection of renewable energy sources to microgrids (MG)-type bipolar dc link and to cover the current needs of new distributed generation units with efficient, economical, and easy way. DC voltage induced from Photovoltaic (PV) cells will be boosted by this new proposed converter. Two three phase inverters were cascaded with the two ends of this SEPIC-Cuk combination. LCL filter smooths the output wave shapes of these two inverters. Hence, the final output can contribute to the national grid. Thus, the whole system can work as a backup during power failure by boosting up DC voltage induced from PV cells, then inverting into AC and finally filtering the output wave shapes with higher efficiency.

6.2 Working principle of the whole system

SEPIC and Cuk are two of the most recent SMPS converters. These two converters are almost identical in structure. The only difference is, SEPIC converter gives positive voltage conversion ratio and Cuk converter gives negative voltage conversion ratio. For both the converter,

$$\left|\frac{Vo}{Vin}\right| = \frac{D}{1-D}$$

At first, we developed a new DC-DC converter by merging SEPIC and Cuk converters. The new proposed converter can be controlled using only one power switch. The new converter has two ends, one is SEPIC end which has positive voltage conversion ratio, another is Cuk end which has negative voltage conversion ratio. So, voltage conversion ratio is doubled across the two ends.

$$\frac{Vo}{Vin} = \frac{D}{1-D} - \left(-\frac{D}{1-D}\right)$$

$$\frac{Vo}{Vin} = \frac{2D}{1-D}$$

However, input inductor of both the SEPIC and Cuk converters are replaced by switched inductors resulting in even higher voltage conversion ratio.

$$\left|\frac{Vo}{Vin}\right| = \frac{D(1+D)}{1-D}$$

Two three phase inverters are cascaded with the two ends of the new SEPIC-Cuk combined converter. Inverter outputs are filtered by two LCL filters. Hence, pure sinusoidal wave shapes are generated by the final inverter outputs. Thus, the final output of the system can contribute to the national grid.

PV cells will induce DC voltage. Induced DC voltage will be boosted up by the new proposed converter. The converter will give positive boosted voltage in the SEPIC side and negative boosted voltage in the Cuk side. Three phase inverters along with LCL filters will invert those boosted DC voltages to the AC line voltage. Thus, the open loop system has been formed. To utilize the whole system more efficiently, closed loop system must be formed.

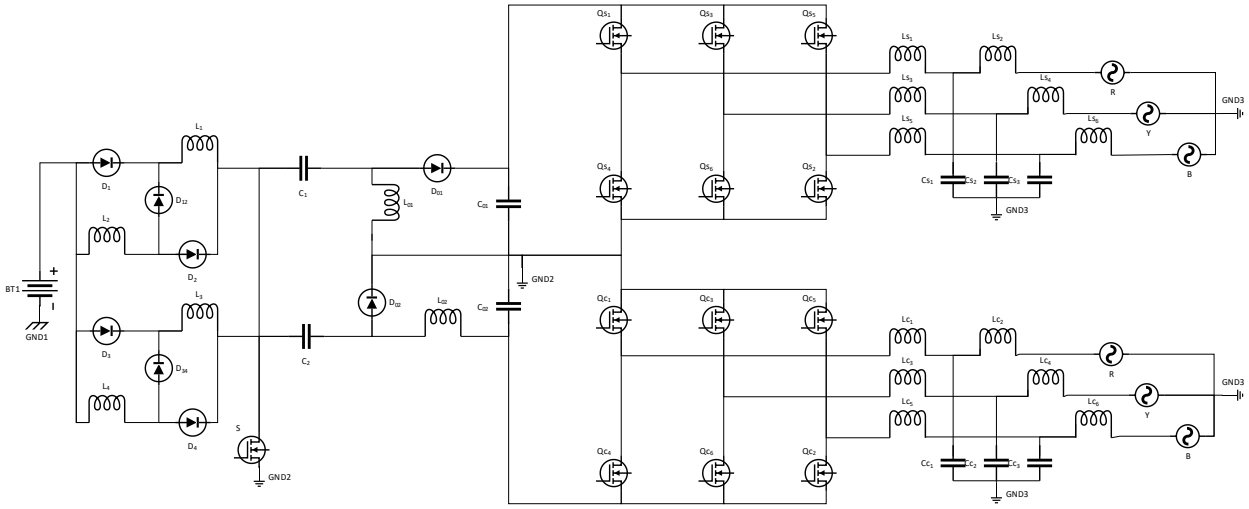

Fig 6.1: Open loop system

Line voltage must remain constant. Hence, with the increase of the load demand, line current is increased. The open loop system can't sense the load demand and perform the switching operation accordingly. Hence, we need to switch manually which is not a smart way indeed. The closed loop version of the proposed system will do this task automatically and can be used in smart grid too.

For PV side power control, MPPT algorithm is used. This is done to maximize the power extraction from the PV Module. For grid side power control, PLL algorithm ensures that the frequency matches with that of the grid. The voltage loop keeps the voltage in line with the grid line voltage, and the current loop varies the current according to the load demand.

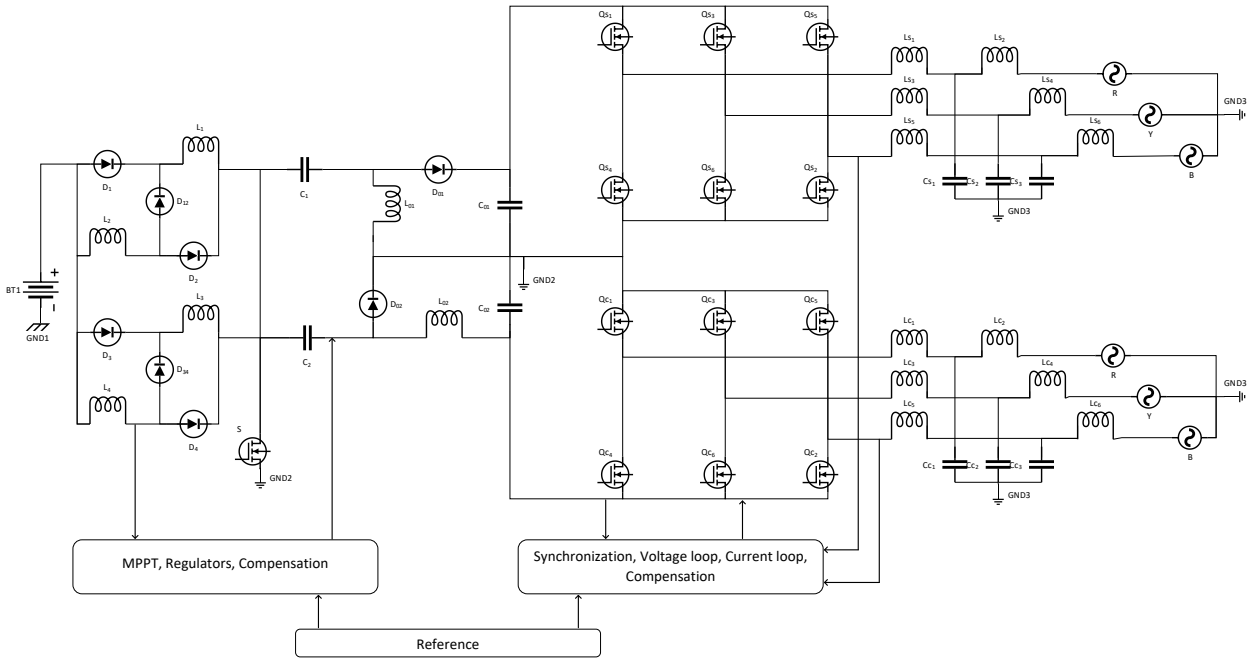

Fig 6.2: Closed loop system

6.3 Various Parameter comparison with existing Generators

The open loop system has been simulated using Cadence Allegro. This software does real time simulation. For different loads, simulation was done. Power factor, efficiency and total harmonic distortion have been recorded for different values of loads. Real power in KW vs these parameters have been plotted. From graphical representation, it's clear that the proposed system has higher efficiency, higher PF and lower THD compared to the already existing topologies.

6.3.1 Efficiency Comparison

Real Power(kW)	Fuel Cell	Diesel Engine	Petrol Engine	Proposed Topology
10	9.80%	6.80%	4.80%	66.20%
30	24.40%	20.10%	15.10%	78.70%
50	34.30%	29.20%	22.30%	85.20%
80	47.20%	35.20%	28.40%	89.40%
100	52.20%	39.40%	33.20%	91.30%
120	58.30%	42.80%	35.50%	93.10%
150	60.20%	48.10%	38.30%	95.50%
180	60.25%	49.60%	39.10%	96.90%
200	60.28%	50.20%	39.70%	97.10%
250	60.30%	50.30%	40.10%	97.30%

Table 6.1: Efficiency comparison of existing generators

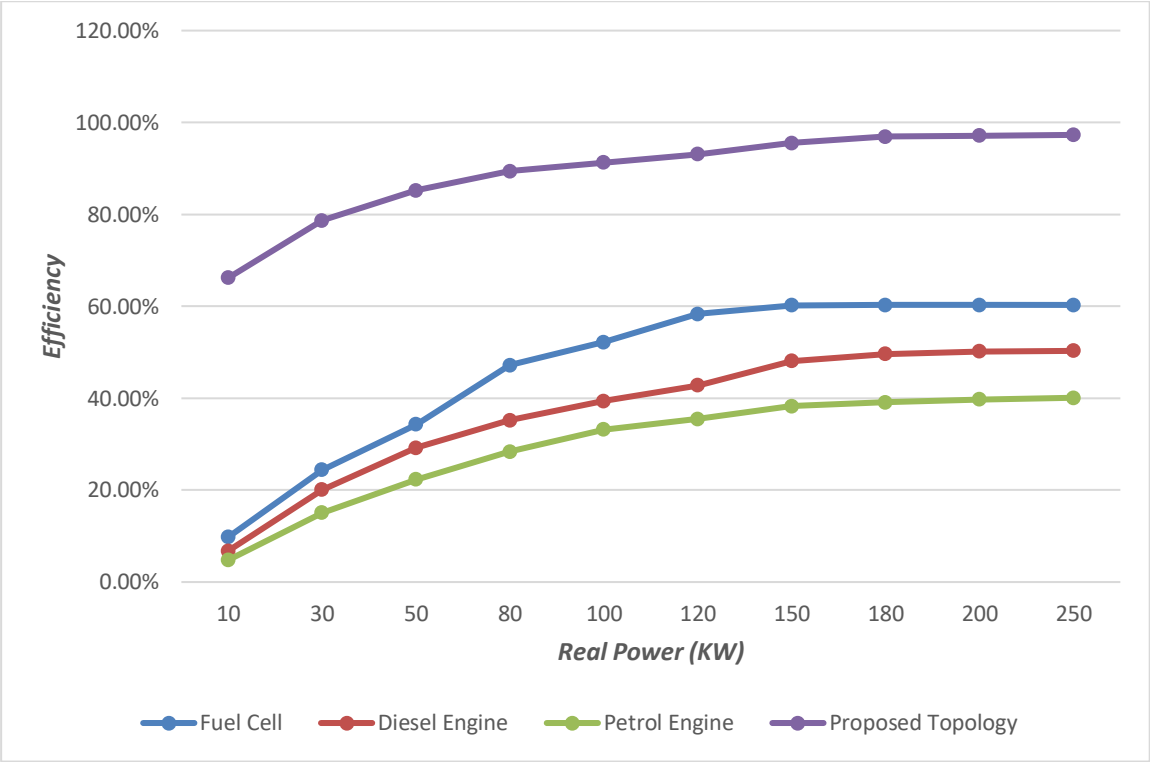

Fig. 6.3: Efficiency comparison of existing generators

6.3.2 THD Comparison:

Real Power(kW)	Fuel Cell	Diesel Engine	Petrol Engine	Proposed Topology
10	25.80%	29.20%	31.10%	19.80%
30	19.20%	21.40%	23.03%	15.20%
50	15.30%	16.60%	17.10%	11.01%
80	13.02%	13.80%	14.40%	9.10%
100	11.50%	12.30%	12.80%	8.20%
120	10.10%	11.20%	11.90%	7.40%
150	9.56%	10.05%	11.10%	6.80%
180	9.52%	9.80%	10.30%	6.20%
200	9.40%	9.78%	9.89%	5.90%
250	9.20%	9.70%	9.80%	5.85%

Table 6.2: THD comparison of existing generators

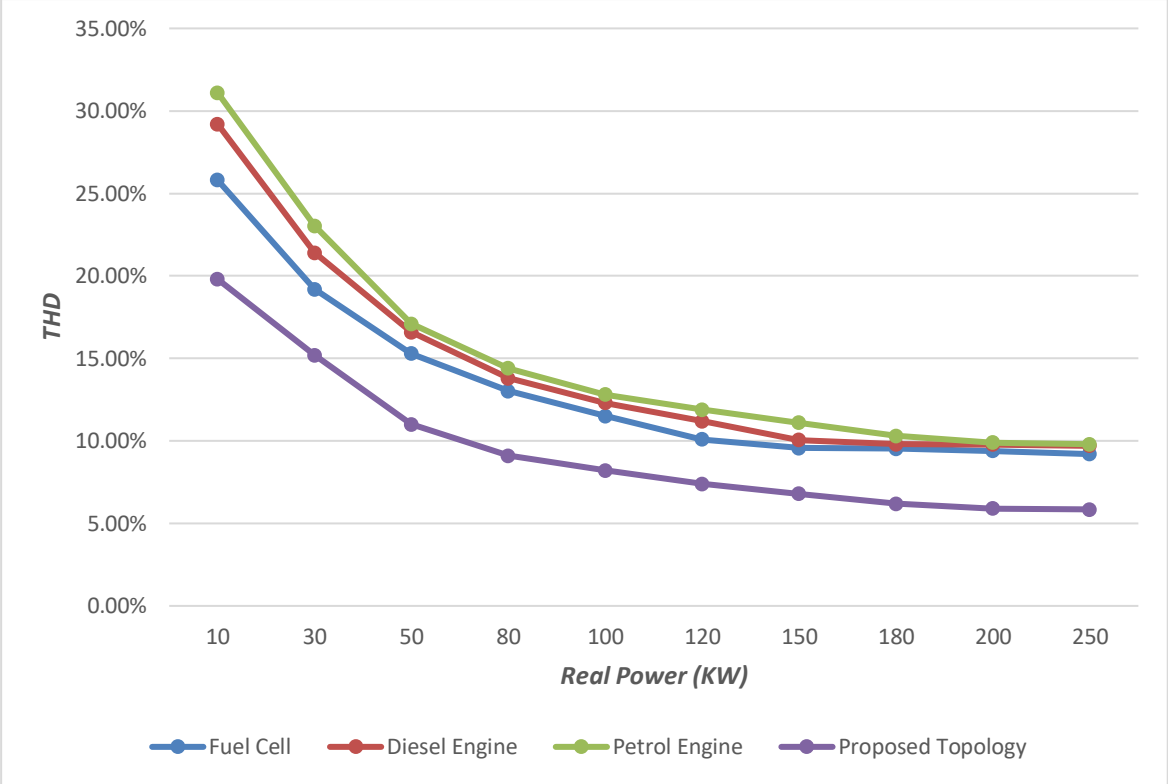

Fig. 6.4: THD comparison of existing generators

6.3.3 PF Comparison:

Real Power(kW)	Fuel Cell	Diesel Engine	Petrol Engine	Proposed Topology
10	0.67	0.65	0.62	0.72
30	0.74	0.71	0.69	0.79
50	0.79	0.76	0.74	0.84
80	0.83	0.79	0.77	0.87
100	0.85	0.82	0.79	0.89
120	0.87	0.84	0.81	0.91
150	0.88	0.85	0.835	0.92
180	0.885	0.87	0.85	0.93
200	0.89	0.88	0.87	0.94
250	0.9	0.89	0.88	0.95

Table 6.3: PF comparison of existing generators

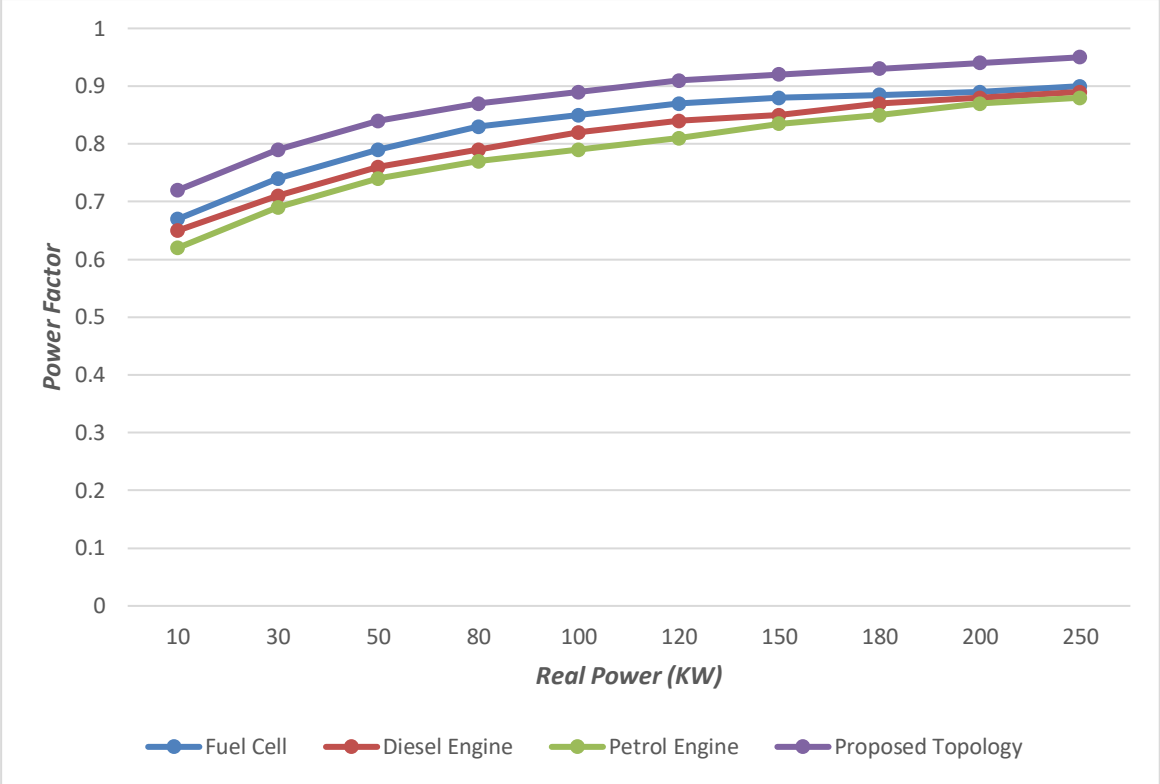

Fig. 6.5: PF comparison of existing generators

6.4 Cost estimation:

Components	Quantity	Cost in Taka
PV modules	15 module (100Wp)	15X9,000 = 1,35,000
Converter and Inverter components	Approximate	4,500
Charge controller	1	1,500
Wiring	Approximate	800
Control circuit, installment, maintenance and others	Approximate	8,000
Total		1,49,800

Table 6.4: Cost estimation

Loads	Quantity	Power Consumption in watt
TV	1	140
Refrigerator	2	2X150 = 300
LED Tube light	16	16X5 = 80
Ceiling fan (50”)	6	6X80 = 480
Total		1kW

Table 6.5: Estimated power supply to various loads

These are the approximate load estimation of CDS and Students' center of IUT. The proposed system can feed these loads. During inclement weather when the PV cells can't be charged properly due to inadequate sunlight, national grid will feed remaining loads. The proposed system should be installed parallelly with the national grid.

The whole system is ecofriendly. It doesn't harm environment by any means. The complete closed loop system can be implemented in smart grid. When the load demand increases, control circuitry will sense the current load demand and adjust switching duty cycle accordingly. The new DC-DC SEPIC-Cuk combined converter has made the whole system more efficient compared to the existing methods. The LCL -filter smooths the final output of the cascaded inverters and thus, reduces the total harmonic distortion of line voltage and current.

Chapter 7

Conclusion

A new hybrid bridgeless buck-boost converter with switched capacitor is presented which improves input power factor, converter efficiency, reduces conduction loss and THD. The classical buck-boost converter has its own set of drawbacks, for instance, the presence of electromagnetic interference and ripple current due to switching of power switch. The use of input LC filter corrects the ripple current and the switched capacitor reduces the THD. Moreover, this proposed bridgeless buck-boost converter with switched capacitor lowers the conduction losses, increases the efficiency and also improves the input power factor, keeping the advantages of both the classical and buck-boost with single stage switched capacitor network. The mathematical equations and simulation results will attest to this fact. This new hybrid bridgeless buck-boost converter can be used in power supply of ICs in microprocessors where 1V-3V is required.

Due to the lower conduction and switching losses, the proposed topology can further improve the conversion efficiency when compared with the conventional Cuk PFC rectifier. Moreover, these proposed Cuk PFC converters with switched capacitor increases the efficiency and also improves the input power factor, keeping the advantages of conventional Cuk converter. The mathematical equations and simulation results verify this. These Cuk PFC converters can be used in power supply of ICs in microprocessors where 1V-3V is required.

In this letter, a converter prototype for dc microgrid applications has been presented. This converter consists the combination of SEPIC and Cuk topologies (SE-CuCC). Both converters have the same voltage conversion ratio with opposite polarities. Therefore, it is possible to combine the two topologies to build a bipolar-type converter. The two combined structures share a common ground reference switch, and an equivalent inductor at the input. The main advantage of the proposed configuration is that it allows implementation bipolar dc link with only one controllable switch, which simplifies the implementation of control strategies, since it is not necessary synchronization of various switches. Moreover, control terminal is connected to ground which simplifies the implementation of the gate drive.

An experimental prototype has been developed and subjected to changing load conditions. Experimental results show its volt-age regulation capacity even in unbalance cases. The proposed SE-CuCC allows us to cover the current needs in new distributed generation units with economical and easy way. Highlighting three aspects of the prototype developed: simple structure since it uses an only switch and fewer passive elements, a driver circuit is simpler since there is only one switch to be controlled and it does not require isolation, and control circuit is simpler since they can be regulated dc bipolar voltages with an only controller.

Adjustments

The output of the supply is to be adjustable between 0 and 30 V and so RVI should be adjusted to make sure that when PI is at its minimum setting, the output of the supply is exactly 0 V. As it is not possible to measure very small values a conventional panel meter, a digital meter was used for this adjustment setting it at a very scale to increase its sensitivity.

Caution

This circuit works off the mains and there are 220 VAC present in some of its parts. Voltages above 50 V are dangerous and could even be lethal. In order to avoid accidents that could be fatal, please observe the following rules:

- It was double checked everything before connecting the circuit to the maim and be ready During constructing the circuit, something looked wrong then it was disconnected and resoled again.
- It was carefully touched every part of the circuit when under power.
- The ICs was connected on the base according to pin configuration, otherwise the circuit may have chance to damage.
- It is not suitable to change the fuses with of higher rating or replace them wire or aluminum foil.
- It was avoided to work with wet hands.
- Used proper sized drill bit to makes the holes in the printed circuit carefully; otherwise it may difficult to proper soldering.
- Used a proper mains lead with the correct plug and earth in circuit properly. The case of the project is made of metal no that it was properly earthen.
- During testing the circuit that works of the mains wears shoes with rubber soles, stand on dry non-conductive floor, and keep one hand in the pocket or behind the back.
- The circuit was carefully build and well insulated, it will not constitute a danger for its user.
- Wearing chain, necklace, or anything that may be hanging and touch an exposed part of the circuit with carefully.
- Electricity can kill when not careful.

If it does not work

- Check the work for possible dry joints, bridges across adjacent tracks or soldering flux residues that usually cause problems.
  Check again all the external connections to and from the circuit to see if them is a mistake there.
- Ensure that there are no components missing or inserted in the wrong places.
- Make sure that all the polarized components have been soldered the right way around.
- Make sure the supply has the correct voltage and is connected the right way around to the circuit.
- Check the project for faulty or damaged components.

Part List

1. R1 = 2,2 KOhm 1W

2. R2 = 82 Ohm 1/4W

3. R3 = 220 Ohm 1/4W

4. R4 = 4,7 KOhm 1/4W

5. R5, R6, R13, R20, R21 = 10 KOhm 1/4W

6. R7 = 0,47 Ohm 5W

7. R8, R11 = 27 KOhm 1/4W

8. R9, R19 = 2,2 KOhm 1/4W

9. R10 = 270 KOhm 1/4W

10. R12, R18 = 56KOhm 1/4W

11. R14 = 1,5 KOhm 1/4W

12. R15, R16 = 1 KOhm 1/4W

13. R17 = 33 Ohm 1/4W

14. 1/22 = 3,9 KOhm 1/4W IS, RV1 = 100K trimmer

16. Ph P2 = 10KOhm linear pontesiometer

17. CI = 3300 uF/50V electrolytic

18. C2, C3 = 47uF/50V electrolytic

19. T9.C4 =1ffiriF polyester

20. C5 = 200nF polyester

21. Co = 100pF ceramic

22. C7 = 10uF/50V electrolytic

23. C8 = 330pF ceramic

23. C9 = 100pF ceramic

25. DI, D2, D3, D4 = 1N5402,3,4 diode 2A - RAX GI837U

26. D5, D6 = 1N4148

27. D7, D8 = 5,6V Zener

28. D9, DIO = 1N4148

29. D11 = 1N4001 diode 1A

30. QI = BC548, NPN transistor or BC547

31. Q2 = 2N2219 NPN transistor

32. Q3 = BC557, PNP transistor or BC327

33. Q4 = 2N3055 NPN power transistor

34. Ul, U2, U3 = TL081, operational amplifier

35. D12 = LED diode

Chapter 8

Published Papers

1. ***Bridgeless AC-DC Buck-Boost Converter with Switched Capacitor for Low Power Applications*** (IEEE Region Ten Conference, Malaysia, 2017)
2. ***New Topologies of Cuk PFC Converter with Switched Capacitor for Low Power Applications*** (IEEE Region 10 Humanitarian Technology Conference, BUET, 2017)

Chapter 9

Reference

1. Kassakian J, Schlecht M, Verghese G (1991) Principles of power electronics. Addison- Wesley, Reading
2. Batarseh I (2004) Power electronic circuits. Wiley, New York
3. Mohan N, Undeland T, Robbins W (2003) Power electronics: converters, applications, and design. Wiley, New York
4. Hart D (2011) Power electronics, 2nd edn. McGraw Hill, New York
5. Holmes D, Lipo T (2003) Pulse width modulation for power converters. IEEE/Wiley- Interscience, New York
6. Wu B (2006) High-power converters and AC drives. Wiley, New York
7. Rossetto L, Spiazzi G, Tenti P (1994) Control techniques for power factor correction converters. In: Proceedings of PEMC, pp 3310–1318
8. Buso S, Matavelli P (2006) Digital control in power electronics. Morgan & Claypool, San Rafael
9. Rodriguez J, Dixon J, Espinoza J et al (2005) PWM regenerative rectifiers: state of the art. IEEE Trans Ind Electron 52:5–55
10. Holtz J (1994) Pulse width modulation for electronic power conversion. Proc IEEE 82:1194–1214
11. da Silva E, dos Santos E, Jacobina C (2011) Pulsewidth modulation strategies. IEEE Ind Electron Mag 5:37–45
12. Schönung A, Stemmler H (1964) Static frequency changers with sub-harmonic control in conjunction with reversible variable speed AC drives. Brown Boveri Rev 51:555–577
13. Bowes S, Mount M (1981) Microprocessor control of PWM inverters. IEEE Proc B:293–305
14. Depenbrock M (1977) Pulse width control of a 3-phase inverter with non-sinusoidal phase voltages. In: Proceedings of the IEEE international semiconductor power converter conference, ISPCC'77, pp 399–403
15. Houldsworth J, Grant D (1984) The use of harmonic distortion to increase the output voltage of a three-phase PWM inverter. IEEE Trans Ind Appl IA-20:1224–1228
16. Kolar JW, Ertl H, Zach FC (1990) Influence of the modulation method on the conduction and switching losses of a PWM converter system. In: Proceedings of the IEEE-IAS'90, pp 502–512
17. Sun J, Grotstollen H (1996) Optimized space vector modulation and regular-sampled PWM: a reexamination. In: Proceedings of the IEEE-IAS'96, pp 956–963
18. Blasko V (1996) A hybrid PWM strategy combining modified space vector and triangle comparison methods. In: Proceedings of the IEEE PESC, pp 1872–1878
19. Hava A, Kerkman R, Lipo T (1998) A high-performance generalized discontinuous PWM algorithm. IEEE Trans Ind Appl 34:1059–1071
20. Alves A, da Silva E, Lima A, Jacobina C (1998) Pulse width modulator for voltage-type inverters with either constant or pulsed DC link. In: Proceedings of IEEE IAS'98, pp 229–1236
21. Seixas P (1988) Commande numérique d'une machine synchrone autopilotée. D.Sc. Thesis, L'Institut Nationale Polytechnique de Toulouse, INPT, Toulouse
22. Holmes D (1996) The significance of zero space vector placement for carrier-based PWM schemes. IEEE Trans Ind App 32:1122–1129
23. Grotstollen H (1993) Line voltage modulation: a new possibility of PWM for three phase inverters. In: Proceedings of the IEEE IAS'93, pp 567–574
24. Jacobina C, Lima A, da Silva E, Alves R, Seixas P (2001) Digital scalar pulse-width modulation: a simple approach to introduce non-sinusoidal modulating waveforms. IEEE Trans Power Electron 16:351–359
25. Oliveira A, da Silva E, Jacobina C (2004) A hybrid PWM strategy for multilevel voltage source inverters. In: Proceedings of the IEEE PESC'2004, pp 4220–4225
26. Van der Broeck H, Skudelny H, Stanke G (1988) Analysis and realization of a pulse width modulator based on voltage space vector. IEEE Trans Ind Appl 24:142–150
27. Jacobina C, Lima A, da Silva E (1977) PWM space vector based on digital scalar modulation. In: Proceedings of the IEEE PESC, pp 100–105
28. Zhou K, Wang D (2002) Relationship between space-vector modulation and three-phase carrier-based PWM: a comprehensive analysis. IEEE Trans Ind Appl 49:186–196
29. Ledwich G (2001) Current source inverter modulation. IEEE Trans Power Electron 6:618–623
30. Dahono P, Kataoka T, Sato Y (1997) Dual Relationships between voltage-source and currentsource three-phase inverters and its applications. In: Proceedings of the PEDS, pp 559–565

31. Zmood D, Holmes DG (2001) Improved voltage regulation for current-source inverters. IEEE Trans Ind Appl 37:1028–1036
32. Espinoza J, Joós G, Guzmán J et al (2001) Selective harmonic elimination and current/voltage control in current/voltage source topologies: a unified approach. IEEE Trans Ind Electron 48:71–81
33. Zargari N, Geza J (1993), A current-controlled current source type unity power factor PWM rectifier. In: Proceedings of the IEEE IAS'93, pp 793–799
34. Acha E, Agelidis V, Anaya-Lara O et al (2002) Power electronic control in electrical systems. Newnes, Oxford
35. Simões G, Farret F (2008) Alternative energy system. CRC Press, Boca Raton
36. Casadei D, Serra G, Tani A et al (2002) Matrix converter modulation strategies: a new general approach based on space-vector representation of the switch state. IEEE Trans Ind Electron 49:370–381
37. Huber L, Borojevic D (1995) Space vector modulated three-phase to three-phase matrix with input power factor correction. IEEE Trans Ind Appl 31:1234–1246
38. Klumpner C, Blaabjerg F (2005) Modulation method for a multiple drive system based on a two-stage direct power conversion topology with reduced input current ripple. IEEE Trans Power Electron 20:922–929
39. Accioly AGH, Bradaschia F, Cavalcanti M et al (2007) Generalized modulation strategy for matrix converters, part I. In: Proceedings of the IEEE PESC'07, pp 646–652
40. Intel Technology Symposium, Tech. Rep, Intel Corporation, Hillsboro, OR, 2001.
41. J. Wei, P. Xu, H. Wu, F. C. Jee, K. Yao, and M. Ye, "Comparison of three topology candidates for 12V VRM," in Proc. IEEE Appl. Power Electron. Conf. (APEC), 2001, pp. 245–251.
42. L. Huber and M. M. Jovanovic´, "A design approach for server power supplies for networking," in Proc. IEEE Appl. Power Electron. Conf. (APEC), 2000, vol. 2, pp. 1163–1169.
43. J. Wei, K. Yao, M. Xu, and F. C. Lee, "Applying transformer concept to non-isolated voltage regulators significantly improves the efficiency and transient response," in Proc. IEEE Power Electron. Specialist Conf. (PESC), 2003, pp. 1599–1604.
44. J. Wie and F. C. Lee, "Two novel soft-switched high-frequency, high efficiency, non-isolated voltage regulators-the phase-shift buck converter and the matrix-transformer phase-buck converter," IEEE Trans. Power Electron., vol. 20, no. 2, pp. 292–299, Mar. 2005.
45. A. Ioinovici, "Switched-capacitor power electronics circuits," IEEE Circuits Syst. Mag., vol. 1, no. 1, pp. 37–42, Jan. 2001.
46. D. Maksimovic´ and S. C´uk, "Switching converters with wide dc conversion range," IEEE Trans. Power Electron., vol. 6, pp. 149–157, Jan. 1991.
47. V. Paceco, A. Nascimento, V. Farias, J. Viera, and L. Freitas, "A quadratic buck converter with lossless commutation," IEEE Trans. Ind. Electron., vol. 47, pp. 264–271, Apr. 2001.
48. M. S. Makowski, "On topological assumptions on PWM converters—a reexamination," in Proc. IEEE Power Electron. Specialist Conf. (PESC), 1993, pp. 141–147.
49. Boris Axelrod, Yefim Berkovich, Adrian Ioinovici, "Switched-Capacitor/Switched-Inductor Structures for Getting Transformerless Hybrid DC–DC PWM Converters"
50. Golam Sarowar, Md. Ashraful Hoque, "High Efficiency Single Phase Switched Capacitor AC to DC Step Down Converter," Procedia - Social and Behavioral Sciences 195 (2015) 2527 – 2536
51. R. Redlinger, P. Andersen, and P. Morthorst, Wind energy in the 21st century: Economics, policy, technology, and the changing electricity industry. Springer, 2016.
52. M. Bilgili, A. Ozbek, B. Sahin, and A. Kahraman, "An overview of renewable electric power capacity and progress in new technologies in the world," Renewable and Sustainable Energy Reviews, vol. 49, pp. 323–334, 2015.
53. K. Barnham, K. Knorr, and M. Mazzer, "Recent progress towards all renewable electricity supplies," Nature materials, 2015.
54. Bing Lu, Ron Brown, Macro Soldnao, "Bridgeless PFC implementation using one cycle control technique," APEC, 2005, no. 2, pp. 812-817
55. Wang Wei, Liu Hongpeng, Jiang Shigong and Xu Dianguo , "A Novel Bridgeless Buck-Boost PFC Converter, " Power Electronics Specialists Conference, 2008. PESC 2008. IEEE
56. M. Mahdavi and H. Farzanehfard, "Bridgeless SEPIC PFC Rectifier with Reduced Components and Conduction Losses," IEEE Transactions Industrial Electronics, vol. 58, No. 9, pp. 4153-4160, Sep. 2011.
57. Y. Jang and M. M. Jovanovic, "Bridgeless High-Power-Factor Buck Converter," IEEE Transactions Power Electron, vol. 26, No. 2, Feb. 2011.
58. Intel Technology Symposium, Tech. Rep, Intel Corporation, Hillsboro, OR, 2001.
59. J. Wei, K. Yao, M. Xu, and F. C. Lee, "Applying transformer concept to non-isolated voltage regulators significantly improves the efficiency and transient response," in Proc. IEEE Power Electron. Specialist Conf. (PESC), 2003, pp. 1599–1604.
60. P. Kong, S. Wang, and F. C. Lee, "Common mode EMI noise suppression for bridgeless PFC converters," IEEE Trans. Power Electron., vol. 23, no. 1, pp. 291–297, Jan. 2008.
61. C.-M. Wang, "A novel single-stage high-power-factor electronic ballast with symmetrical half-bridge topology," IEEE Trans. Ind. Electron., vol. 55, no. 2, pp. 969–972, Feb. 2008.

62. W.-Y. Choi, J.-M. Kwon, and B.-H. Kwon, “Bridgeless dual-boost rectifier with reduced diode reverse-recovery problems for power-factor correction,” IET Power Electron., vol. 1, no. 2, pp. 194–202, Jun. 2008.
63. Y. Jang, M. M. Jovanovic, and D. L. Dillman, “Bridgeless PFC boost rectifier with optimized magnetic utilization,” in Proc. IEEE Appl. Power Electron. Conf. Expo., 2008, pp. 1017–1021.
64. M. S. Makowski, “On topological assumptions on PWM converters—a reexamination,” in Proc. IEEE Power Electron. Specialist Conf. (PESC), 1993, pp. 141–147.
65. Boris Axelrod, Yefim Berkovich, Adrian Ioinovici, “Switched Capacitor/Switched-Inductor Structures for Getting Transformerless Hybrid DC–DC PWM Converters
66. N. Hatziargyriou; H. Asano; R. Iravani; C. Marnay, “Microgrids,” IEEE Power and Energy Magazine, vol. 5, issue 4, pp. 78–94, Jul/Aug 2007.
67. H. Kakigano, Y. Miura, T. Ise, R. Uchida, “DC Micro-grid for Super High Quality Distribution – System Configuration and Control of Distributed Generations and Energy Storage Devices,” *IEEE IPEMC Power Electron Motion Control Conf.*, 2004 (3), pp. 1740–1745.
68. J. M. Guerrero, J. C. Vasquez, and R. Teodorescu, “Hierarchical control of droop-controlled DC and AC microgrids: A general approach towards standardization,” *IEEE Conf. Ind. Electron. (IECON)*, pp. 4305–4310, 2009.
69. J. M. Guerrero, “Microgrids: Integration of distributed energy resources into the smart-grid,” *in Proc. IEEE Int. Symp. Ind. Electron*., Bari, Italy, 2010, pp. 4281–4414.
70. J. C. Vasquez, J. M. Guerrero, J. Miret, M. Castilla, and L. Vicuña, “Hierarchical control of intelligent microgrids,” *IEEE Ind. Electron. Mag*., vol. 4, no. 4, pp. 23–29, Dec. 2010.
71. Lie Xu and Dong Chen, “Control and operation of a DC microgrid with variable Generation and energy starge,” IEEE Trans. Power delivery, vol. 26, no 4, pp. 2513–2522, Oct. 2011.
72. J. J. Justo, F. Mwasilu, J. Lee, J. W. Jung, “AC-microgrids versus DC microgrids with distributed energy resources: a review,” Renewable and Sustainable Energy Reviews, nº 24, pp. 387-405, 2013.
73. J. Lago, J. Moia, and M. L. Heldwein, “Evaluation of power converters to implement bipolar dc active distribution networks—DC–DC converters,” in Proc. Energy Convers. Congr. Expo., 2011, pp. 985–990.
74. E. Landsman, "A Unifying Derivation of Switching dc-dc Converter Topologies", Proc. IEEE Power Electronics Specialists Conference, PESC1979, pp. 239-243.
75. J. White, and W. Muldoon, "Two-Inductor Boost and Buck Converters", Proc. IEEE Power Electronics Specialists Conference, PESC1987, pp. 387-392.
76. D. Maksimovic, and S. Cuk, "General Properties and Synthesis of PWM DC-to-DC Converters", Proc. IEEE Power Electronics Specialists Conference, PESC1989, pp. 515-525.
77. J. Wang; W.G. Dunford; and K E. Mauch, "Synthesis of two-inductor DC-DC converters", Proc. IEEE Power Electronics Specialists Conference, PESC1997, pp. 1367-1373, vol. 2.
78. J.Chen, D. Maksimovic, and R. Erickson, "Buck-Boost PWM Converters having two independently controlled Switches", Proc. IEEE Power Electronics Specialists Conference, PESC2001, pp. 736-741.
79. E. Duran, M. Sidrach-de-Cardona, J. Galan and J.M. Andujar, “Comparative analysis of buck-boost converters used to obtain I–V characteristic curves of photovoltaic modules", Proc. IEEE Power Electronics Specialists Conference, PESC2008, pp. 2036-2042.
80. B. R. Lin and F. Y. Hsieh, “Soft-switching Zeta-flyback converter with a buck-boost type of active clamp,” IEEE Trans. Ind. Electron., vol. 54, no. 5, pp. 2813–2822, Oct. 2007